

Modeling the effect of dual-core energy recovery ventilator (ERV) unit on the energy use of houses in northern Canada compared with the single-core ERV unit

Jing Li

A Thesis

in

Department of Building, Civil and Environmental Engineering

Presented in Partial Fulfillment of the Requirements

for the Degree of Master of Applied Science (Building Engineering) at

Concordia University

Montreal, Quebec, Canada

August 2021

© Jing Li, 2021

CONCORDIA UNIVERSITY
School of Graduate Studies

This is to certify that the thesis is prepared

By: Jing Li

Entitled: Modeling the effect of dual-core energy recovery ventilator (ERV) unit on the energy use of houses in northern Canada compared with the single-core ERV unit

and submitted in partial fulfillment of the requirements for the degree of

Master of Applied Science (Building Engineering)

complies with the regulations of the University and meets the accepted standards with respect to originality and quality.

Signed by the final examining committee:

Dr. A. Athienitis Chair

Dr. Bruno Lee Examiner

Dr. Hua Ge Co-Supervisor

Dr. Radu Zmeureanu Co-Supervisor

Approved by Dr. Michelle Nokken, Graduate Program Director

27/08/2021 Dr. Mourad Debbabi, Dean, Gina Cody School of Engineering and Computer Science

ABSTRACT

Modeling the effect of dual-core energy recovery ventilator (ERV) unit on the energy use of houses in northern Canada compared with the single-core ERV unit

Jing Li

The conventional preheating defrost used in the single-core energy recovery ventilator (ERV) is not optimal for housing in northern Canada due to its significant energy consumptions. Therefore, the recirculation defrost and dual-core operation have been the focus for addressing the frosting issues of the ERV in northern Canada. The use of single-core ERV using the defrost by air recirculation has the disadvantage of reducing the outdoor air supplied to the house, which might affect the indoor air quality. First, this thesis presents new correlation-based models of the single-core ERV with recirculation defrost, based on laboratory-controlled experimental data, of supply air temperature and humidity after the single-core ERV unit during normal and defrost operation modes. Then the dual-core ERV model, in compliance with the manufacturing schedules in each unit, is developed based on the single-core correlation-based models. Second, the seasonal energy use for space and ventilation of houses are simulated in TRNSYS program at three arctic locations with heating degree-days (HDD) of 8798, 8888 and 12208, respectively, and Montreal (4356) as the reference. The ERV unit is studied in the Net Zero Energy Housing (NZEH) model and Conventional Northern Housing (CNH) and Northern Sustainable Housing (NSH) northern housing models for the following cases: i) with and without single-core ERV, ii) different threshold temperatures for defrost, iii) preheating and iv) dual-core operation. The single-core ERV unit reduces heating energy use, compared with the case without heat recovery, by 24% (Montreal), 26% (Inuvik), 27% (Kuuujuaq), and 27% (Resolute), respectively. However, the outdoor airflow rate during the defrost is smaller than minimum standard requirements for 1038 hours (19% of time) in Inuvik, 701 hours (13%) in Kuuujuaq, 1320 hours (24%) in Resolute,

and 223 hours (4.7%) in Montreal, respectively. The factory schedules are recommended since the increase of normal operation time leads to a significant increase in the energy use of heating the outdoor air. The preheating defrost is not economical to use in northern Canada because it significantly increases the energy use of heating the outdoor air, compared with the single-core ERV with the recirculating defrost and dual-core ERV units. The dual-core ERV unit removes the frost while continuously supplying the minimum required outdoor air to the indoors. This advantage comes at the cost of minor increases in the heating and fans energy use compared with the single-core ERV unit.

ACKNOWLEDGEMENTS

I would like to express my thanks and gratitude to my supervisor, Dr. Hua Ge and Dr. Radu Zmeureanu. They have provided me with a really interesting research topic in heat/energy recovery ventilator in northern Canada, and this is valuable research for the northern habitants. At the same time, the knowledge and skills I mastered in the project will contribute a lot to my future PhD studies. I am extremely thankful that they received me as a thesis-based student which is the foundation for me to start the research work and also have a profounding impact on my career. I would like to also appreciate their continuous guidance, suggestions and support during the period of revision of my first conference paper and journal paper. Without their diligent revision and guidance, it was impossible for me to present successfully in this good stage.

Special thanks to Li Ma, a master student supervised by Dr. Hua Ge, I appreciate so much for her rich knowledge on the model development and practical materials and good perspective in the northern-Canada-related research, which provided me with a general understanding of what I was working on the model development for the northern residential housing.

My sincere thanks also go to Ying Sun, who currently is a PhD student under the supervision of Dr. Fariborz Haghighat. She supported me at the beginning when I was just involved in using TRNSYS software. She taught me from the beginning and step by step until today I have been professional of using it. I really appreciate all her efforts and time spent on my research. And I send my gratitude to Daniel Baril, a PhD student supervised by Dr. Hua Ge, who is very experiencing on the on-site work. He has given me the experience of what the on-site works look like and never felt tired to share his first-hand experience and thought on the installment of the device he acquired during the works in the

northern communities before. All these good suggestions will benefit a lot for my future onsite testing of the ERV unit.

I would like to say thank you to my friends and colleagues in the office, Dr. Guojie Chen and Dr. Zhongjian Sun as visiting scholars from China, Dr. Lin Wang, Villu Kukk, Cheng Zhang, and Sahar M Sahyoun, for bringing happiness during the school years. They are the people I am willing to get along with, share my happiness or sadness in life and give me responsible help whenever I am in difficulties.

I also would like to acknowledge the financial supports received from The Fonds de recherche du Québec Nature et technologies (FRQNT) [No. 2019-PR-254829] and Gina Cody School of Engineering and Computer Science at Concordia University.

Finally, I want to send my appreciation to my parents, who support me, comfort me and encouraged me during my master's years.

TABLES OF CONTENTS

LIST OF FIGURES	ix
LIST OF TABLES	xi
1. INTRODUCTION	1
1.1. Context and Motivation	1
1.1.1. Northern Canada	1
1.1.2. Housing in Northern Canada	1
1.1.3. Household Ventilation	3
1.2. Research Objectives	5
1.3. Thesis Overview	6
2. LITERATURE REVIEWS	7
2.1. Northern sustainable housing projects	7
2.2. Air-to-air Heat/Energy Exchangers	12
2.3. Frost controls of heat/energy recovery ventilator in arctic climates	15
2.3. Summary of literatures review	22
3. Methodology	24
3.1. Correlation-based models of supply air temperature T_2 in single-core ERV unit during normal and defrost operations	24
3.1.1. Correlation-based model of supply air temperature T_2 during normal operation	26
3.1.2. Correlation-based model of supply air temperature T_2 during defrost operation	27
3.1.3. Verification of correlation-based models of T_2 for normal and defrost operations	28
3.1.4. Prediction of ice mass formation during different normal operation times	30
3.2. Correlation-based models of supply air humidity ratio w_2 in single-core ERV unit during normal and defrost operations	36
3.2.1. Correlation-based models of supply air humidity ratio w_2 during normal operation	37
3.2.2. Correlation-based models of supply air humidity ratio w_2 during defrost operation	38
3.2.3. Verification of correlation-based models of w_2 for normal and defrost operations	39
3.3. Application of correlation-based models of supply air temperature T_2 and humidity ratio w_2 during normal and defrost operation of dual-core ERV	40

3.4. Housing models incorporating with the new ERV correlation-based models in TRNSYS..	44
3.5. Summary.....	48
4. SIMULATION RESULTS AND ANALYSIS	49
4.1. Simulation results of single-core ERV unit: correlation-based models versus Type 667b of TRNSYS program.....	50
4.2. Single-core ERV with the NZEH model	53
4.3. Impact of different operation schedules of the single-core ERV with the NZEH model	64
4.4. Dual-core ERV with the NZEH model.....	65
4.5. Single-core versus dual-core ERV with northern CNH and NSH Models.	67
4.6. Summary.....	69
5. CONCLUSIONS	71
REFERENCES.....	74
APPENDIX A. THE DEVELOPMENTS OF CORRELATION-BASED MODELS.	80
A.1. <i>Supply air temperature T_2 / humidity w_2 during the defrost.</i>	80
A.2. <i>Different proposed operation schedules.</i>	80
APPENDIX B. PARAMETERS AND INPUTS FROM TRNSYS TYPE	84
B.1. <i>Ground coupling – TYPE 1244.</i>	84
B.2. <i>Energy recovery component – Type 667b.</i>	85
APPENDIX. C. SIMULATION RESULTS.....	86
C.1. <i>Single-core ERV in compliance with the different proposed normal/defrost operation schedules in the NZEH house model.</i>	86

LIST OF FIGURES

Figure 1: Simplified airflow diagram of a cross-flow fixed-plate exchanger core [21]	13
Figure 2: the multiple section heat recovery [63].....	19
Figure 3: Schematic representation of dual-core air-to-air energy recovery system [67].	20
Figure 4: The heat exchanger with two connected fix-plate in [66].....	21
Figure 5: Schematic representation of air-to-air energy recovery system.	24
Figure 7: Predicted versus measured [21] supply air temperature at different outdoor air temperature T_1 during normal operation.....	27
Figure 8: Predicted supply air temperature T_2 (Equation 1) based on [21] and [34] during normal operation at outdoor air temperature $T_1 = -20^\circ\text{C}$	29
Figure 9: Predicted supply air temperature T_2 (Equation 2) with the model coefficients derived from [34] during defrost operation at outdoor air temperature $T_1 = -20^\circ\text{C}$	29
Figure 10: The predicted supply air temperature during the defrost operation in terms of the 30 minutes (37 min at -35°C) normal operation.....	32
Figure 11: The predicted supply air temperature T_2 during the defrost operation for the 40 minutes (37 min at -35°C) normal operation.	33
Figure 12: The predicted supply air temperature during the defrost operation in terms of the 50 minutes (37 min at -35°C) normal operation.	33
Figure 13: The comparison between the heat to cold channels from calculations $Q_{channel\ from\ calculations}$ and assumptions $Q_{channel\ from\ assumptions}$ at the proposed operations time	35
Figure 14: Comparison between the predicted accumulated ice mass and measurements [21] for the different operation times.	36
Figure 15: Schematic variation of supply air humidity ratio from single-core ERV unit with time at $T_1 = -20^\circ\text{C}$ and $w_2 = 0.36\text{g/kg}$	37
Figure 16: Predicted versus measured [21] supply air humidity w_2 at outdoor air temperatures $T_1 = -20^\circ\text{C}$ during normal operation.....	38

Figure 17: Predicted supply air humidity w_2 (Equation 11) based on [21] and [34] during normal operation at outdoor air temperature of -20°C	39
Figure 18: Predicted supply air humidity w_2 (Equation 12) based on [34] at outdoor air temperature of -20°C , during defrost operation.	40
Figure 19: Defrost operation schedules of the dual cores ERV unit [70].....	41
Figure 20: Supply air temperature T_2 for the alternative operation of ERV1 and ERV 2.	42
Figure 21: Supply air humidity ratio w_2 for two ERV units with alternating defrost at $T_1 = -20^{\circ}\text{C}$, $w_1 = 0.36$ g/kg.	43
Figure 22: Schematic representation of the NZEB house.....	46
Figure 23: Schematic representation of CNH the NSH houses	47
Figure 24: Air to air Heat Recovery Device Schematic [68].....	51
Figure 25: Comparison of supply air temperature T_2 and sensible heat transfer effectiveness predicted	52
by the correlation-based models versus Type667b of TRNSYS, in the case of NZEH house.	52
Figure 26: Comparison of the exhaust air relative humidity RH_3 and latent heat transfer effectiveness	53
predicted by correlation-based models versus Type667b of TRNSYS, in the case of NZEH.	53
Figure 27: The monthly energy savings rate in three arctic locations (Inuvik, Kuujjuaq and Resolute) and Montreal for the heating months.	61
Figure 28: Indoor humidity ratio with and without single-core ERV unit during the heating season.....	64
Figure 29: Monthly average indoor humidity ratio: comparison of cases without ERV, single-core ERV and dual-cores ERV units for NZEH model.	67
Figure A.1: Predicted versus measured [21] supply air temperature at different outdoor air temperature T_1 during 30 minutes normal operation	81
Figure A.2: Predicted versus measured [21] supply air temperature at different outdoor air temperature T_1 during 40 minutes normal operation	82
Figure A.3: Predicted versus measured [21] supply air temperature at different outdoor air temperature T_1 during 50 minutes normal operation	83

LIST OF TABLES

Table 1: Summary of Northern Sustainable House (NSH) configuration	8
Table 2: The heat transferred to the cold channel during the defrost and ice mass at the manufacturer’s operation time, 3 hours operation in [21] and proposed operation time.....	32
Table 3: Different operation times of the ERV unit.	34
Table 4: Factory set schedule of operation [70].....	41
Table 5: Building envelope features of NZEH in Montreal and CNH [70] and NSH [36] housing models in arctic locations.....	45
Table 7: Information about three selected arctic locations compared with Montreal [74]	49
Table 8: Performance matrix for the evaluation of ERV unit.....	50
Table 9: Energy use for space heating and heating of ventilation air of the case study NZEH model with and without single-core ERV in Montreal.	54
Table 10: Energy use for space heating and heating of ventilation air of the case study NZEH model with and without single-core ERV in Inuvik.....	54
Table 11: Energy use for space heating and heating of ventilation air of the case study NZEH model with and without single-core ERV in Kuujjuaq.	55
Table 12: Energy use for space heating and heating of ventilation air of the case study NZEH model with and without single-core ERV in Resolute.	55
Table 13: Comparison of annual heating energy use and defrost hours under three arctic climates (Inuvik, Kuujjuaq, and Resolute) compared with the cold climate of Montreal, in the case of NZEH model.	56
Table 14: Annual energy use and defrost hours of single-core ERV in the NZEH model in Montreal, comparison of the case of -10°C and -20°C threshold temperature for defrost of single-core ERV unit.	57
Table 15: Annual energy use and defrost hours of single-core ERV in the NZEH model in Inuvik, comparison of the case of -10°C and -20°C threshold temperature for defrost of single-core ERV unit.	58
Table 16: Annual energy use and defrost hours of single-core ERV in the NZEH model in Kuujjuaq, comparison of the case of -10°C and -20°C threshold temperature for defrost of single-core ERV unit.	59
Table 17: Annual energy use and defrost hours of single-core ERV in the NZEH model in Resolute, comparison of the case of -10°C and -20°C threshold temperature for defrost of single-core ERV unit.....	60

Table 18. Annual energy use for heating the outdoor air of NZEH. Comparison of single-core ERV with recirculation defrost, single-core ERV with preheating defrost, and dual-core ERV with recirculation defrost. ..	63
Table 19: Increase of annual energy use for heating ventilation air and decrease of percentage of defrost hours of the NZEH model with the increase of normal operation time.....	65
Table 20: The fan energy use of the single-core ERV in the NZEH model with the increase of normal operation time.....	65
Table 21: Annual energy use for heating the outdoor air and fans: comparison between the single-core ERV and dual-core ERV, in the case of NZEH model.	66
Table 22: Annual energy use for heating the outdoor air: comparison between single-core and dual-core ERV units used in CNH and NSH models.	68
Table 23: Annual space heating energy use and energy use of heating the outdoor air: comparison between dual-core and pre-heating ERV used with CNH and NSH models.	68
Table A.1: Supply air temperature T_2 at the beginning and end of defrost operation [21]......	80
Table A.2: Supply air humidity w_2 at the beginning and end of the defrost operation [21]	80
Table A.3: Supply air temperature T_2 at the beginning and end of the defrost operation.....	81
Table A.4: Supply air temperature T_2 at the beginning and end of the defrost operation corresponding to 40 minutes normal operation.	82
Table A.5: Supply air temperature T_2 at the beginning and end of the defrost operation for the 50 minutes normal operation.....	83
Table C.1: Annual energy use for the space heating and heating the outdoor air and defrost hours in the NZEH house in Montreal with the increase of normal operation time, comparison of the case with the single-core ERV unit and without ERV unit.....	87
Table C.2: Annual energy use for the space heating and heating the outdoor air and defrost hours in the NZEH house in Inuvik with the increase of normal operation time, comparison of the case with the single-core ERV unit and without ERV unit.....	88
Table C.3: Annual energy use for the space heating and heating the outdoor air and defrost hours in the NZEH house in Kuujuaq with the increase of normal operation time, comparison of the case with the single-core ERV unit and without ERV unit.....	89
Table C.4: Annual energy use for the space heating and heating the outdoor air and defrost hours in the NZEH house in Resolute with the increase of normal operation time, comparison of the case with the single-core ERV unit and without ERV unit.....	89

LIST OF SYMBOLS AND UNITS

Name	Symbol	Units
Outdoor air temperature	T_1	°C
Outlet supply air temperature after the ERV unit	T_2	°C
Inlet exhaust air temperature	T_3	°C
Outlet exhaust air temperature	T_4	°C
Supply air temperature after the heating coil	T_5	°C
The water temperature entering the radiant floor tank	T_{in}	°C
The water temperature exiting the radiant floor tank	T_{out}	°C
Outdoor air humidity ratio	w_1	g/kg
Outlet supply air humidity ratio after the ERV unit	w_2	g/kg
Inlet exhaust air humidity ratio	w_3	g/kg
Outlet exhaust air humidity ratio	w_4	g/kg
Supply air humidity ratio after the heating coil	w_5	g/kg
Outdoor relative humidity	RH_1	%
Outlet supply air relative humidity after the ERV unit	RH_2	%
Inlet exhaust air relative humidity	RH_3	%
Outlet exhaust air relative humidity	RH_4	%
Supply air relative humidity after the heating coil	RH_5	%
Inlet supply air mass flow rate	m_1	kg/s
Outlet supply air mass flow rate	m_2	kg/s
Inlet exhaust air mass flow rate	m_3	kg/s
Outlet exhaust air mass flow rate	m_4	kg/s
Water mass flow rate in the radiant heating loops in Zone A1	m_{water}	kg/s
Mass flow rate of the exhaust air recirculating through ERV	m	kg/s
Sensible heat transfer effectiveness of the ERV unit	$\varepsilon_{sensible}$	-
Latent heat transfer effectiveness of the ERV unit	ε_{latent}	-
Space heating demand	$Q_{radiant}$	kWh
Ventilation heating demand with the recirculation defrost	$Q_{recirculation}$	kWh
Ventilation heating demand with the preheating defrost	$Q_{preheating}$	kWh
The volume of the house	V_{house}	m ³
The heat capacity of the water	C	kJ/kg·°C
Specific heat of air	c_p	kJ/kg·°C
Air density	ρ_{air}	kg/m ³
Effective thermal resistance	RSI	m ² K/W
Air changes per hours	ACH	(1/hr)

1. INTRODUCTION

1.1. Context and Motivation

1.1.1. Northern Canada

Northern Canada, colloquially the North, is the vast northernmost region of Canada variously defined by geography and politics. Politically, the term refers to three territories of Canada: Yukon, Northwest Territories and Nunavut. Similarly, *the Far North* (when contrasted to *the North*) may refer to the Canadian Arctic: the portion of Canada that lies north of the Arctic Circle, east of Alaska and west of Greenland. This area covers approximately 40% of Canada's total land area but has less than 1% of Canada's population [1].

There is a limited network of roads connecting these communities, where most of the communities are accessible only by aircraft or seasonal boats. As a result of this limited mobility, the availability of materials and goods is infrequent and typically constrained to the warmer summer months. A by-product of refined oil imported from the southern provinces dominated fuel markets in Northern Canada accounting for the three quarters of all fuel consumption [2].

These fuels are primarily used for heating, transportation, and electricity generation. The high cost of importing energy products along with the method of energy production have let northern Canada become the most expensive regions in end-use energy costs nationally [2]. Even with these regional limitations, the people in Northern Canada are least likely to consider moving from their communities because many rely on their family ties, social support of each other, and traditional activities [3]

1.1.2. Housing in Northern Canada

The largest city in the region, Iqaluit, is located on Baffin Island in Nunavut. The Inuit city is one of the fastest growing communities in Canada with a 8.3% increase in population for the 5 year

period between 2006 and 2011 [4]. The Canadian national average for the same period was 5.9%. Regionally, Arctic Canada has the youngest and fastest growing population in Canada, with a median age in 2009 nearly half that for the rest of Canada and a fertility rate more than double that for the rest of the country [5]. The increase in population, particularly in Iqaluit, has been accompanied by an increase in the demand for housing. During the same period between 2006 and 2011 the percent increase in the number of private dwellings occupied by residents was nearly as twice as the national average [4]. Even though there was a significant increase in the number of private dwelling, the majority of housing in Nunavut is public or government housing. There are approximately 8550 regularly occupied households in Nunavut, of which 51% are public housing, 16% are government staff housing and 33% are privately-owned [6]. At present, Nunavik alone needs 1030 housing units to deal with the shortage of adequate housing [7]. In Nunavut, these numbers are even higher. The housing shortage has led to lengthy waitlists for public housing unit [7].

The need for more housing is not only linked to the increase in population. The increased risk of moisture-related problems, such as mould growth, mildew and frost, due to inadequate temperature control, humidity control and high air leakage in the building envelopes in northern housing are also contributing to the increased need for housing in northern Canada [8].

One major problem facing northern communities is that the National Canadian Building Codes are not sufficient for building in northern climates [9]. Consequently, many houses in northern Canada are lack of good repair and do not meet the current needs of many habitants. Eighteen percentage of the households in the region require major repairs while the average percentage of households requiring major repairs in Canada is only 7.5% [10]. Overcrowding, primarily due to the lack of quality housing, is another significant issue in northern Canada. 31 % of Inuvit live in the region are considered to be overcrowded [11]. The overcrowding contributes to the spread of communicable diseases rarely

occurring in southern Canada, mental health challenges [7]. In the meanwhile, Nunavut has the most serious overcrowding issues among the territories in northern Canada, with 35% of households considered overcrowded [8]. However, this thesis only presents the ventilation of northern housing to ensure the sufficient fresh air supply to occupants rather than addressing the overcrowding issues faced in the northern community.

The high rate of physical and mental illness and suicide rates in northern Canada has been linked to the poor housing condition in the regions as one of many contributing socio-economic factors of these issues [12]. Furthermore, the life expectancy for people living in the territories in northern Canada was nearly ten years lower than the rest of the Canadian population [4]. This is all underlined by the fact that only one in two people in Arctic Canada self-identify as being in very good health [13].

1.1.3. Household Ventilation

Reducing energy consumption in buildings plays an important role in reducing CO₂ emissions since the building sector accounts for 40% of global energy use [14]. New houses with higher airtightness and energy efficiency (e.g., R-2000-certified houses) have been increasingly constructed to reduce heat losses and energy use for heating [15]. For cold climates, the search for optimum mechanical ventilation of residential well-insulated buildings [16] must take into account the minimum requirements for indoor air quality, acceptable thermal comfort of occupants, and the reduction of heating energy use. Since the energy used by ventilation systems without heat/energy recovery is significant in cold climates, it is essential to focus on high energy efficient ventilation with heat/energy recovery systems [17].

The membrane energy exchanger (MEE) is recommended for cold climate applications because of better frost resistance and energy savings compared with other types of heat/energy exchangers [18-

20]. The formation of frost in the energy recovery ventilator (ERV) is the primary operation concern in cold climates. The frost starts inside a cross-flow membrane-based ERV when the outdoor air temperature is between -8°C and -12°C [21]. Due to the reduced cross-sectional area and increased roughness of the accumulated frost, the airflow rate of warm exhaust air through the exchanger is reduced. As a result, the thermal efficiency of the unit diminishes, and the unit can be damaged if no actions are taken to remove the frost [21-23].

Publications [24-32] focused on the development of frost protection techniques and investigation of defrosting methods for the air-to-air heat/energy exchangers in order to maintain high energy recovery effectiveness. Methods such as preheating the outdoor air, bypassing the outdoor airflow, reducing the supply airflow rate, and recirculating warm exhaust air have proven to be effective for the mitigation of frost impacts on heat exchangers [24, 26]. The existing operating procedure for air exchangers in northern Arctic climates typically requires the pre-heating of inlet supply air before entering the heat/energy exchanger in order to reduce the potential for frost formation. This can be costly because as previously mentioned that Northern Canada has the highest end-use energy costs nationally. Conventional defrosting practices, while adequate in more temperate locations in Canada, are not optimal for managing the accumulation of frost in an exchanger in these regions. New frost control methods are needed to overcome the operational limitations in Arctic climates [33]. Compared to the conventional preheating defrost, the recirculation defrost and dual-core operation are recommended to use in northern Canada due to their energy-efficiency and good performance in removing the frost. Although the recirculation defrost has been studied under the laboratory-controlled condition under the cold climates [21, 34], there is only one publication for the seasonal analysis of the recirculation defrost under the extremely cold climates. The dual-core operation [21] has been the focus recently since it can not only remove the frost effectively but provide the continuous fresh air supply,

compared with the recirculation defrost. The dual-core ERV unit has been tested under the laboratory-controlled condition [21], while this dual-core ERV units based on the set-up in [21] need to be simulated further in the northern housing models to assess its long-term thermal performance. The correlation-based models of the ERV unit with the recirculation defrost are needed for the following reasons: 1) the correlation-based models of the single-core ERV unit with the defrost will take into account the frosting and defrosting effect on the supply air temperature and humidity ratio of the HRV/ERV unit, 2) the correlation-based models of the unit are easy to be developed based on the experimental data and can be used as the general equations of the single-core ERV unit in other simulated projects, and 3) the correlation-based models can be validated by the experimental data to ensure the reliability of the developed correlation-based models.

1.2. Research Objectives

The main objective of this paper is the evaluation of the effect of dual-core ERV unit compared with the use of single-core ERV unit on (1) the energy use for pre-heating outdoor air, (2) the energy use by ventilation fans that supply the required ventilation airflow rate during the normal and defrost by recirculation operation modes, and (3) the indoor air humidity.

Since there are no published simulation models of HRV/ERV units under defrost used in arctic houses, this thesis starts with the development of correlation-based models for single-core HRV/ERV unit based on laboratory experiments [21], followed by the validation with experimental data of reference [34]. The models predict the supply air temperature and humidity ratio of the HRV/ERV unit under normal and defrost operations. These models are then used for the simulation of single-core and dual-core ERV units, using the manufacturer's recirculation defrost schedule. The models are connected in TRNSYS program, and used for the assessment of the defrost by recirculation method

when applied to houses at three northern Canadian locations. The results are compared with those obtained from the base case house in Montreal.

The correlation-based model developed in this thesis was only applicable for plate-type ERV, while generic correlation-based models for other types of HRV/ERV, such as MERV or energy wheel, is beyond the scope of this thesis; the approach of model development can be applied to other types of HRV/ERV with experimental data available.

1.3. Thesis Overview

The thesis is structured as follows: **Chapter 2** presents the literatures review on the northern housing projects and defrost strategies at the cold/ arctic climates. **Chapter 3** presents the development and validation of single-core models of supply air temperature and humidity ratio that leave the ERV unit, under normal and defrost operations. The dual-core models that use the defrost schedules are developed based on the single-core models. **Chapter 3** also presents the computer model of a Net Zero Energy House (NZEH), and two northern housing models, all developed by using TRNSYS -18 program along with the newly developed single-core and dual-core ERV models. **Chapter 4** compares the simulated annual heating energy use and defrost hours in the cases of single-core ERV and dual-core ERV units. **Chapter 5** presents the main conclusions of this study.

2. LITERATURE REVIEWS

2.1. Northern sustainable housing projects

The ERV unit deployed in [21] is only assessed under the laboratory-control condition, To test its reaction when operating in the real house, the housing models featured with the energy-efficiency and adequate for the northern climate are expected to be established. However, the existing housing models (etc. NZEH model [35]) are only aiming at the cold climate. Thereby, the new northern housing models need to be established for the simulation of energy performance of energy recovery ventilators (ERV) in the residential house under the arctic (cold) climates. As mentioned previously that the current northern housing in compliance with the National Building Code is not sufficient for the goal to provide the inhabitants with comfort, energy-efficiency and health. Therefore, the update to the sustainable northern house has been the concerns in the northern communities. The Northern Sustainable House (NSH) program funded by Canada Mortgage and Housing Corporation (CMHC) in collaboration with the local housing corporation and construction was announced, the scope of which was to minimize the energy consumption up to 50 % less than that of similar housing specified by the 1997 Model National Energy Code for Houses (MNECH) and simultaneously promote the culture-friendly house in the Northern Canada (CMHC, 2009). The six projects [36-39], located at Dawson City, Yukon And Inuvik, Northwest Territories, respectively are constructed under the NSH project. The configurations of the six sustainable houses are presented in **Table 1**.

Table 1: Summary of Northern Sustainable House (NSH) configuration

	Arviat E/2 Northern Sustainable House (E/2 NSH), Nunavut [37]	Arviat E/2 Northern Sustainable House (E/2 SIP), Nunavut [37]	NHC SIP A and B, Nunavut [37]	The Dawson E/2 Northern Sustainable House, Yukon [38]	The Dawson E/9 Northern Sustainable House, Yukon [39]		The Northern Sustainable House – Inuvik, Northwest Territories [36]	
Building Layout	One story; Three bedrooms and an open-concept living room/ dining room/ kitchen area; bathroom; sewing room; a large cold storage area	One story; Three bedrooms and an open-concept living room/ dining room/ kitchen area; bathroom; sewing room; a large cold storage area		Three bedrooms and an open concept living room/dining room/kitchen area; bathroom	Solar Unit: three bedrooms; an open-concept living room/ dining room/ kitchen area; one bathroom	Flex Unit: two bedrooms; an open-concept living room/ dining room/ kitchen area; one bathroom	Unit A: three bedrooms; an open-concept living room/ dining room/ kitchen area; one bathroom; one storage room	Unit B: two bedrooms; an open-concept living room/ dining room/ kitchen area; one bathroom; one storage room
Building Area	142 m ² footprint and 128 m ² heated floor area	one story 142 m ² footprint and 128 m ² heated floor area	one story 118 m ² heated floor area	one story 141.41 m ² heated floor area	one story 150.3 m ² footprint and 138.8 m ² heated floor area	one story 150.3 m ² footprint and 120.9 m ² heated floor area	one story of duplex 247 m ² footprint and 210 m ² heated floor area	
Occupancy	4 persons	2-3 adults 4 children	2 adults 5-7 children (in each unit)	4 persons	4 persons	4 persons	4 persons in each unite	
Wall	RSI 8.0 (R 46)	RSI 7.8 (R 44) (effective)	RSI 7.0 (R 40) (effective)	RSI 7.2 (R 41)	RSI 8.4 (R 47.5)		RSI 8.8 (R 50)	
Ceiling/Roof	RSI 11.6 (R 66)	RSI 12.7 (R 72) (effective)	RSI 8.8 (R 50) (effective)	RSI 10.6 (R 60)	RSI 14.1 (R 80)		RSI 14.1 (R 80)	
Floor	RSI 9.1 (R 52)	RSI 7.8 (R 44) (effective)	RSI 8.8 (R 50) (effective)	RSI 7.8 (R 44)	RSI 7.8 (R 44)		RSI 9.3 (R 53)	
Window	RSI 0.92 (R 5.2)	RSI 0.92 (R 5.2)	RSI 0.92 (R 5.2)	RSI 0.97 (R 5.5)	RSI 0.97 (R 5.5)		RSI 0.97 (R 5.5) - South RSI 0.74 (R 4.2) - North	
Window Area	9.64 m ² in total South glazing-to-floor ratio: 7.2% (7.57 m ²)	9.64 m ² in total South glazing-to-floor ratio: 7.2% (7.57 m ²)	9.64 m ² in total South glazing-to-floor ratio: 7.2% (7.57 m ²)	17.5 m ² in total South glazing-to-floor ratio: 4.5% (6.4 m ²)	19.4 m ² in total South glazing-to-floor ratio: 6.9% (9.6 m ²)	19 m ² in total South glazing-to-floor ratio: 9.0% (10.9 m ²)	27.7 m ² in total South glazing-to-floor ratio: 5.29% (11.1 m ²)	
Airtightness	E/2 NSH unit pre-drywall: 1.44 ACH at 50 Pa; E/2 NSH unit post-drywall: 1.42 at 50 Pa	E/2 NSH unit pre-drywall: 1.44 ACH at 50 Pa; E/2 NSH unit post-drywall: 1.42 at 50 Pa	E/2 NSH unit pre-drywall: 1.44 ACH at 50 Pa; E/2 NSH unit post-drywall: 1.42 at 50 Pa	1.7 ACH at 50 Pa	0.75 ACH at 50 Pa	0.83 ACH at 50 Pa	2.36 ACH at 50 Pa	2.7 ACH at 50 Pa
HRV	Yes 55% efficiency at -25 °C (-13 °F), and 62.5% efficiency at 0 °C (32 °F), two-mode of airflow rate 20 or 50 L/s (39 or 98	Yes 55% efficiency at -25 °C (-13 °F), and 62.5% efficiency at 0 °C (32 °F), two-mode of airflow rate 20 or 50	Yes 55% efficiency at -25 °C (-13 °F), and 62.5% efficiency at 0 °C (32 °F), two-mode of airflow rate 20 or 40	Yes Inlet air preheated by a hot water coil from the boiler, 45 L/s (95 CFM)	Yes 45 L/s (95 CFM)		Yes Inlet air preheated by a preheat coil. Heat recovery has 89% efficiency at -25 °C (-13 °F), and 83% efficiency at 0 °C (32 °F)	

	CFM). Inlet air preheated by a preheat coil	L/s (39 or 98 CFM). Inlet air preheated by a preheat coil	50 L/s (39 or 98 CFM). Inlet air preheated by a preheat coil				
Space Heating	Oil-fired boiler with hydronic baseboard heater Type: Boiler with 86% efficiency and 98 MBH output capacity	Oil-fired boiler with hydronic baseboard heater Type: Boiler with 86% efficiency and 98 MBH output capacity	Oil-fired boiler with hydronic baseboard heater Type: Boiler with 86% efficiency and 98 MBH output capacity	Oil-fired boiler with hydronic baseboard heater Type: Boiler is 70,000 BTU high-efficiency	Electric baseboard heaters updated from E2 project in Dawson given the problems in E2 1. 500 W baseboard placed under small windows of a living room, entry and bathroom. 2. 1,000 W baseboard placed in the remaining windows of the living room, dining room and bedrooms. 3. 300 W baseboard placed in the laundry room	Natural gas boiler with radiant baseboard Type: Boiler has a maximum output of 141,000 BTU/h with 96% efficiency	
Domestic Hot Water	Oil-fired boiler with tank Type: Boiler with 86% efficiency and 98 MBH output capacity. Hot Water Tank with 151 L (40 US gallon) capacity. Water holding tank with 1,500 L (400 US gallon) capacity	Oil-fired boiler with tank Type: Boiler with 86% efficiency and 98 MBH output capacity. Hot Water Tank with 151 L (40 US gallon) capacity. Water holding tank with 1,500 L (400 US gallon) capacity	Oil-fired boiler with tank Type: Boiler with 86% efficiency and 98 MBH output capacity. Hot Water Tank with 151 L (40 US gallon) capacity. Water holding tank with 1,500 L (400 US gallon) capacity	Electric hot water heater Type: 150-L (40-gallon) capacity	Solar thermal collector and electric water heater with a tank 1. Two 3.0 m ² (32 ft ²) solar thermal collectors, providing two-third of domestic hot water and, connected with the preheat tank with 320 L (85 US gallon) capacity; 2. Electric hot water heater, as the backup heating source, with 150 L (40 US gallon) capacity and 0.9 efficiency.	Electric hot water tank with the 150 L (40 gallon) of capacity and 0.9 of energy efficiency	Flat-plate solar collectors and boiler with tank Type: preheated by 4 flat-plate solar collectors and heated by boiler as the auxiliary heating source. The water tank has 450-L (120 US gallon) storage
Extra Heating Load	Oil-fired boiler (86.5% rated AFUE) External hydronic heating line for sewage tank	Oil-fired boiler (86.5% rated AFUE) External hydronic heating line for sewage tank	Oil-fired boiler (86.5% rated AFUE) Heated crawl space	N/A	N/A	N/A	
Solar System	N/A	N/A	N/A	N/A	1. For the "solar house", two 3.0 m ² (32-ft ²) solar thermal collectors mounted at a 60 degree slope on the south porch roof serving as the domestic hot water source. For the "flex house", conventional house. 2. 6 m ² or 80 m ² PV placed on the south-facing roof will update in the further project when having enough budget	PV: Each unit has 8 224 W photovoltaic modules on the 75 degree angled roof facing south, 3.6 kW totally; Solar collectors: 4 flat-plate solar collectors mounted on the 75 degree angled south-facing roof	

Energy Performance	296 kWh/m² with 43% less energy consumption than MNECH 1997 based on HOT200 results; 538 kWh/m² with 14% less energy consumption than MNECH 1997 with respect to actual billed data 2013/2014; 4 kWh/m² of HRV ventilation	457 kWh/m² with the 15% less energy consumption than E/2 NSH with respect to actual billed data 2013/2014;	490 kWh/m² with the 15% less energy consumption than E/2 NSH with respect to actual billed data 2013/2014; 454 kWh/m² with 21.5% less energy consumption than E/2 NSH with respect to actual billed data 2013/2014;	168 kWh/m² with 54% less energy consumption than MNECH 1997 as predicted; 4.19 kWh/m² of HRV ventilation	121.77 kWh/m² with the 68% energy consumption reduction compared with the MNECH 1997 as predicted; 7.17 kWh/m² of HRV ventilation	145.43 kWh/m² with the 67% energy consumption reduction compared with the MNECH 1997 as predicted; 8.23 kWh/m² of HRV ventilation	225 kWh/m² Consumes about 49% less energy than MNECH 1997 as predicted; 3 kWh/m² of HRV ventilation
---------------------------	--	---	--	---	--	--	---

In the Arviat E/2 Northern Sustainable House (E/2 NSH), 43% of energy consumption reduction (296 kWh/m²) compared with the MNECH 1997, as predicted, is achieved including 1600 kWh (4500 \$) of energy saving in electricity and 1600 Litres (\$1900) of energy saving in oil annually. It could be estimated that two years to pay off \$11000 of cost of building envelope upgrade is needed with the annual saving of \$4500 for electricity and \$1900 for oil. The HRV ventilation consumes 4 kWh/m². An assessment among the four sustainable building projects (E/2 NSH, E/2 SIP, NHC SIP A and NHC SIP B, respectively) is made based on the energy bills. It was revealed that E/2 NSH has the largest energy consumption (538 kWh/m²), compared with the other three projects. The E/2 SIP and NHC SIP A followed behind, 457 kWh/m² and 490 kWh/m², respectively. The NHC SIP B is the most energy-efficient building with 454 kWh/m² of energy consumption. The E/2 NES used 35 percent less electricity than the E/2 NSH, and 35 percent less electricity than the E/2 SIP house and 6 percent more and 1 percent less than the NHC SIP A and B houses respectively.

The predicted consumption in the Dawson E/2 Northern Sustainable House is 168 kWh/m², 54% less than that in MNECH 1997, where it consists of the 91.64 kWh/m² of space heating, the 25.92 kWh/m² of domestic water heating, the 45.56 kWh/m² of appliances/lighting and the 4.19 kWh/m² of mechanical ventilation (HRV ventilation). It is estimated that although it costs an extra \$51300 on the update of the project compared with the MNECH 1997, energy-efficient measurement taken in place could annually save \$3000. Therefore, based on the analysis above, it will take about 17 years to pay off the investment on the energy-efficient upgrade. One year monitoring test is conducted and found that, due to the occupant behaviour and some issues in the space heating, such as the oversized boiler, the actual energy saving is only 25 percent less than the MNECH 1997 far lower than the expected. Additionally, the hydronic space heating system and additional control increase the cost of the project, where the complexity of the hydronic heating system also makes it more challenging to install, maintain and operate.

The Dawson E/9 Northern Sustainable House reduce 68% of energy consumption for the “Solar House” and 67 % for the “Flex House” compared with the MNECH 1997 while the “Solar House” consumes 121.77 kWh/m² totally with 7,17 kWh/m² of HRV ventilation and “Flex House” 145.43 kWh/m² with 8.23 kWh/m² of HRV ventilation. If the predicted 67 percent reduction in annual energy use is achieved, it will take approximately 15 years for “Solar House” to recover the \$52042 of cost on the energy saving feature, whereas for “Flex House”, 9 and half years to recover the \$33291 of cost.

The predicted consumption reduction of the modelled Inuvik NSH was 49 percent (totally 225 kWh/m² of energy consumption including 3 kWh/m² of HRV ventilation) less than the expected performance of the MNECH baseline involving the space heating and domestic hot water consumption. Given the estimated annual energy cost savings of \$6800 per unit, the simple payback would be approximately 16.8 years to recover the cost of the energy-saving measurement at the given cost of energy at the time.

2.2. Air-to-air Heat/Energy Exchangers

There are many types of air-to-air heat/energy exchangers, which are typically divided into two categories: (i) air-to-air heat exchangers only allowing the exchange of sensible heat between two air-streams (ii) air-to-air energy exchangers allowing the exchange of both sensible heat and latent heat (through the transfer of water-vapor) between two airstreams.

Air-to-air heat recovery exchangers and air-to-air energy recovery exchangers are often referred to as HRVs and ERVs, respectively. Where HRV stands for “heat recovery ventilator” and ERV stands for “energy/enthalpy recover ventilator”.

Both heat and energy exchangers are used in residential and commercial buildings for the preheating and/or pre-cooling of supply air. Heat/energy recovery technologies deployed in the passive ventilation and building practice have been extensively reviewed in [40-42]. Heat/energy recovery technologies for applications in zero energy buildings (ZEBs) in cold climate countries,

which is very relevant to the ventilation in northern Canada, are also reviewed in [18], covering the different types of HRV/ERV technologies and system integrations.

There are multiple types of air-to-air heat/energy exchangers [40, 41] (rotary wheel, recovery loop, run around heat exchanger, heat pipe, phase change materials etc.). However, the fixed-plate heat/energy exchangers are most commonly applied in low-rise residential housing. This type of exchanger will be the focus of this thesis.

Fixed-plate heat/energy exchangers (**Figure 1**) consist of a core constructed of laminated fixed-plates. Within these plates are several channels where the supply and exhaust airstreams pass through. The flow of the supply and exhaust air alternates between each plate of the core allowing for the transfer of heat and/or water-vapour between airstreams. The direction of the supply and exhaust air as it passes through the core depends on the orientation of the plates. Cross-flow and counter-flow are the two most common orientation. Cross-flow cores is the focus in this study because they are the most commonly used cores for residential applications.

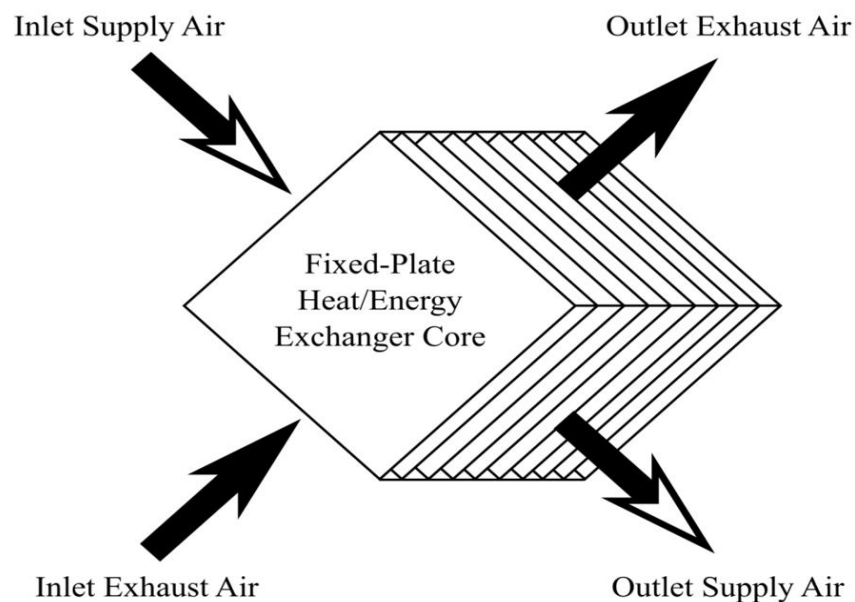


Figure 1: Simplified airflow diagram of a cross-flow fixed-plate exchanger core [21]

The geometry and material of the cores, as one of the most significant parts of the fixed-plate HRV/ERV, varies depending on design constraints and the intended purpose of the air-to-air heat/energy exchanger. Exchanger cores that transfer only sensible heat are typically constructed of corrugated plastic sheets made of polycarbonate. Metal (aluminum or stainless steel) fixed-plate cores are also available, however are more expensive and not as easy to manufacture as the corrugated plastic alternative. Corrugated plastic cores are durable, waterproof and are thermally stable for typical residential ventilation applications.

Vapour-permeable core is typically recommended for hot and humid climates where considerable energy savings are made by using it [43-45]. Conversely, although the cores have been recommended for over 30 years [46], only a few research [21, 34] has been completed for applications in very cold climates. There are many types of vapour permeable materials available, however most of which are proprietary designs owned by the respective manufacturer. Typically, vapour permeable materials are combined with a substrate that is treated to allow for water-vapour transfer. One of the most common types of vapour permeable core materials is polymerized paper. Membrane-based cores are becoming more popular as research in vapour transfer performance progresses. One commonly used membrane core consists of a porous desiccant-loaded polymer substrate that is coated on one surface with a thin layer of water permeable polymer [47]. The porous polymer substrate provides structural rigidity while different types of water permeable polymer coats are applied for different applications. The permeability of the material is highly dependent on the sorption curve affected by the temperature of the material itself. For the membrane exchanger cores, materials with linear sorption curves have better performance under typical conditions [48]. Thinner membranes increase heat and water-vapour transfer between airstreams [49].

Membrane exchanger cores have low containment ratios. The mass transfer of contaminant between the supply and exhaust airstream is independent of the inlet indoor and outdoor air temperatures and relative humidity. Air leakage due to core construction, not through the membrane

material itself, is the primary concern regarding the mass transfer of contaminants [50]. The implementation of membrane materials for heat and moisture recovery has been extensively reviewed in [51] including the progress of heat and mass transfer analysis, exchanger structures and membrane design.

2.3. Frost controls of heat/energy recovery ventilator in arctic climates

Compared with the other frosting controls such as the preheating supply air, bypassing supply air and reducing supply air, the defrost by exhaust air recirculation was found to be the most appropriate for extremely cold climates [52]. When frost formation within the exchanger core reaches a critical level, the unit stops the supply of outside air, and the exhaust air is recirculated through the exchanger core to melt the accumulated frost.

HRV/ERV units with the recirculation defrost were investigated through laboratory-based experiments or field tests [21,27, 34, 53, 54]. The defrost duration of the ERV unit [27, 53, 54], the thermal performance (i.e., supply air temperature and humidity, and sensible and latent heat transfer effectiveness) [21, 27, 34], and the effect on fan power input [21, 34] have been studied. The different defrost durations have been proposed depending on the outdoor air temperature [27, 53, 54]. It was recommended to run a 4–5 min defrosting cycle after every 40 min of working time. The main limitations of [27] are a lack of empirical correlations for frosting and no experimental data to validate the results. Fisk found that 6–26% of the heat exchanger operational time was used for defrosting under supply air temperatures of -12 °C to -20 °C. However, Ninomura & Bhargava [53] underlined that frost protection should be the onset for outside temperatures below -4°C, and the evaluation of defrost cycle duration for the recirculation method showed that the defrost cycle duration account for around 13% of entire operation hours of the unit for outside temperature below -4°C and 22% for temperatures below -25°C. Ninomura & Bhargava [53] also suggested that the defrosting time should not exceed 20% of the total operational time. The fan speed increased during the recirculation defrost cycle [19, 21], which enhanced the frosting melting. The defrost duration

of the unit was identified depending on the variation of outdoor air temperature. The HRV/ERV with recirculation were only tested in the house in Iqaluit during two months, February and March 2019 [55].

Since the long-term test of HRV/ERV units with the recirculation defrost throughout the entire year is costly and time-consuming, computer simulation could be an effective alternative approach to investigate the annual or seasonal performance of such units. There is only one publication [52] about the numerical seasonal analysis of HRV/ERV unit with the recirculation defrost for extremely cold climates, that is locations with heating degree-days (18°C) greater than 7000.

Several simulation studies evaluated the heat and mass transfer characteristics when the HRV/ERV unit was incorporated into the ventilation system of a house, and the energy savings potential [56- 61]. Firstly, the energy efficiency of the ventilation heat recovery system significantly increases in cold climatic conditions [61]. Recently, Rasouli et al. have studied the effects of the ERVs on the annual cooling and heating energy consumption under the climatic condition from hot to cold. The ERV achieves 40% of energy saving for annual heating, depending on the climate and system effectiveness [59, 61], which is 5% higher than the energy saved with HRV, In the cold Finnish climate investigated in [60], the efficiency of heat recovery has a significant effect on energy consumption. Total annual specific energy consumption at 80% temperature efficiency was 11% (18.1 kWh/m^2) less than at 60% efficiency. Rafati Nasr, Kassai, Ge & Simonson [56] deduced the weighted coefficient equations for describing the performance of ERV in different areas in the range from the extremely cold zone to the warm zone in China. The major contributions of this study on ERV incorporated into the house are the following four findings: (i) the higher enthalpy efficiency the heat/energy recovery unit has, the more energy can be saved, but the two appear not to be linear relation, which is also proven in [60], (ii) The more difference between indoor and outdoor enthalpy, the higher percentage of energy is saved, which is also observed in ERV in [61]. the same findings are also revealed in [58] that ERV has better performance in

Shanghai (warm and humid) than that of Beijing (cold and dry) under the winter conditions. (iii) It implies that improving fan efficiency plays a key role for the energy saving, (iv) saved energy percentage increases with the increase of fresh air change rate. However, a great increase in total energy consumption was also seen which is attributed to the increase of fresh air change rate. The house, installed with HRV, in the cold climate [60] showed the opposite results on the sensitivity of the energy consumption to the ventilation rate with only 4.6% of total energy consumption decrease when the air change rate dropped from 0.85 to 0.69 ACH. It can finally be concluded [57] that ERV is better for the special buildings that need more fresh air. The effect of ERV on annual cooling and heating energy consumption was investigated by conducting TRNSYS simulations [61]. The comparison of the heat/energy saving potentials through the use of heat/energy exchangers with different defrosting methods (preheating and bypassing) was made in three cold cities (Chicago, Anchorage and Saskatoon) where each of these cities represents a different type of cold region in terms of outdoor temperature and humidity level. Two findings were generalized [56] when the frosting effect are ignored. Firstly, there are almost the same saving percentages for each type of heat/energy exchanger in different cities. Second, the heat/energy exchangers can recover most heat/energy from the exhaust stale airflow in the range from 54–66%. Overall, it can be underlined in [56-61] that although the thermal performance of ERV/HRV has been widely investigated, the frosting effect, as the concern of the HRV/ERV operation in the cold climate, is ignored. This deficiency of investigation will influence the accuracy of the HRV/ERV investigation regarding its thermal characteristic and energy performance under cold climatic condition. Some conclusions from the review of these publications, which did not consider the frost/defrost operation, are summarized here: (1) The heat recovery effectiveness is significantly greater in cold climates [61]; (2) the energy savings depend on the efficiency of the HRV/ERV unit, indoor/outdoor condition, fan efficiency, and the air ventilation rate [57-61]; and (3) the difference of energy savings by using preheating or bypassing defrost in different cold climates are insignificant [56-61], because the frost and defrost operation of HRV/ERV units were not taken into consideration.

Other simulation models [19, 26, 62] addressed the case of frost and defrost in the HRV/ERV units. The recirculation defrosts in a housing model [19] led to the reduction of heating energy use. In the meanwhile, when the HRV unit had the sensible heat transfer effectiveness of 65%, its normal operation duration was 19 hours before stopped by the frost thickness criteria [26]; while the operation duration was shorter at lower effectiveness, for example, 16 hours at 50%.

The recirculation defrost strategy used in a single-core HRV/ERV unit has the negative outcome of insufficient ventilation airflow rate, leading to poor indoor air quality. To overcome this issue, a dual-core ERV unit with two heat exchangers has been proposed to address the frost protection and continuous supply of the required outdoor airflow rate into the house. There are two types of dual-core HRV/ERV units: dual cores in parallel [16, 63, 64, 67] and dual cores in series [65, 66]. References [6, 63, 64, 67] investigated the thermal performance and energy savings potential of dual-core HRV/ERV units in parallel.

Kragh, Rose, Nielsen & Svendsen [63] demonstrated an example of dual-core HRV in parallel (**Figure 2**) consisting of two identical side-by-side polycarbonate heat exchangers allowing for cyclic defrosting while continuous ventilation. In position 1, the damper is adjusted to allow 90% of the inlet exhaust air to exchange with the 100% supply airstream in HRV 1. Defrosting for the previously active section can be completed by having the remaining 10% of the warm exhaust air into HRV 2 exchanged with the other inactive section of HRV2. In position 2, the damper flips allowing 10% inlet exhaust airflow to the HRV1 and 90% supply airflow to the HRV2. The 10% inlet exhaust warm air is used to defrost in HRV1 being affected by the frost in the previous phase while 100% of the supply air absorbs the heat from the 90% of the exhaust air in HRV2. The alternating between position 1 and position2 stayed happened as the unit operates under frosting conditions.

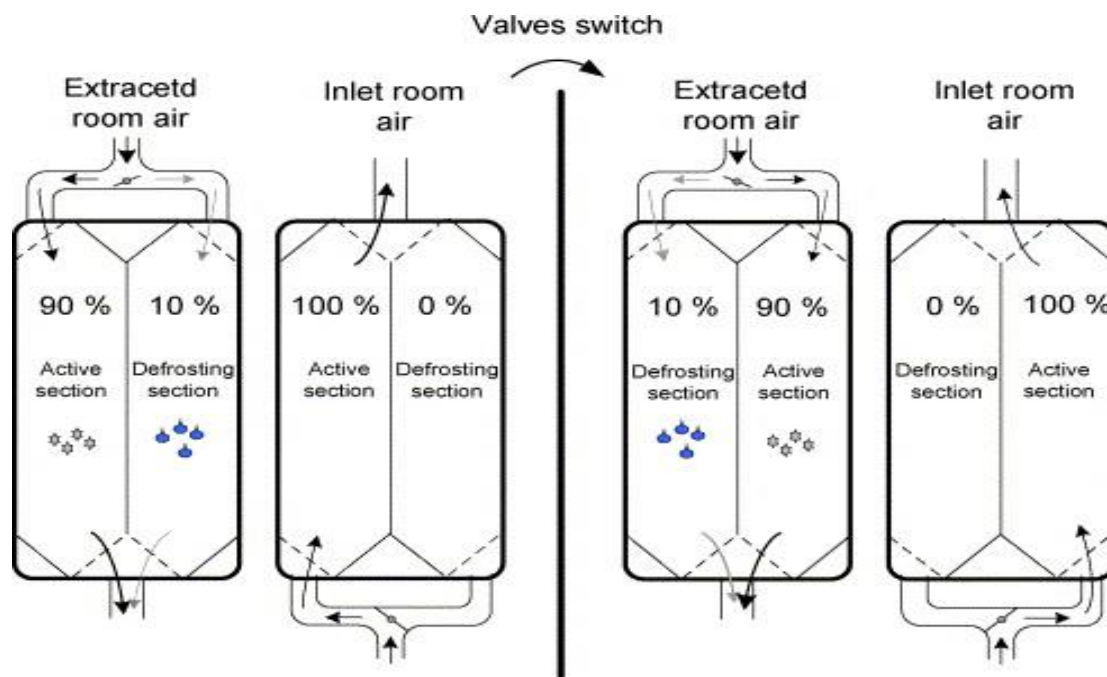


Figure 2: the multiple section heat recovery [63].

The long-term test of the system under the frost condition is carried out under the laboratory set-up, and the experimental condition in this test is set as -6°C of outdoor air temperature, 20°C of indoor air temperature and 55-60% of indoor relative humidity. The temperature efficiency of 88% was achieved. Given the limitation of the appliance, the airflow rate was adjusted to lower than the expected (25l/s) in order to maintain the interior condition. Under the setup conditions, the system could run continuously for 4 days not affected by frost. However, it was noted that 60 minutes of the section switch time for defrosting were not efficient to remove all of the frosts in the unit. Consequently, the uncontrolled frost would finally result in the system failure on both sections if the inlet supply temperature further decreased. The researchers concluded that the volume of the exchanger could be a barrier and hence the focus of the optimization of the exchanger in the future will be on the minimization of the volume of the exchanger. Moreover, they clarified that there was a possibility to control the section switch time as the function of the inlet temperature and variable diversion of inlet exhaust air for defrosting.

Another example of dual-core ERV in parallel is presented in **Figure 3** [67]. When core A is in defrosting mode, core B (active core) is in normal operation for the heat exchange between the

exhaust air and supply air. As the amount of frost is accumulated in core B (active core) to be the critical level, a set of the dampers switch and distribute the outlet supply airflow into core A which has been defrosted previously. This process is repeated periodically to manage the frost.

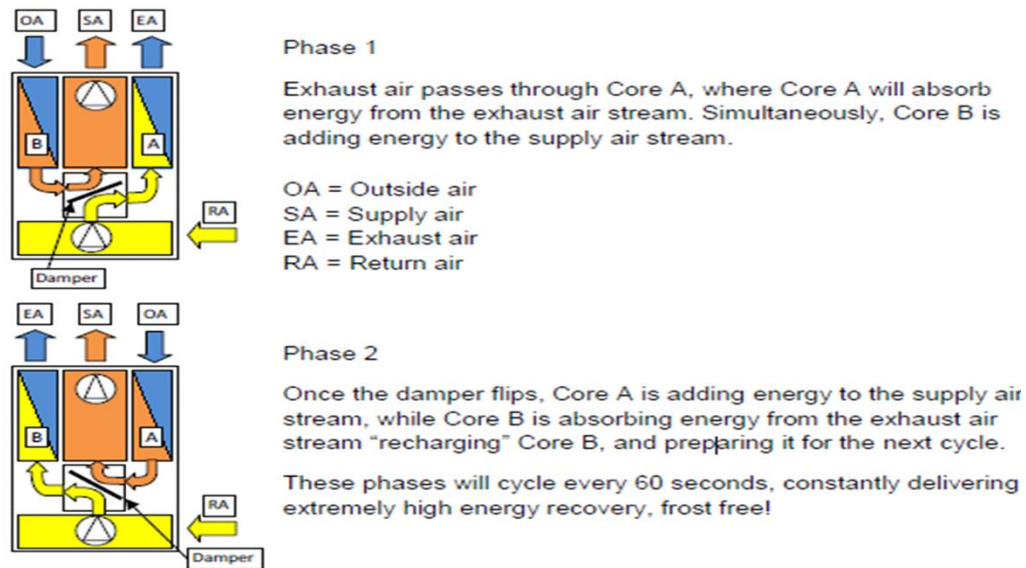


Figure 3: Schematic representation of dual-core air-to-air energy recovery system [67].

Firstly, a laboratory-controlled testing of the proposed dual-core ERV was made at different outdoor temperature from 0 °C to -35 °C in twin houses, one of which was used as the reference house coupled with single-core ERV [67]. Compared with the single-core HRV/ERV unit, the dual-cores HRV/ERV tested in a house of Cambridge Bay (Nunavut) could operate at extremely cold climate of -40°C of outdoor temperature without the performance reduction. The hourly average supply air temperature leaving the dual-cores HRV/ERV unit could be increased by around 2.6 °C higher than the single-core HRV/ERV unit [64]. The implementation of the dual-core unit in parallel [64] could save up to 5% more energy for pre-heating outdoor air and operation of fans than the single-core unit.

Kragh, Rose & Svendsen [65] proposed the heat exchanger with two connected fix-plate in series as shown in **Figure 4**. The system is comprised of two fixed-flat heat exchangers in series. In position 1, frost is accumulated in exchanger 1 due to the cold outdoor air. After a while, a series of

dampers are adjusted to allow airflow to pass through the channels in the opposite direction. the exchanger 1 is in the defrost mode, which means that the accumulated frost in the previous stage is defrosted by the warm exhaust air. On the contrary, frost starts to form in the exchanger 2. The process demonstrated before is repeated periodically in the whole operation when the defrost is required.

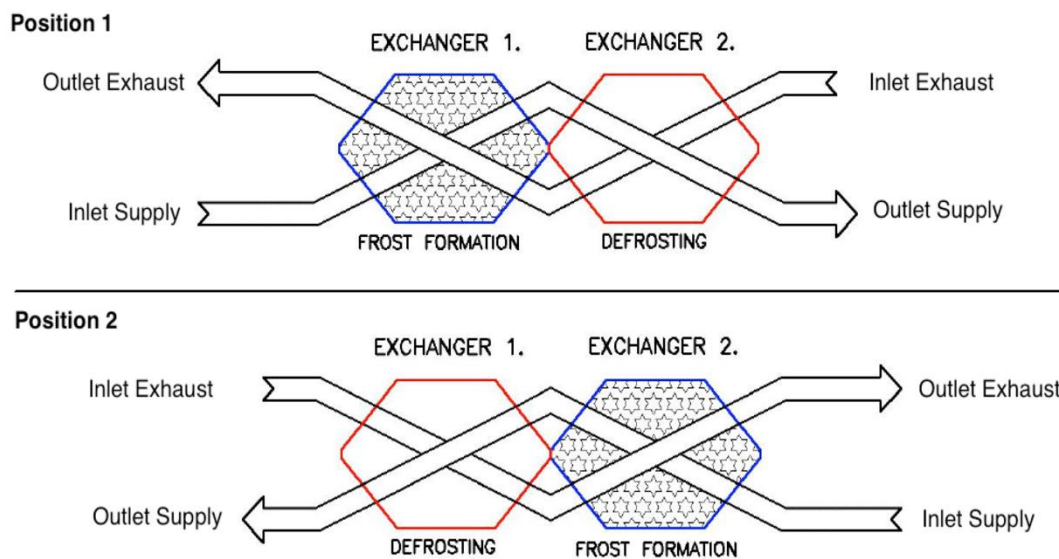


Figure 4: The heat exchanger with two connected fix-plate in [66].

Vladykova, Rode, Kragh & Kotol [66] discussed the performance of dual-core HRV units in series installed in Sisimiut, Greenland for five years. The sensible heat transfer effectiveness of the system was expected to be around 90%. However, because of the poor damper control, the sensible heat transfer effectiveness was only between 55% and 80%, and the annual average of 60%. Furthermore, the application of dual-core HRV in series lead to a small amount of energy that was required for after-heating of supply air to the room. Based on the five years field measurements, it was recommended that the dampers should be activated only when the defrost is required instead of using the pre-determined set time. The dual-core HRV might be blockage of the dual-core HRV due to the formation of ice might be identified when the pressure loss in the exhaust part of the heat exchanger is increased in the period with outdoor temperatures below $-10\text{ }^{\circ}\text{C}$. To prevent heat loss

from the system, it was recommended to install the heat recovery system under the conditioned room.

Beattie, Fazio, Zmeureanu & Rao [21] concluded based on laboratory measurements that the dual-core ERV unit can adequately manage the removal of frost in both cores while providing a continuous supply of required outdoor air. There was no reduction of the time-average supply outdoor airflow rate, as witnessed in the case of single-core ERV.

Due to its advantages of high heat transfer effectiveness and continuous and constant supply of outdoor air, the dual-core ERV unit is recommended [64] for extremely cold climate over the single-core ERV unit with the recirculation defrost. However, there are very limited publications [48] about simulated studies of the dual-core ERV unit. The dual-core ERV unit in [21] was only tested for a short period in the laboratory-controlled experiment. A large difference was observed between measurements during the defrost operation and numerical studies of dual-core HRV [62].

Thereby, long-term simulation studies of the dual-core ERV unit installed in the ventilation system of houses in extremely cold climates are needed.

2.3. Summary of literatures review

The literatures review in this section primarily presented the northern sustainable projects and new frosting controls in the arctic climates.

The current housing stocks in northern Canada are not suitable for the northern communities and conditions. The overcrowding, faulty design and inadequate temperature and relative humidity controls has made the building costly to maintain/operate, uncomfortable, and, in some cases, threatening to the health of occupants. Therefore, the Northern Sustainable House program was announced to achieve the 50% of energy saving compared with the conventional northern house in compliance with the Model National Energy Code for Houses (MNECH). Six northern projects built within the NSH program in Dawson City, Yukon And Inuvik, Northwest Territories, showed

good outcomes in terms of the energy savings, electricity savings and pay-back for the investment on renovation.

The air-to-air heat/energy recovery ventilator plays a key role in the sufficient fresh air supply and ventilation energy savings in the northern airtight houses. The membrane-based energy recovery ventilators are recognized as the most adequate for the cold (arctic) climates. However, the primary concerns for the HRV/ERV operation in the cold (arctic) climates are the frost formation leading to the blockage and further deterioration on the thermal performance of the unit if no proper defrosting is undertaken. The conventional preheating of the supply air is costly due to the high price of end-use oil, and thereby two new frosting controls (recirculation and dual-core, respectively) are introduced. The recirculating exhaust air is seen as the most adequate for the cold (arctic) climates, but the fresh air supply is interrupted in the period of defrost, which will lead to the insufficient fresh air supply and deterioration on the indoor air quality (IAQ). Therefore, the two types of dual-core HER/ERV, either in parallel or series configurations, are introduced to not only protect the unit from the risk of frosting but provide sufficient fresh air. Compared to the single-core HRV/ERV, the utilization of dual-core HRV/ERV leads to higher supply air temperature, significant energy savings and more tolerance to the extremely cold climate.

Based on the research gap identified of rare publications focusing on the single-core ERV under the extremely cold climate, this thesis focus on the development of correlation-based models of the single-core ERV. Then, the single-core ERV models are applied in the development of the dual-core ERV modes. Then, the ERV models are integrated into the two developed northern housing models and one referenced NZEH housing model of TRNSYS to predict the heating energy consumption and defrost hours of ERV in the case with single-core unit with recirculating and preheating, versus dual-core unit.

3. Methodology

The thesis shortly introduces the steps for achieving the goal: (i) the development of correlation-based models, from experimental data, for normal and defrost operations, of supply air temperature and humidity ratio leaving the single-core ERV unit, (ii) the application of correlation-based models to the analysis of dual-core ERV unit, (iii) the simulation of energy use in houses at different Canadian northern locations, and (iv) the assessment of performance of ERV on the heating energy use of those case study houses.

3.1. Correlation-based models of supply air temperature T_2 in single-core ERV unit during normal and defrost operations

The supply air temperature T_2 leaving the ERV unit varies with the outdoor air temperature $T_1 = T_{outdoor}$, and the operation mode (**Figure 5**). The supply air temperature T_5 that enters the house is kept constant at $T_5 = T_{indoor}$, being controlled by the heating coil (HC), installed after the ERV unit. P is the total air pressure at inlets and outlets of the ERV unit.

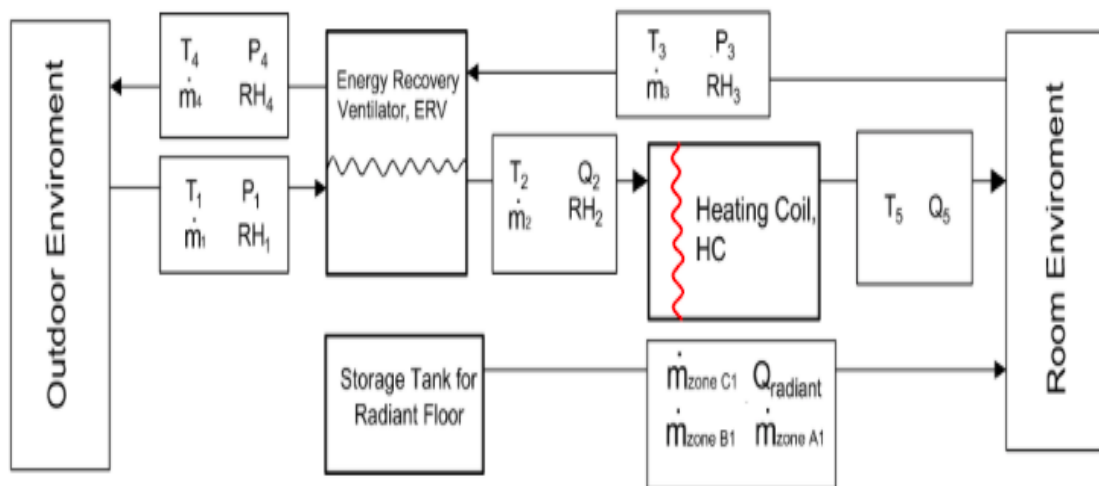


Figure 5: Schematic representation of air-to-air energy recovery system.

The electric power input to the heating coil (HC), used to increase the temperature of the outdoor air stream from T_2 to T_5 , is added to the space heating energy use, for the estimation of total energy use of the house during the heating season. The normal operation of the ERV unit, as set by the manufacturer, takes 22-25 minutes and it is followed by the defrost operation of 7-10 minutes (**Figure 6**). After the defrost operation, the cycle of normal and defrost operations are repeated.

The effect of frost accumulation in the ERV core and subsequent defrost on the supply air temperature T_2 and humidity ratio w_2 is not considered in the energy recovery component (Type 667b) of the TRNSYS program [68], which is used in this study for the simulation of energy efficiency of such a system. Therefore, correlation-based models of supply air temperature T_2 and humidity ratio w_2 during the normal operation and defrost operations, respectively, are developed from measurements of [21]

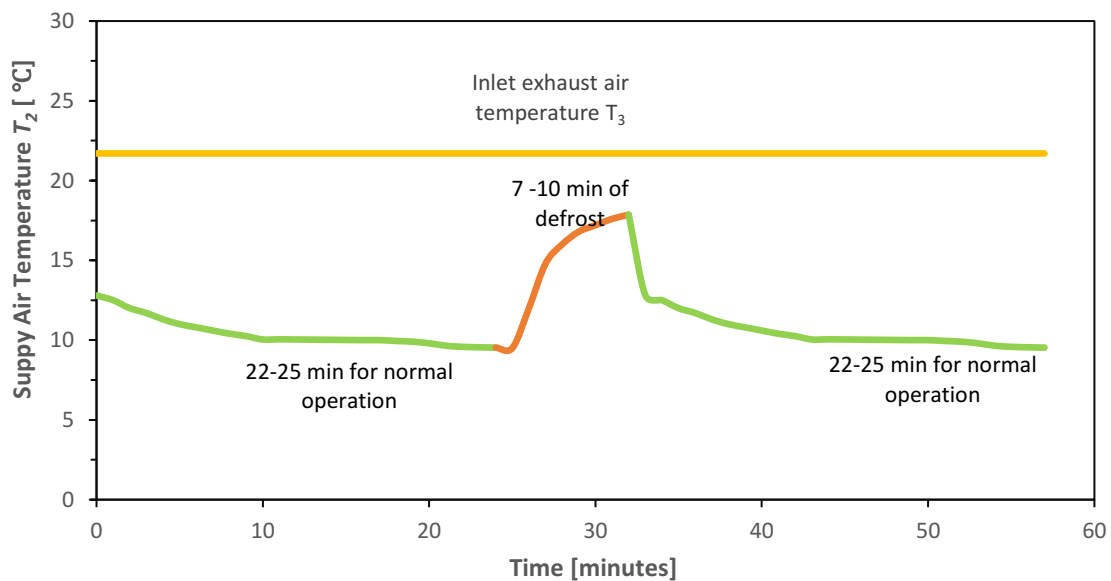


Figure 6: Schematic variation of supply air temperature T_2 in single-core ERV unit with time at outdoor temperature $T_1 = -20^\circ\text{C}$

3.1.1. Correlation-based model of supply air temperature T_2 during normal operation

The correlation-based model (**Equation 1**), which considers the effect of frost on the heat exchange process, if the frost occurs in the exhaust air channel, is developed and inserted in TRNSYS model of house by using an equation box.

$$T_2 = T_{2(t=0)} \cdot [A \cdot T_1 - B \cdot (1 - e^{-Ct}) + D] \quad (1)$$

Where $T_{2(t=0)}$ is the air temperature leaving the heat recovery unit at the beginning of the normal operation in APPENDIX A, which is equal to air temperature at the end of the defrost operation in APPENDIX A. T_1 is the outdoor air temperature entering the ERV unit, and t is the time during normal operation [minute].

The coefficients are determined by curve fitting of measured data from [21]: $A=0.006$, $B=0.328$, $C=0.097$, and $D=1.102$ at $T_l = -10^\circ\text{C}$, -15°C , -20°C and -25°C ; and $A=0.004$, $B=0.559$, $C=0.18$ and $D=1.126$ at $T_l = -35^\circ\text{C}$. The predicted supply air temperature T_2 (**Figure 7**) agrees well with the measurements; the coefficient of determination R^2 has values between 0.96 and 0.99.

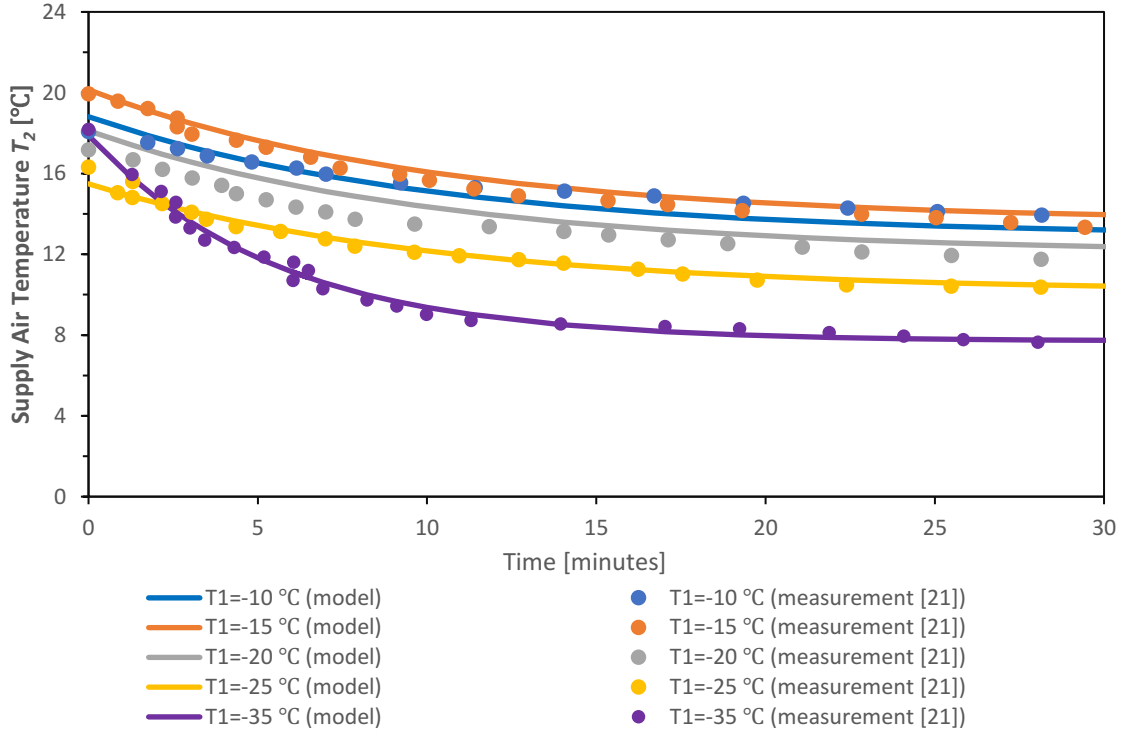


Figure 7: Predicted versus measured [21] supply air temperature at different outdoor air temperature T_1 during normal operation

3.1.2. Correlation-based model of supply air temperature T_2 during defrost operation

When defrost is required, the supply air inlet damper and exhaust air outlet damper are closed. The exhaust airflow is recirculated from the exhaust air inlet to supply air outlet. The supply air temperature T_2 during the defrost operation is modelled with **Equation 2**, which is developed based on the pattern of variation presented in [34], and using measurements of [21].

$$T_2 = AT_1 + T_{2(t=0)} + (T_{2(t=7 \text{ or } 10)} - T_{2(t=0)}) \cdot (1 - e^{-Bt}) \quad (2)$$

with:

$$T_{2(t=0)} = 0.2497 T_1 + 17.124 \quad (3)$$

Where $T_{2(t=0)}$ is the supply air temperature [°C] at the beginning of defrost in APPENDIX A; A and B are coefficients determined by curve fitting of measured data from [21]: A = 0.0, and B

= 0.533; T_2 ($t=7$ or 10) is the supply air temperature at the end of defrost; and t is the time during defrost [minute].

3.1.3. Verification of correlation-based models of T_2 for normal and defrost operations

The results of correlation-based models of T_2 are compared with measurements from [34], which were obtained at a time step of one minute under laboratory-controlled conditions. The comparison is carried out at the same initial supply air temperature and outdoor air temperature of $T_1 = -20^\circ\text{C}$ (**Figure 7** for normal operation, and **Figure 8** for defrost operation).

First, the model of normal operation (**Equation 1**) with the coefficients determined from [21] fitted well the measurements of [34] except the first 10 minutes of normal operation (**Figure 8**), which may be attributed to the different physical characteristics of ERV units used by [21] and [34]. Second, to reduce such a difference, the coefficients of model of normal operation (**Equation 1**) are identified using data points of T_2 extracted from the graphs presented in [34] as follows: $A=0$, $B=0.265$, $C=0.28$ and $D=0.965$. For the defrost operation, the model coefficients (**Equation 2**) derived from [34] are: $A=0$ and $B=0.525$.

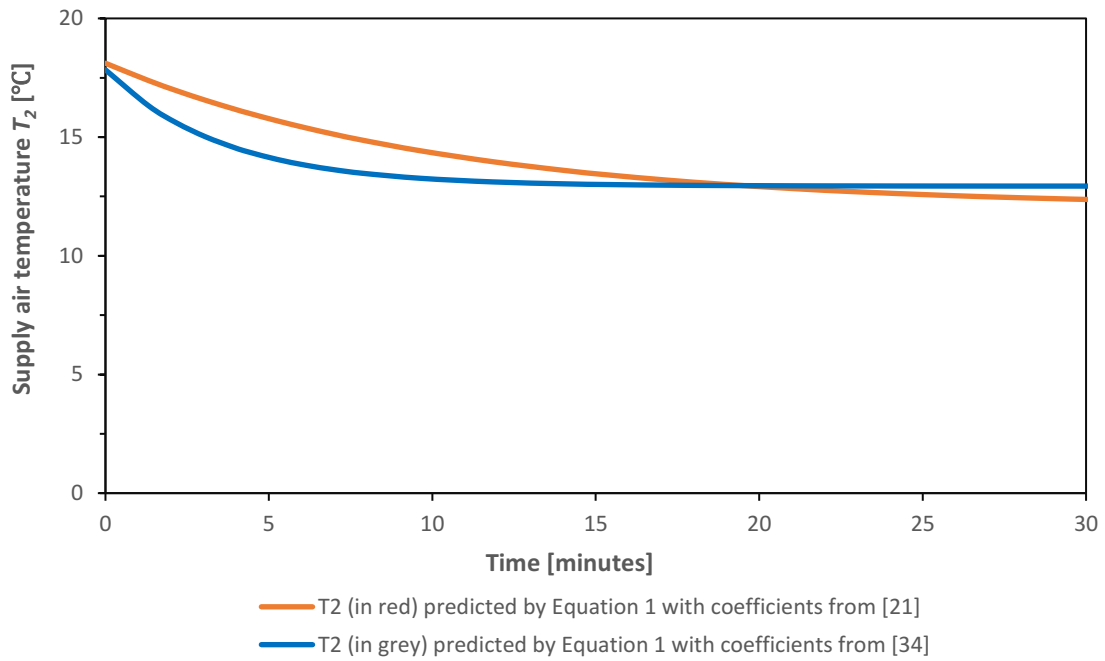


Figure 8: Predicted supply air temperature T_2 (**Equation 1**) based on [21] and [34] during normal operation at outdoor air temperature $T_1 = -20^\circ\text{C}$.

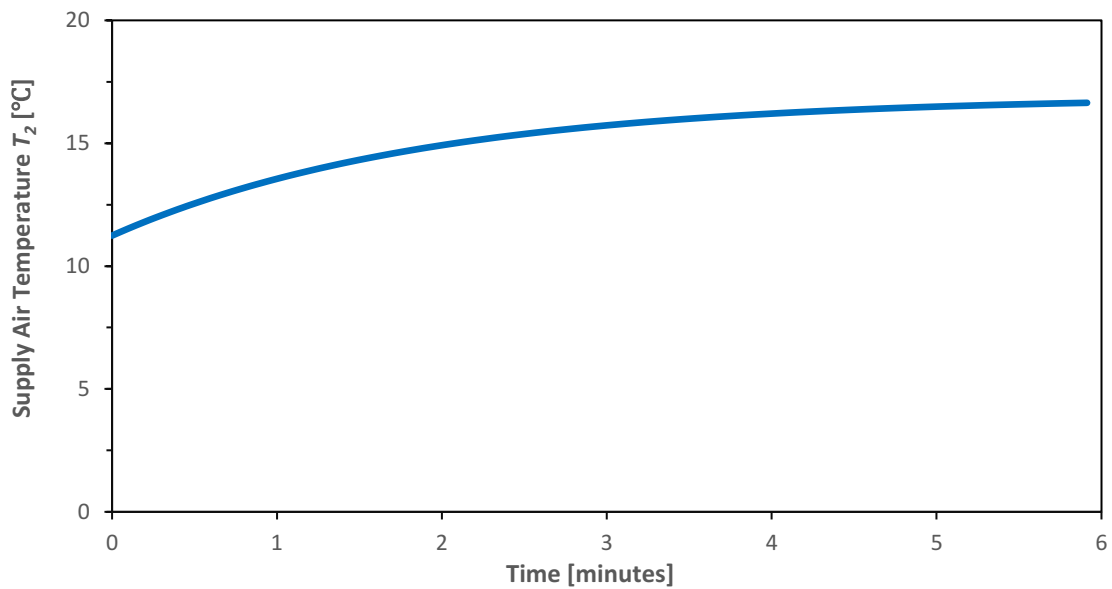


Figure 9: Predicted supply air temperature T_2 (**Equation 2**) with the model coefficients derived from [34] during defrost operation at outdoor air temperature $T_1 = -20^\circ\text{C}$.

3.1.4. Prediction of ice mass formation during different normal operation times

With longer normal operation time of the ERV unit at low outdoor air temperature T_1 , more ice is accumulated, and the supply air temperature T_2 is lower. On the other hand, longer normal operation time reduces the defrost frequency and the risk of reduced outdoor supply air flow rate. The impact of longer normal operation time, i.e., 30, 40, and 50 minutes, different from the manufacturer's set schedule, on the development of ice mass is presented in this section.

For the manufacturer's operation time (MO), the heat transferred to the cold channel during the defrost (**Table 2**) $Q_{ice\ in\ MO}$ is determined using **Equation 4**. For the proposed operation time (PO), it is assumed that $Q_{channel}$ is constant over the 50 minutes of the proposed operation time (PO) and the $Q_{channel}$ calculated according to MO is used in the proposed operations. The ice mass measured by [21] in the manufacturing operation time $m_{ice\ in\ MO}$ (**Table 21**) is modified to convert measurements from 3 hours (**Table 21**) to the manufacturer's operation time implemented here with the assumption that the ice growth is linear over time according to [69]. For the proposed operation time (PO), the heat transferred to the ice is calculated using **Equation 6** and then the predicted ice mass is determined by **Equation 7**. 334 is the melting heat of ice, kJ/kg. The models of predicting the ice mass for other operation times are supposed to meet the two principles as follows: 1) the linear relationship of predicted ice mass should be seen among proposed operations; 2) the predicted ice mass at proposed operations (PO) should be larger than the ice mass calculated from the measurements in [21] accordingly, indicating the fully melting of ice by the recirculation defrost and 3) the predicted supply air temperature (**Equation 2**) at proposed operations in **Figures 10 - 12** should be in compliance with the variation pattern of supply air temperature during the defrost in [34].

Manufacturer's operation (MO):

$$Q_{channel\ in\ MO} = Q_{warm\ exhaust\ air} - Q_{ice\ in\ MO} \quad (4)$$

With:

$$Q_{ice\ in\ MO} = m_{ice\ in\ MO} \cdot 334 \quad (5)$$

Proposed operation (PO):

$$Q_{ice} = Q_{warm\ exhaust\ air} - Q_{channel\ from\ assumption} \quad (6)$$

$$m_{ice} = \frac{Q_{ice}}{334} \quad (7)$$

With:

$$Q_{warm\ exhaust\ air} = \int_0^t C \cdot m \cdot (T_3 - T_2) \Delta t \quad (8)$$

Where:

$m_{ice\ in\ MO}$ = the measured ice mass inside the ERV unit (**Table 2**) at the manufacturing operation, kg

$Q_{channel\ from\ assumption}$ = the heat transferred to the cold channel in the proposed operations (PO), assumed to be equivalent to $Q_{channel\ in\ MO}$ in **Table 2**, kWh

t = the defrost time varying with the different operation time, s

T_2 = supply air temperature during the defrost for the different operation time presented in **Figures 10 - 12**.

C = the heat capacity of the warm exhaust air recirculating through the ERV tunnel, KJ/(kg· °C)

m = the mass flow rate of the exhausted air recirculating through the ERV unit, kg/s

Table 2: The heat transferred to the cold channel during the defrost and ice mass at the manufacturer’s operation time, 3 hours operation in [21] and proposed operation time

Outdoor air temperature [°C]	Heat transferred to the cold channel $Q_{channel\ in\ MO}$ [kWh]	Ice mass [kg]				
		3 hours [21]	Manufacturer’s operation	30	40	50
-10	107.17	0.26	0.036	0.043	0.057	0.072
-15	106.474	0.32	0.044	0.053	0.071	0.089
-20	114.316	0.4	0.056	0.067	0.089	0.111
-25	108.48	0.5	0.104	0.125	0.167	0.208
-35	135.87	0.46	0.192	0.23	0.307	0.383

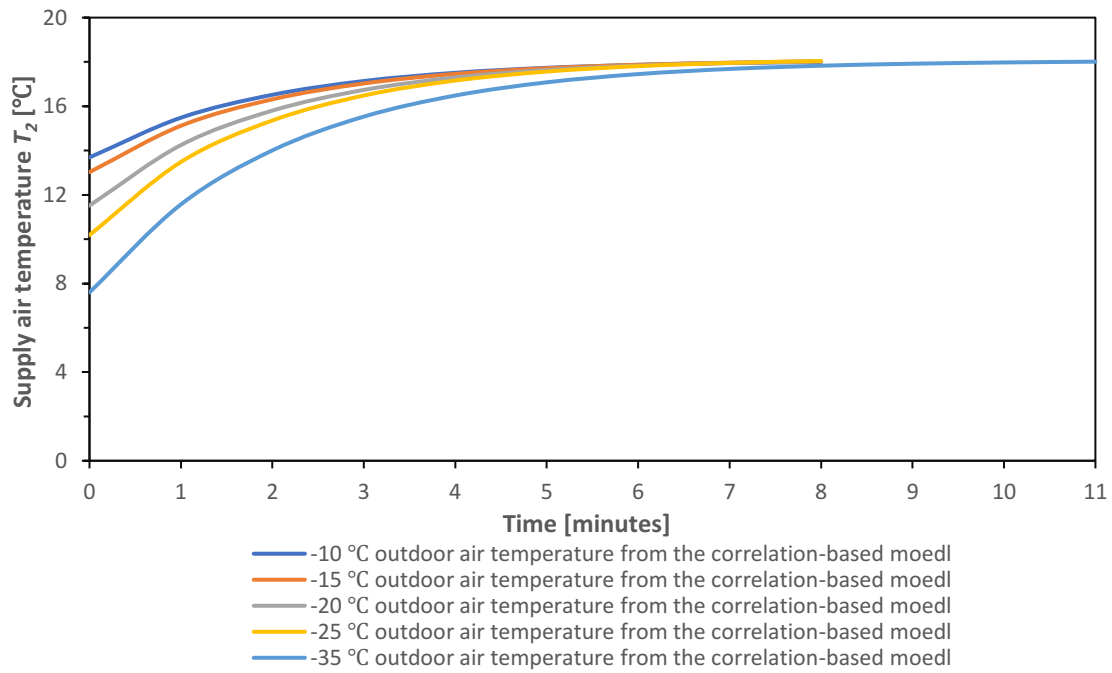


Figure 10: The predicted supply air temperature during the defrost operation in terms of the 30 minutes (37 min at -35°C) normal operation.

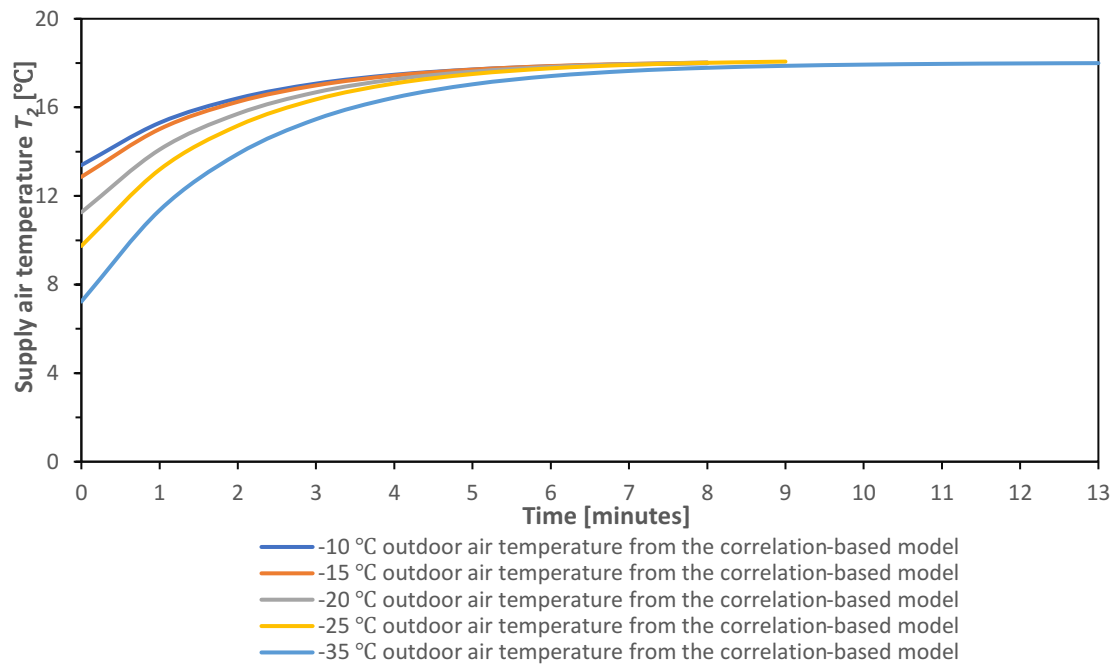


Figure 11: The predicted supply air temperature T_2 during the defrost operation for the 40 minutes (37 min at -35°C) normal operation.

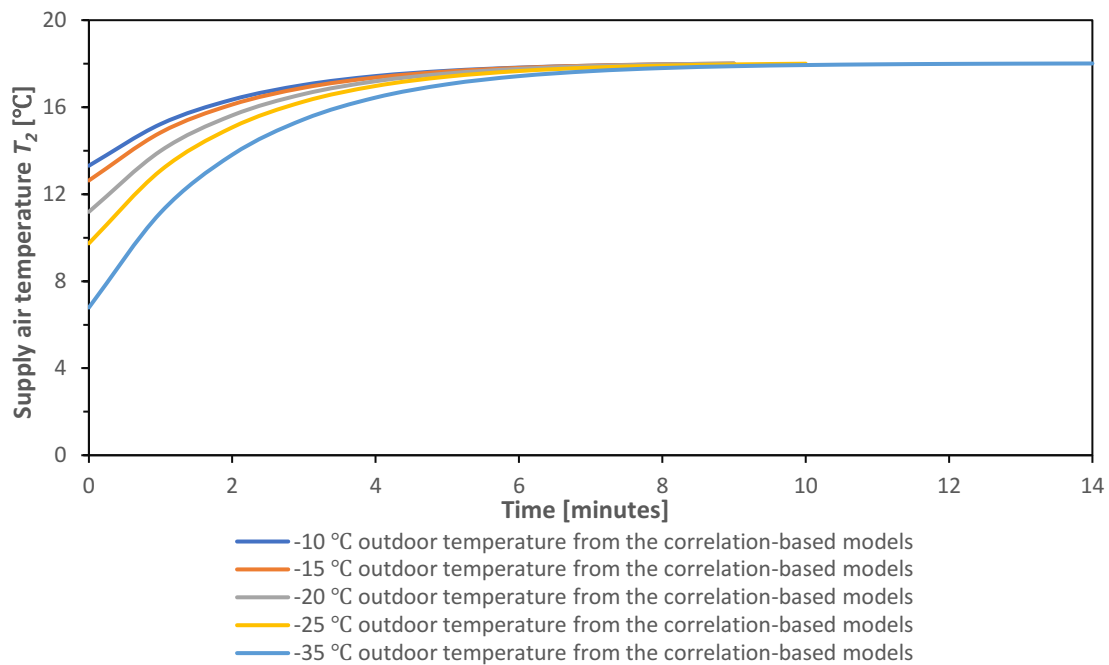


Figure 12: The predicted supply air temperature during the defrost operation in terms of the 50 minutes (37 min at -35°C) normal operation.

The defrost duration required for different operation times, from 30 min to 50 min, is evaluated (**Table 3**) based on the models of ice mass.

Table 3: Different operation times of the ERV unit.

Normal operation time [min]	Defrost operation time [min]	outdoor air temperature
30	8	$25\text{ °C} < T_l < -10\text{ °C}$
	11	$T_l < -25\text{ °C}$
40	8	$-20\text{ °C} < T_l < -10\text{ °C}$
	9	$-20\text{ °C} < T_l < -25\text{ °C}$
	13	$T_l < -25\text{ °C}$
50	9	$-20\text{ °C} < T_l < -10\text{ °C}$
	10	$-20\text{ °C} < T_l < -25\text{ °C}$
	14	$T_l < -25\text{ °C}$

To verify the assumption of the same value of heat to the cold channel used over 50 minutes, the heat to the cold channel in proposed operations time by using the ice mass converted from the measurements in [21] are calculated (**Equation 9**) to compare with the value of assumed heat to the cold channel under the same condition (**Figure 13**). The CV-RSME between calculated heat to the cold channel and assumed one in proposed operation time (PO) is 22% at -10 °C, 23% at -15 °C, 22% at -20 °C, 20% at -25 °C and 25% at -35 °C, respectively.

$$Q_{channel\ from\ calculation} = Q_{warm\ exhaust\ air} - Q_{ice\ from\ measurements} \quad (9)$$

$$Q_{ice\ from\ measurements} = m_{ice\ from\ measurements} * 334 \quad (10)$$

Where:

$m_{ice\ from\ measurements}$ = ice mass inside the ERV unit (**Table 2**) at the proposed operation time converted from the measurements in [21], kg

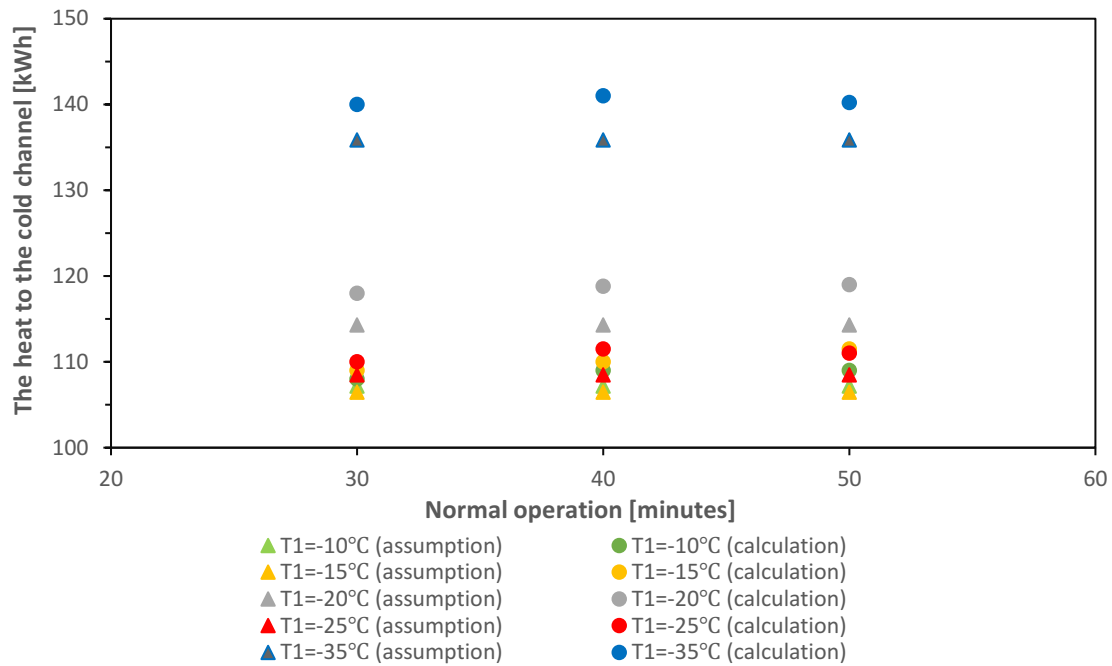


Figure 13: The comparison between the heat to cold channels from calculations $Q_{channel}$ from calculations and assumptions $Q_{channel}$ from assumptions at the proposed operations time

The accumulated ice mass during the normal operation time, as predicted by correlation models, is compared with the measured ice mass [21] (**Figure 14**). The CV-RSME between predicted ice mass and measurements is 71% at -10 °C, 55% at -15 °C, 29% at -20 °C, 17% at -25 °C and 22% at -35 °C, respectively.

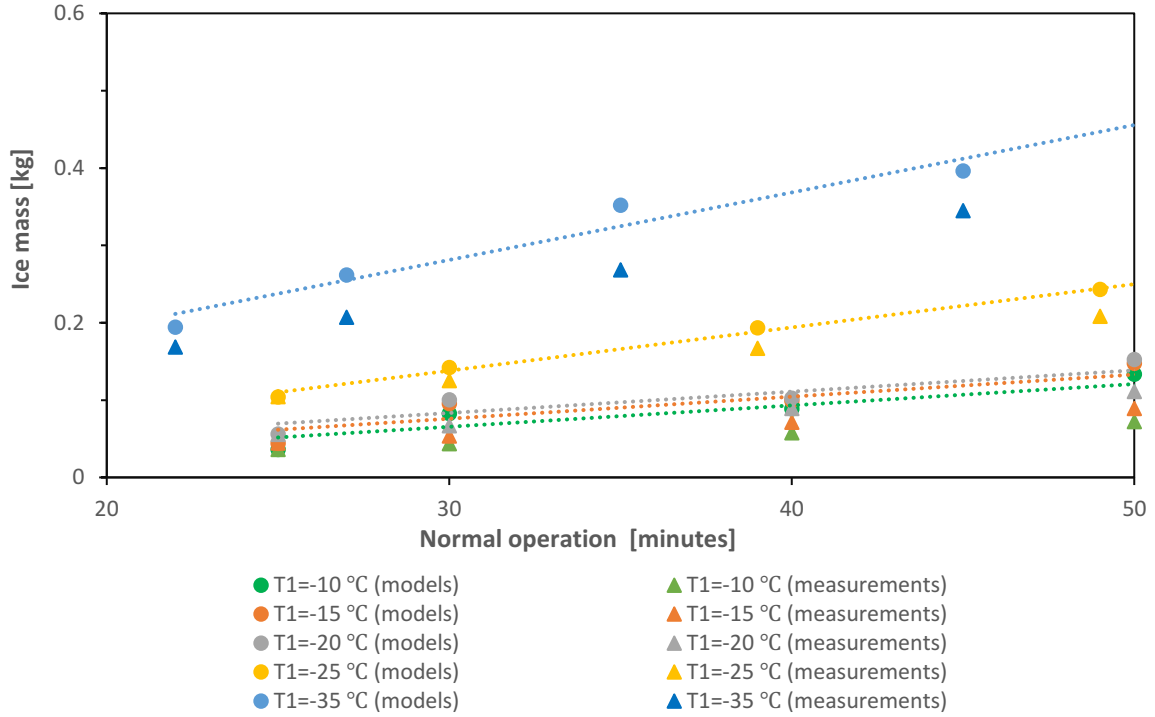


Figure 14: Comparison between the predicted accumulated ice mass and measurements [21] for the different operation times.

3.2. Correlation-based models of supply air humidity ratio w_2 in single-core ERV unit during normal and defrost operations

Correlation-based models of supply air humidity w_2 during the normal operation and defrost operation, respectively, are developed from measurements of [21]. The supply air humidity ratio w_2 , leaving the ERV unit, decreases quickly during the first 5 minutes of normal operation, from about 6 g/kg to 3 g/kg, and then remains constant (**Figure 15** for outdoor air temperature of -20°C). During the 7-10 min defrost operation, the supply air humidity ratio w_2 increases due to the ice melting. After the defrost operation, the normal cycle is repeated (**Figure 15**), where w_2 rapidly decreases in the first 10 minutes.

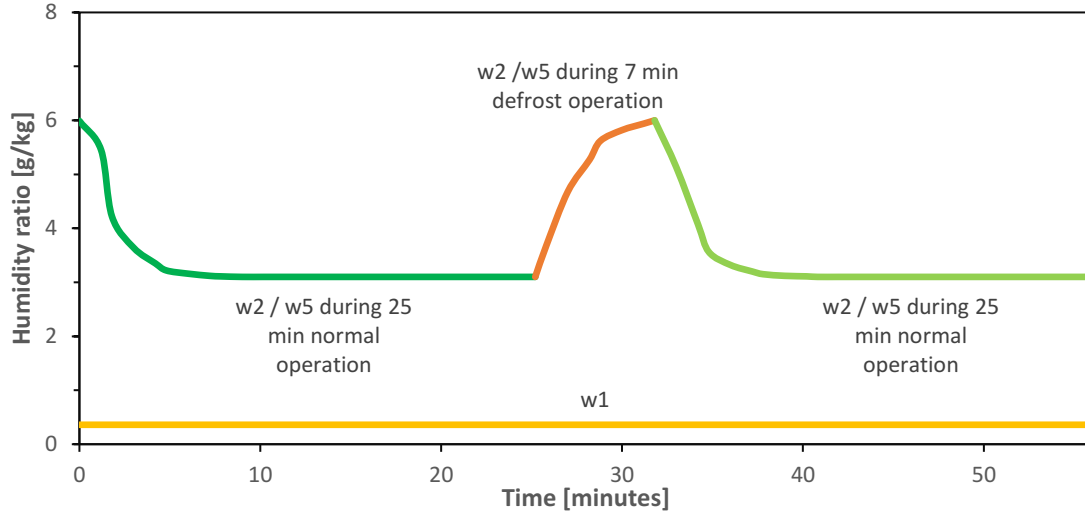


Figure 15: Schematic variation of supply air humidity ratio from single-core ERV unit with time at

$$T_1 = -20^\circ\text{C} \text{ and } w_2 = 0.36\text{g/kg.}$$

3.2.1. Correlation-based models of supply air humidity ratio w_2 during normal operation

Equation 11 predicts the supply air humidity w_2 , in terms of time t and outdoor air temperature T_1 from measurements [21]. **Figure 16** shows the results at outdoor air temperature of -20°C .

$$w_2 = w_{2(t=0)} \cdot [A \cdot T_1 - B \cdot (1 - e^{-Ct}) + D] \quad (11)$$

Where $w_{2(t=0)}$ is the supply air humidity leaving the ERV unit at the beginning of the normal operation in APPENDIX A, which is equal to supply air humidity w_2 at the end of the defrost operation in APPENDIX A; t is the time during the normal operation, from 0 to 25 minutes. The coefficients are determined by curve fitting measured data [21]: $A=0$, $B=0.448$, $C=0.738$, and $D=0.96$ at $T_1 = -10^\circ\text{C}$, -15°C , -20°C and -25°C ; and $A=0.005$, $B=0.47$, $C=0.363$ and $D=1.16$ at $T_1 = -35^\circ\text{C}$.

Predicted supply air humidity w_2 (**Figure 16**) is in good agreement with measurements [21]; the coefficient of determination R^2 is between 0.96 and 0.99.

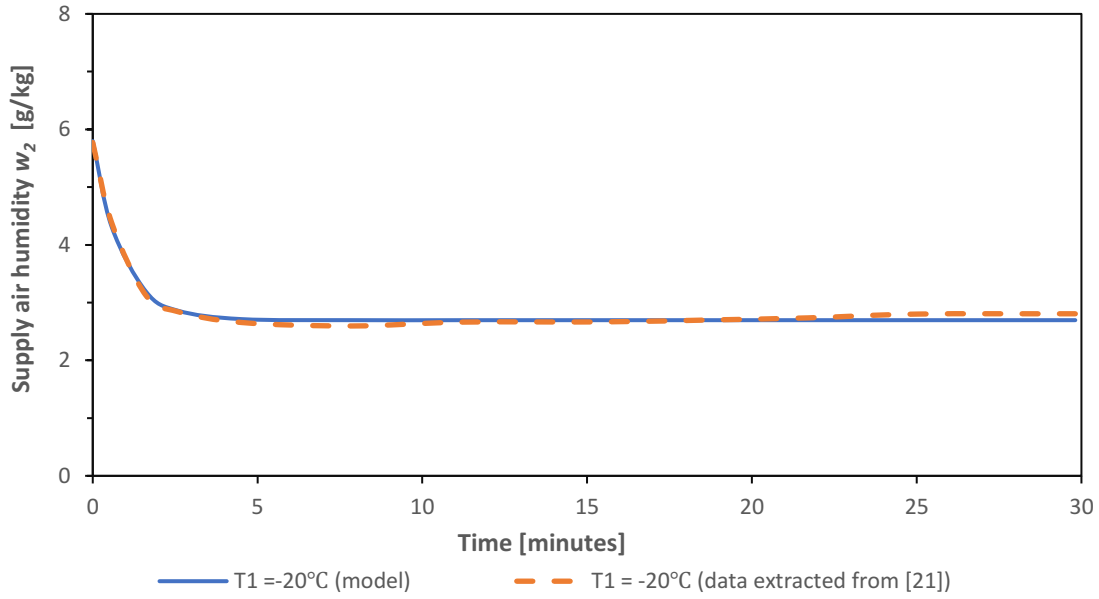


Figure 16: Predicted versus measured [21] supply air humidity w_2 at outdoor air temperatures $T_1 = -20$ °C during normal operation

3.2.2. Correlation-based models of supply air humidity ratio w_2 during defrost operation

The supply air humidity w_2 during the defrosting operation [21] is modelled with **Equation 12**, which represents the general pattern of variation as presented in [34].

$$w_2 = AT_1 + w_2(t=0) + (w_2(t=7 \text{ or } 10) - w_2(t=0)) \cdot (1 - e^{-Bt}) \quad (12)$$

with:

$$w_2(t=0) = 0.0409 T_1 + 4.2133 \quad (13)$$

Where $w_2(t=0)$ is the supply air humidity ratio at the beginning of defrost in APPENDIX A; $A = 0.0$, and $B = 0.539$ are determined from curve fitting of measured data [21]; $w_2(t=7 \text{ or } 10)$ is the supply air humidity ratio w_2 at the end of defrost at APPENDIX A; and t is the time during defrost [minute].

3.2.3. Verification of correlation-based models of w_2 for normal and defrost operations

The correlation-based models of w_2 for the normal and defrost operations are compared with measurements from [34], as presented in section 2.1.3 for air temperature T_2 . **Figures 17 and 18** present the comparison under the same initial supply air temperature, and with the outdoor air temperature $T_1 = -20^\circ\text{C}$.

First, the model of normal operation (**Equation 11**) with the coefficients determined from [21] fitted well the measurements of [34] except the first 10 minutes of normal operation (**Figure 17**), which may be attributed to the different physical characteristics of ERV units used by [21] and [34]. Second, to reduce such a difference, the coefficients of model of normal operation (**Equation 11**) are identified using data points of T_2 extracted from the graphs presented in [34] as follows: $A=0.002$, $B=0.537$, $C=1.136$ and $D=1.04$. For the defrost operation, the model coefficients (**Equation 12**) derived from [34] are: $A=0$ and $B=0.525$.

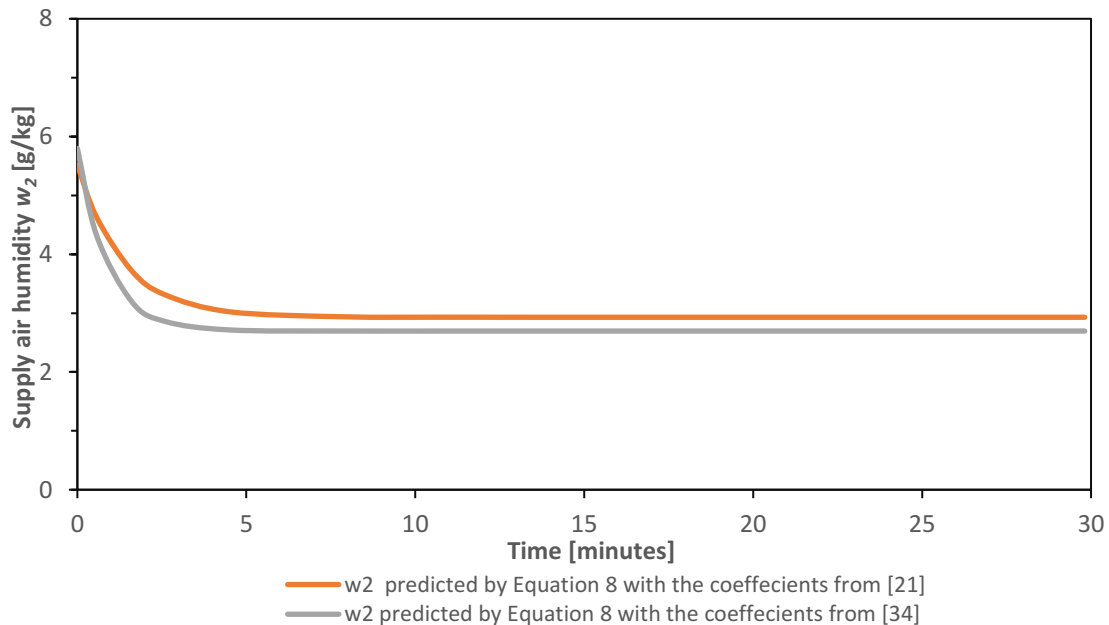


Figure 17: Predicted supply air humidity w_2 (**Equation 11**) based on [21] and [34] during normal operation at outdoor air temperature of -20°C .

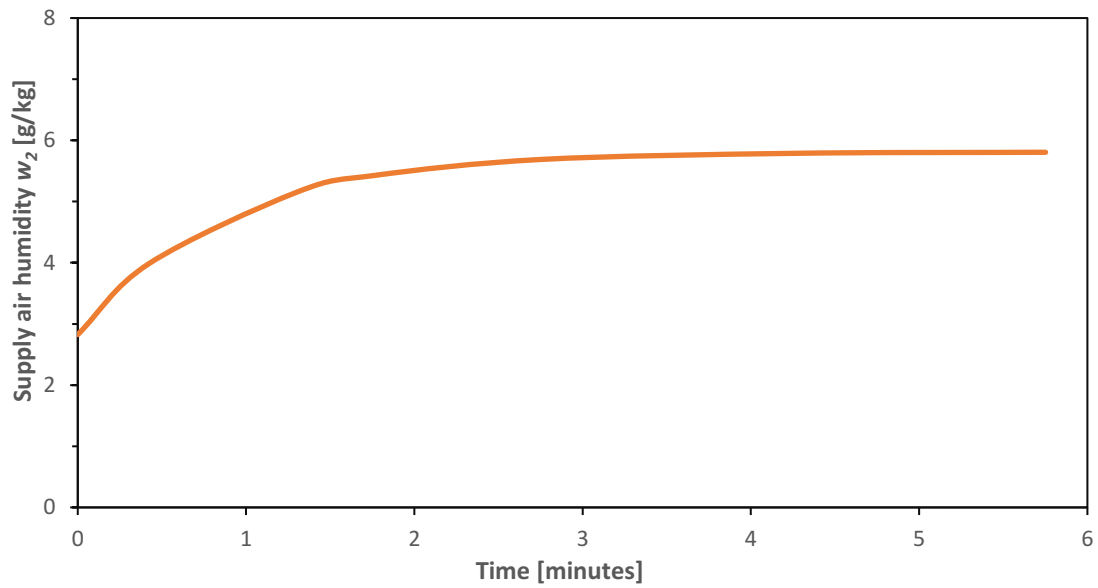


Figure 18: Predicted supply air humidity w_2 (Equation 12) based on [34] at outdoor air temperature of -20°C , during defrost operation.

3.3. Application of correlation-based models of supply air temperature T_2 and humidity ratio w_2 during normal and defrost operation of dual-core ERV

To overcome the insufficient ventilation and performance reduction of the conventional single-core ERV unit, the dual-core ERV unit (composed of ERV 1 and ERV 2) operating in parallel is proposed in [21]. The alternative dual-core operation ensures the continuous supply of the required outdoor airflow rate. According to the manufacturer's specifications, the defrost operation is required only when the outdoor air temperature is lower than -10°C .

The dual-core ERV unit operates in three modes: the normal operation mode (heat/moisture exchange), the defrost mode and the standby mode. The duration of each mode is controlled by the factory set schedule (Table 4) for the ERV unit.

Table 4: Factory set schedule of operation [70]

Outside temperature	Defrost duration [min]/Normal operation duration [min]
Warmer than -10 °C	No defrost
$-10 < T_i < -27$ °C	7/25
$T_i < -27$ °C	10/22

The two cores run alternatively, that is when one core is in normal operation mode, supplying 100% of outdoor air, the other core is either in defrost operation mode and recirculates air from the house, or is in standby mode (**Figure 19**). The correlation-based models of the supply air temperature T_2 (**Equations 1 and 2**) and supply air humidity ratio w_2 (**Equation 11 and 12**) for the normal and defrost operations, respectively, are applied in each mode of ERV operation.

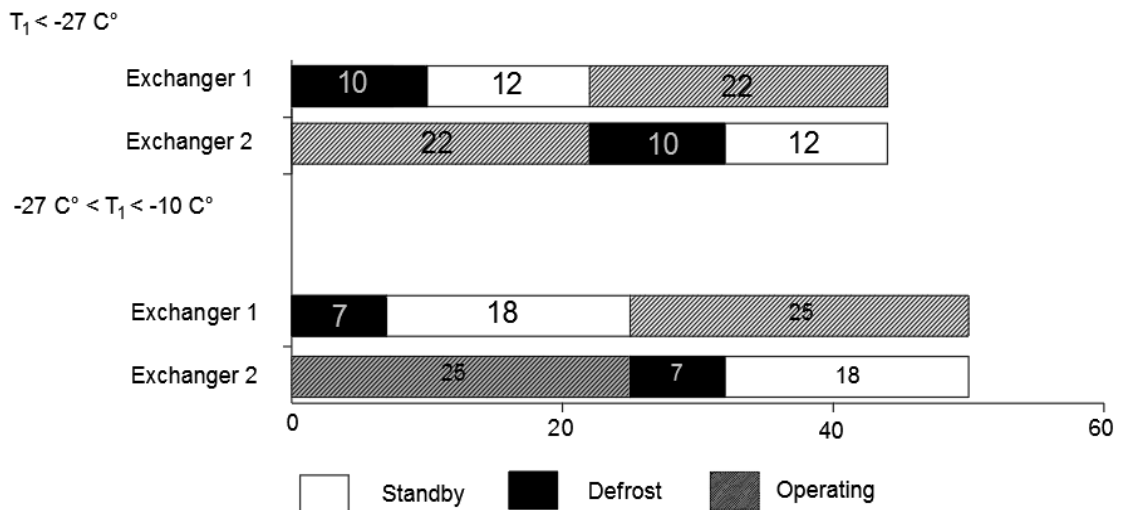


Figure 19: Defrost operation schedules of the dual cores ERV unit [70].

During the defrost recirculation, the supply outdoor air stream in ERV 1 mixes with the recirculated air stream, and then passes through the heating coil (HC). Blue curve shows the variation of T_2 and humidity w_2 after ERV 1 (**Figures 20 and 21**), and red curve shows the variation of T_2 and humidity w_2 after ERV 2 (**Figures 20 and 21**). During standby operation ERV units do not supply air.

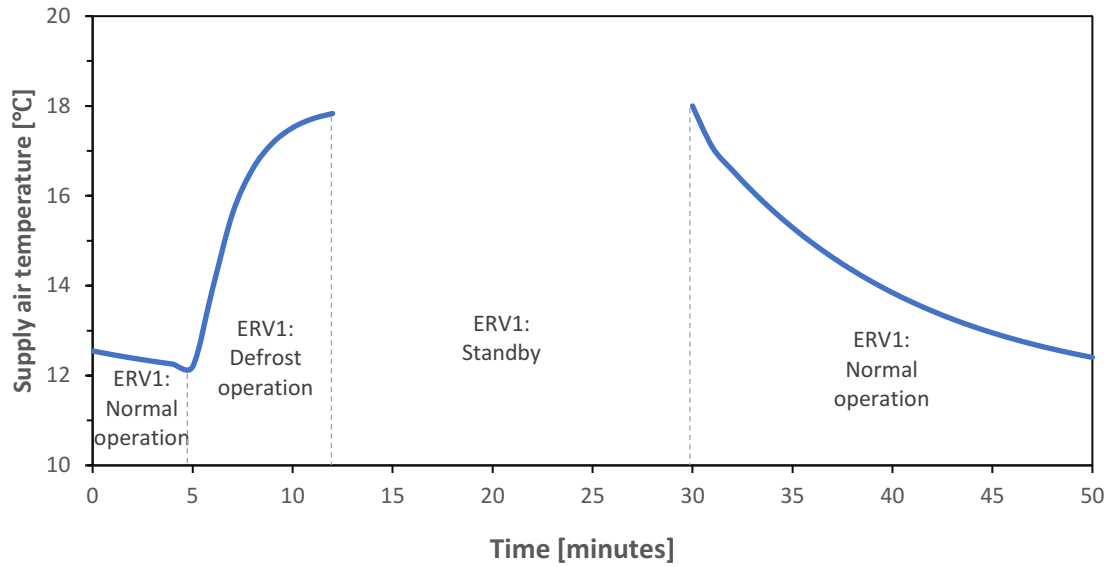


Figure 20a. Supply air temperature T_2 of ERV1 in defrost operation from 5 min to 12 min, and standby from 12 min to 30 min, followed by normal operation from 30 min to 50 min.

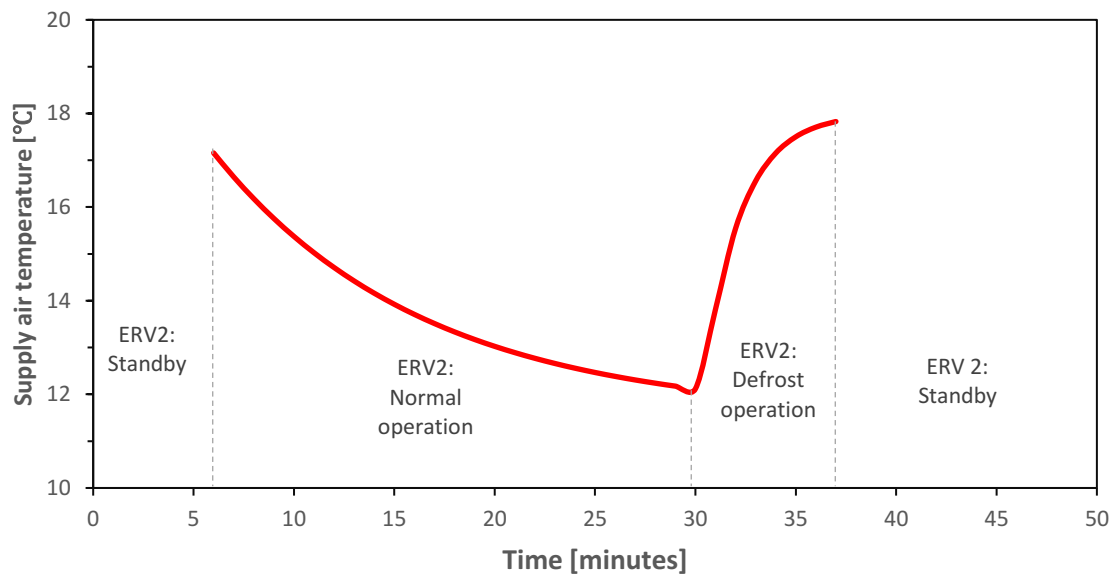


Figure 20b. Supply air temperature T_2 of ERV2 in normal operation from 6 min to 30 min, and defrost from 30 min to 38 min, followed by standby mode from 38 min to 50 min

Figure 20: Supply air temperature T_2 for the alternative operation of ERV1 and ERV 2.

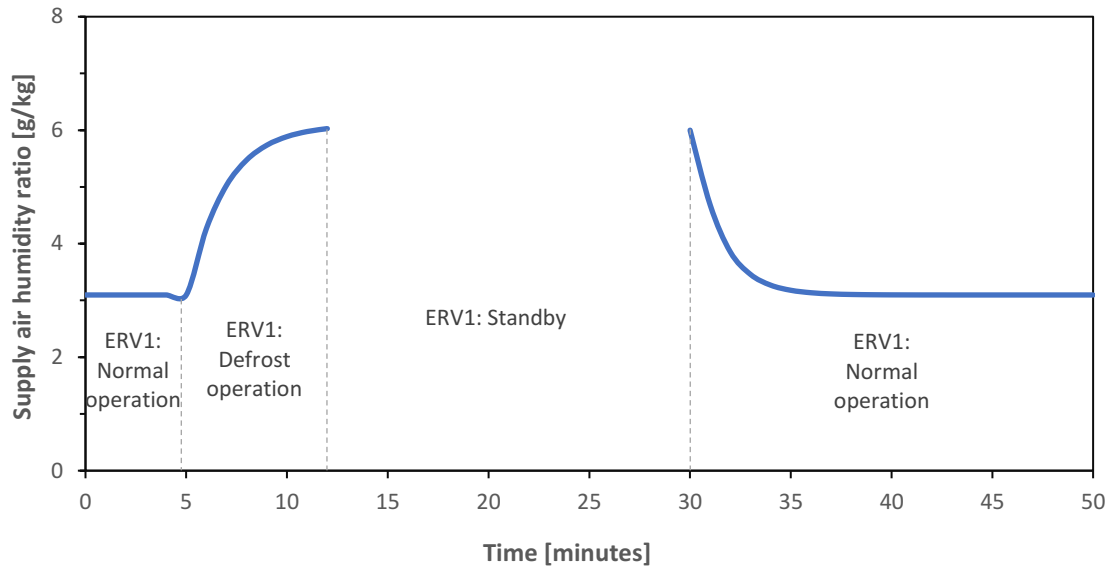


Figure 21a. Supply air humidity ratio w_2 of ERV1 in defrost operation from 5 min to 12 min, and standby from 12 min to 30 min, followed by normal operation from 30 min to 50 min.

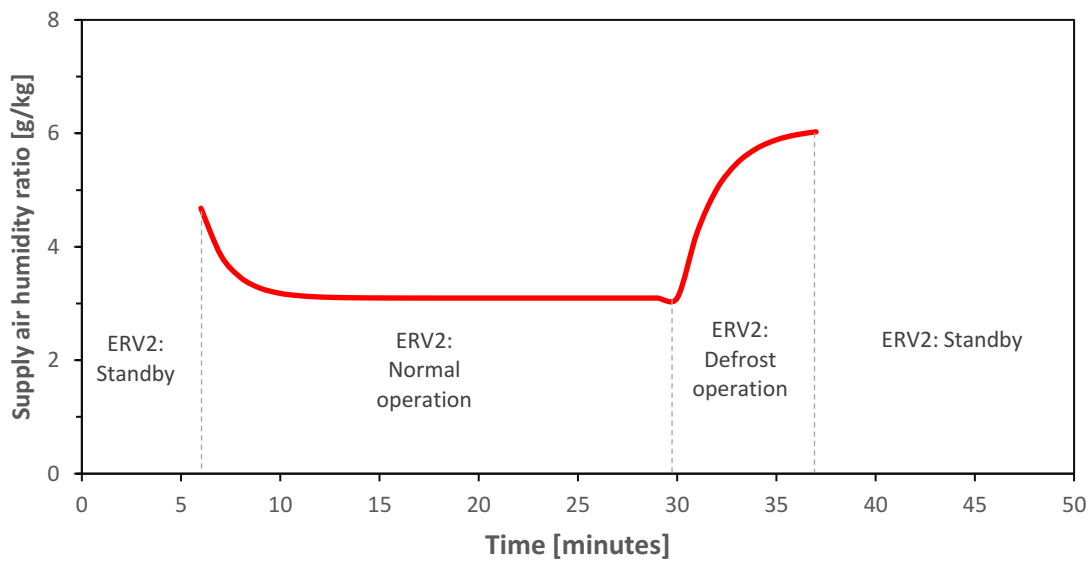


Figure 21b. Supply air humidity ratio w_2 of ERV2 in normal operation from 6 min to 30 min, and defrost from 30 min to 38 min, followed by standby mode from 38 min to 50 min

Figure 21: Supply air humidity ratio w_2 for two ERV units with alternating defrost at $T_I = -20^\circ\text{C}$,
 $w_I = 0.36$ g/kg.

3.4. Housing models incorporating with the new ERV correlation-based models in TRNSYS

The effect of single-core and dual-core ERV units, on the heating energy use is evaluated for three different house types. The study starts with the simulation of a Net Zero Energy House the Conventional Northern House (CNH) that complies with the 1997 Model National Energy Code for Houses (MNECH) [71], and the Northern Sustainable House (NSH) [36] that is expected to lead to 50% reduction in energy consumption compared with CNH. The prescriptions of thermal insulation of envelope and air infiltration rate for the NZEH are more restrictive than those of CNH and NSH. The energy performance of these three house types, i.e., NZEH, CNH and NSH, is simulated at three arctic locations (Inuvik, Kuujuaq and Resolute), and compared with Montreal.

TRNSYS (Transient System Simulation program) [72] is the software used in this thesis to develop the model of the home and simulate its energy use performance. This software has its roots in predicting the energy consumption of solar buildings and has become well established over the past 33 years. TRNSYS is a very powerful and versatile tool. The software can be used to model many different types of systems, ranging from something as simple as a domestic hot water system to a more complex multi-story, multi-zone building with all of its functioning and interdependent systems. The software has been developed to allow the user to include various types of components (called "Types") in the system/building being simulated, such as solar panels, boiler or heat/energy recovery ventilators. If the specific component does not exist in the fairly comprehensive TRNSYS library, the modular architecture of the software allows the user to create a custom component in all common programming languages using the DLL format and add it to the model. Moreover, the software can be linked to other software programs, such as Microsoft Excel, Matlab and EES to perform other tasks [73]

The NZEH model was initially developed by using TRNYS v17 [35], converted to TRNSYS v18, and modified by adding the newly developed correlation-based models presented in section 2. This is a two-storey house, with a total floor area of 334 m², having five thermal zones

with a basement and ventilated attic. Characteristics of building envelope in NZEH in Montreal and in CNH and NSH in arctic locations are listed in **Table 5**. More details are available in reference [35].

Table 5: Building envelope features of NZEH in Montreal and CNH [70] and NSH [36] housing models in arctic locations

Building envelope	NZEH house (Montreal)	CNH house (Arctic locations)	NSH house (Arctic locations)
Thermal resistance ($m^2 \cdot K/W$)			
Walls	6.25	6.7	8.8
Ceiling	10.42	10.8	14.1
Floor	1.9	8.1	9.6
Windows	1.03 – Fixed picture (50% of south façade) 0.862 – Operable casement (All other windows)	5 - South and North	0.97 – South ; 0.74 - North
Air infiltration rate at 50 Pa pressure difference (ach)			
	1.22	5.3 at unit A and unit B	2.36 at unit A; 2.7 at unit B

A ground coupling – Type 1244 (**Figure 22**), featured with the grids around the NZEH house, converted from TRNSYS v17 in [35] to v18 for present project with the change of input values, can simulate the heat transfer between the ground floor and surrounding soil compared with the case of the constant underground temperature. The detailed on parameters of Type 1244 are presented in APPENDIX B.

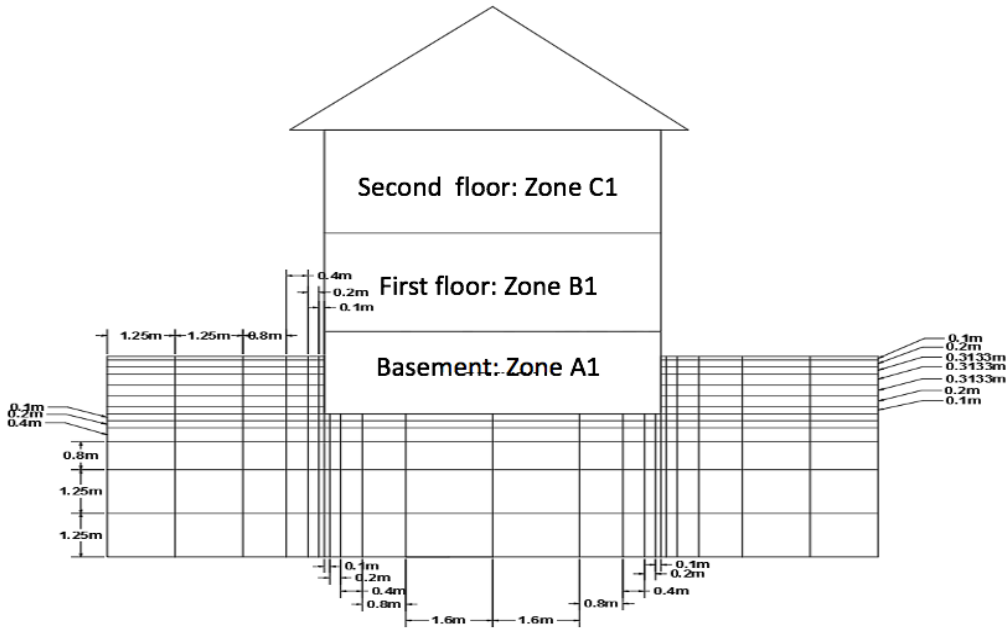


Figure 22: Schematic representation of the NZEB house.

The heating and ventilation systems are decoupled. The hydronic radiant floor heating, supplied from a water storage tank (Type 534 of TRNSYS) equipped with two electric heaters, maintained all rooms at the setpoint temperature of 22°C. The storage tank also receives heat from evacuated tube solar collectors (Type 71 of TRNSYS) that reduces the electric demand. The ventilation system supplies 0.35 ach of outdoor air [35]. Two types of ERV units, the dual-core and single-core units, are compared in terms of energy use and hours of adequate ventilation. Single-core ERV unit has 67% apparent sensible heat transfer effectiveness and 46% latent heat transfer effectiveness at 57 L/s and 0°C outdoor air temperature [70]. The operation times of ERV units are listed in **Table 4**.

The house energy demand for heating is composed of space heating demand (due to the use of radiant floor) Q_{radiant} , and the energy demand with the recirculation defrost $Q_{\text{recirculation}}$ for heating the outdoor airflow rate of 0.35 ach from temperatures T_2 to T_5 .

$$Q_{\text{radiant}} = \int_0^t C \cdot m_{\text{water}} \cdot (T_{\text{in}} - T_{\text{out}}) \cdot \Delta t \quad (14)$$

$$Q_{recirculation} = \int_0^t \frac{ach}{3600} \cdot V_{house} \cdot \rho_{air} \cdot C_p \cdot (T_5 - T_2) \cdot \Delta t \quad (15)$$

Where:

C = the heat capacity of the water in the radiant heating loop, kJ/kg· °C

T_{in} = the water temperature entering the radiant floor tank. °C

T_{out} = the water temperature exiting the radiant floor tank. °C

m_{water} = the water mass flow rate of radiant heating loop, kg/s

Both CNH [71] and NSH [36] (**Table 5**) are one-story duplex houses with two suits, each house with 119 m² and a shared mechanical room in 9.5 m² (**Figure 23**). The hydronic radiant baseboard heaters are supplied by a natural gas boiler (Type 122 of TRNSYS). The ventilation system and ERV units are of the same type as in the case of NZEH model. More details are presented in [36].

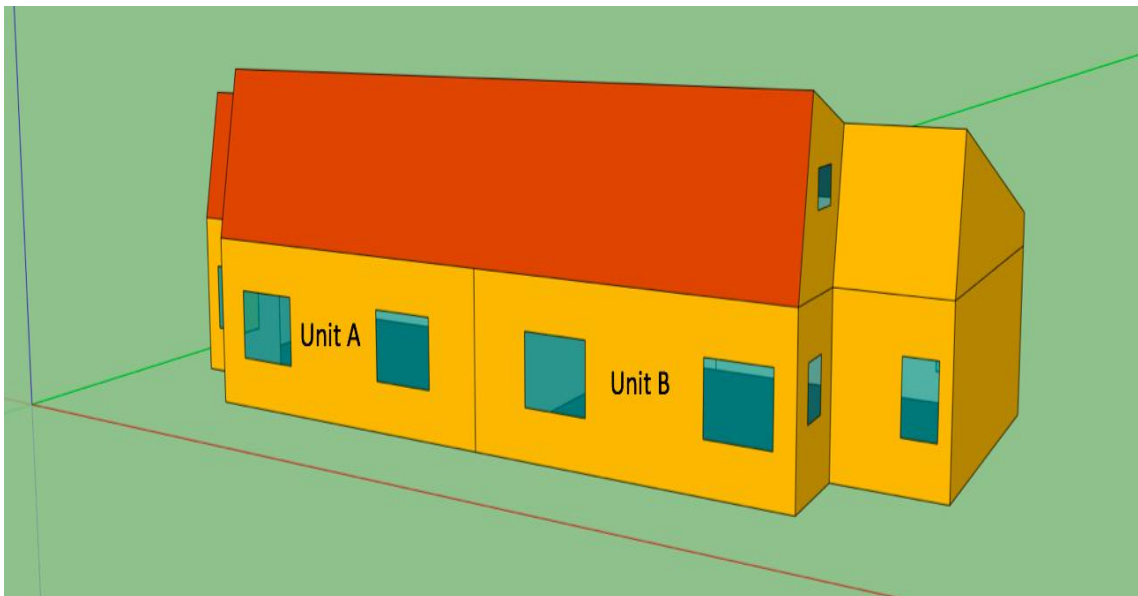


Figure 23: Schematic representation of CNH the NSH houses

3.5. Summary

The correlation-based models of the single-core ERV unit are developed by using the measurements in [21]. Moreover, the predicted models of ice mass are established based on the correlation-based models of the ERV unit and then used to predict the different normal/defrost operation time. In addition, the dual-core ERV models based on the set-up in [21] in compliance with the manufacturer’s schedules for each unit are developed for comparison with the single-core ERV unit. Finally, one NZEH housing model and two northern housing models (CNH and NSH) are also established in TRNSYS, and the HVAC and building envelope of these two models are presented. The comparison between the single-core unit with the recirculating and preheating defrost and dual-core ERV units are conducted by using the correlation-based models in the three housing models (NZEH, CNH and NSH) with the four locations (**Table 6**).

Table 6: The different scenarios for the comparison of the single-core ERV with the recirculating and preheating defrost and dual-core ERV.

Locations (4)		Inuvik, Kuujjuaq, Resolute and Montreal	
Housing models (3)		NZEH, CHN, NSH	
ERV (1)	• Without ERV		
	• Single-core ERV	• preheating	No defrost
		• Re-circulation	-manufacturer’s operation time - 30, 40, 50 minutes
• Double-core ERV		Manufacturer’s operation time	

4. SIMULATION RESULTS AND ANALYSIS

Sections 4.1 compare the difference of using the built-in ERV unit (Type 667 b) and the correlation-based models.

Sections 4.2 and 4.3 compare the predicted seasonal heating results of single-core ERV when used with a NZEH, and section 4.4 compares the results of dual-core ERV with a NZEH. Simulations are performed with weather data files of three arctic locations (Inuvik, Kuujjuaq and Resolute), and the results are compared with the case study of Montreal (**Table 7**). The heating season is determined whenever the indoor temperature is lower than setpoint indoor temperature of the house, as follows: (i) from September 5 to June 4 (Kuujjuaq and Inuvik), and (ii) the entire year (Resolute), (iii) from October 17 to May 1 (Montreal). The factory set defrost schedule is used (**Table 4**). The performance matrix used for the evaluation of ERV unit are presented in **Table 8**.

Section 4.5 compares the predicted seasonal heating results of single-core and dual-core ERV units with northern CNH and NSH models at the same four locations.

Table 7: Information about three selected arctic locations compared with Montreal [74]

Location	Inuvik	Kuujjuaq	Resolute	Montreal
Latitude	68.36°N	58.10°N	74.70°N	45.50°N
Heating-degree days HDD (18°C)	8798	8888	12208	4356
Minimum outdoor air temperature (°C)	-47.2	-40.6	-43.9	-28.9
Maximum wind speed [km/h]	44.56	85.0	82.6	62.0

Table 8: Performance matrix for the evaluation of ERV unit

Types	Performance matrix
Energy use	<ul style="list-style-type: none"> • The energy use for heating the outdoor air • The energy use for the space heating Total heating energy use (space heating and ventilation) Energy savings for heating the outdoor air (with single-core ERV vs without single-core ERV) Energy increase for heating the outdoor air (preheating vs recirculating) Energy increase for heating the outdoor air (-10 °C threshold temperature vs -20°C threshold temperature) Energy increase for heating the outdoor air (single-core vs dual-core)
Defrost hours	<ul style="list-style-type: none"> • The defrost hours reductions (-10 °C threshold temperature vs -20°C threshold temperature) • decrease of percentage of defrost hours (different operation schedules)

4.1. Simulation results of single-core ERV unit: correlation-based models versus Type 667b of TRNSYS program

The model available in TRNSYS, named Type 667b, that simulates the operation of heat recovery units does not include the frost/defrost operation mode of ERV unit. **Figure 24** presents the process of heat/moisture recovery and inputs used in the built-in ERV models in TRNSYS (e.g. $T_{exhaust,in}$ and $T_{fresh,in}$; $w_{exhaust,in}$ and $w_{fresh,in}$; ϵ_{sens} and ϵ_{lat}). Some of these inputs (e.g. $T_{exhaust,in}$ and $T_{fresh,in}$; $w_{exhaust,in}$ and $w_{fresh,in}$), for the calculation of heat/moisture transfer (**Equation 16 and 17**), are varying with time. However, the sensible and latent effectiveness ϵ_{sens} and ϵ_{lat} are not changed once setup when the frosting is occurred, consequently, there are no change in supply air temperature T_2 and humidity w_2 over time due to the frosting. The details of input values are presented in APPENDIX B.

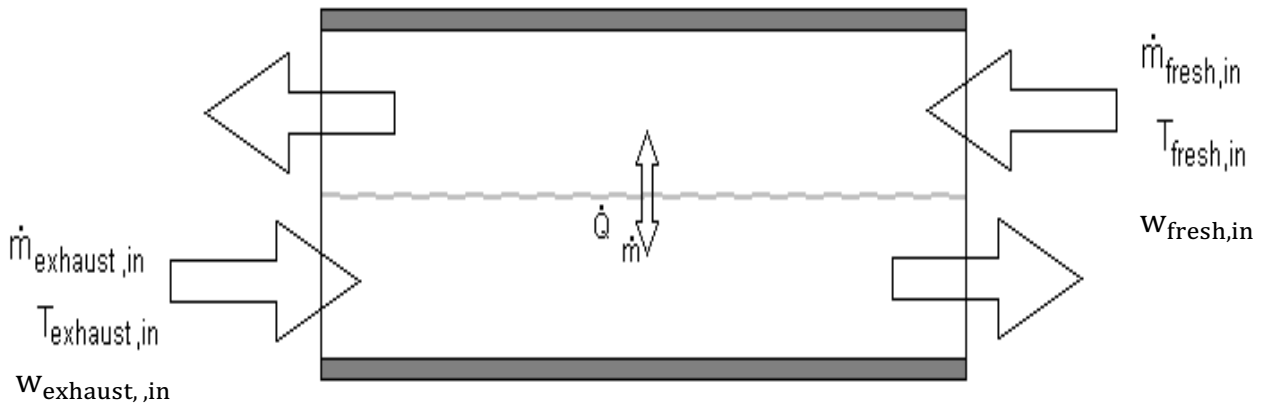


Figure 24: Air to air Heat Recovery Device Schematic [68]

$$\dot{Q}_{sens} = \varepsilon_{sens} C_{min} (T_{exhaust,in} - T_{fresh,in}) \quad (16)$$

$$\dot{m}_{sens} = \varepsilon_{lat} m_{min} (w_{exhaust,in} - w_{fresh,in}) \quad (17)$$

Hence, the new correlation-based models are included in TRNSYS by using equation boxes. As an example for NZEH, the difference is observed in the pattern of variation of supply air temperature T_2 , and of sensible heat transfer effectiveness, which is calculated only during the normal operation time (**Figure 25**). The seasonal energy use for heating the outdoor airflow rate is estimated at 2616 kWh by using the new correlation-based model with a single-core ERV unit, compared with 3139 kWh as predicted by Type 667b, a difference of 16.6%.

The relative humidity RH_3 calculated based on the exhaust air humidity ratio w_3 from the house, which is predicted by the new model, varies with time and has greater values compared with RH_3 obtained from TRNSYS (**Figure 26**). The latent heat transfer effectiveness changes rapidly during the first moments of normal operation mode, due to the hygrothermal memory of heat exchanger from the defrost mode.

All results presented in sections 5.1, 5.2, 5.3 and 5.4 are obtained from TRNSYS with the new models included.

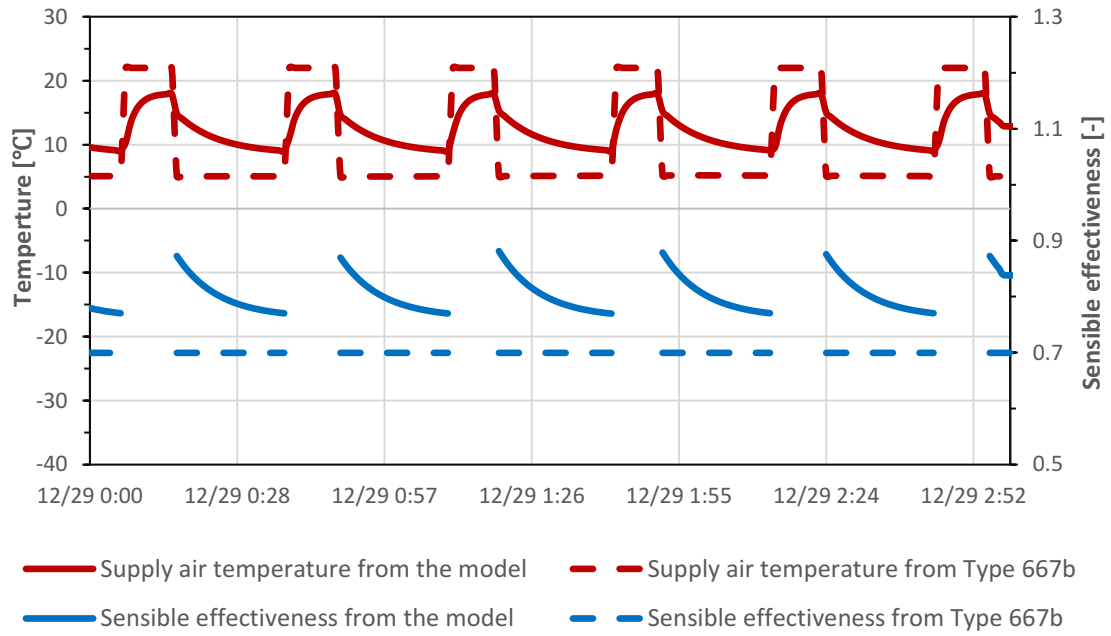


Figure 25: Comparison of supply air temperature T_2 and sensible heat transfer effectiveness predicted by the correlation-based models versus Type667b of TRNSYS, in the case of NZEH house.

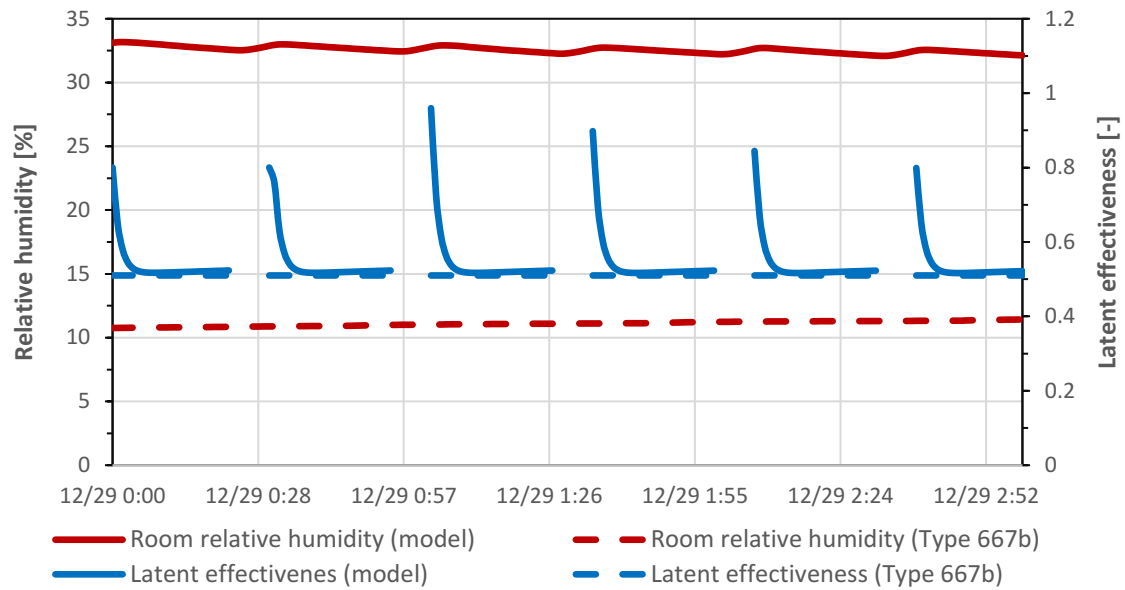


Figure 26: Comparison of the exhaust air relative humidity RH_3 and latent heat transfer effectiveness predicted by correlation-based models versus Type667b of TRNSYS, in the case of NZEH.

4.2. Single-core ERV with the NZEH model

The monthly simulation results at four locations with and without single-core ERV are presented as an example, (Table 9 - 12). In Montreal (Table 9), the use of single-core ERV reduces the energy use for heating the ventilation air by 7718 kWh (energy savings of 29%) over the heating season, compared with the case without an ERV unit. The recirculation defrost occurs over 223 hours. In Inuvik (Table 10), the implementation of single-core ERV reduces the energy use for heating the ventilation air by 11473 kWh over the heating season, or average energy savings of 25% compared with the case without an ERV unit. The recirculation defrost occurs over 1043 hours. In Kuujuaq (Table 11), the use of single-core ERV lead to the energy savings for heating the ventilation air by 9512 kWh over the heating season, or average energy savings of 24% compared with the case without an ERV unit. The recirculation defrost occurs over 702 hours. In Resolute (Table 12), the use of single-core ERV reduces the energy use for heating the ventilation air by

15150 kWh over the heating season, or average energy savings of 24% compared with the case without an ERV unit. The recirculation defrost occurs over 1379 hours.

Table 9: Energy use for space heating and heating of ventilation air of the case study NZEH model with and without single-core ERV in Montreal.

Months	With single-core ERV unit				Without ERV unit		
	Space heating (kWh)	Heating of ventilation air (kWh)	Total heating energy use (kWh)	Defrost hours	Heating of ventilation air (kWh)	Total heating energy use (kWh)	Energy savings (kWh)
Oct.	733	237	970	0	691	1424	454
Nov.	1877	444	2321	0	1343	3220	899
Dec.	3005	559	3564	50	1923	4928	1364
Jan.	3244	573	3817	78	2244	5488	1671
Feb.	2846	503	3349	70	1940	4786	1437
Mar.	2364	527	2891	23	1695	4059	1168
Apr.	1317	362	1679	0	1087	2404	725
Total	15394	3201	18595	223	10923	26317	7718

Table 10: Energy use for space heating and heating of ventilation air of the case study NZEH model with and without single-core ERV in Inuvik.

Months	With single-core ERV unit				Without ERV unit		
	Space heating (kWh)	Heating of ventilation air (kWh)	Total heating energy use (kWh)	Defrost hours	Heating of ventilation air (kWh)	Total heating energy use (kWh)	Energy savings (kWh)
Sep.	1631	237	1868	0	761	2393	525
Oct.	2861	354	3215	58	1364	4225	1010
Nov.	3731	392	4123	163	1840	5571	1448
Dec.	4301	449	4750	191	2118	6419	1669
Jan.	4517	458	4975	192	2219	6736	1761
Feb.	4019	414	4433	170	1979	5998	1565
Mar.	4149	429	4578	175	2032	6181	1603
Apr.	3233	350	3583	93	1507	4740	1157
May.	2169	283	2452	1	964	3133	681
June	174	21	195	0	75	249	54
Total	30785	3387	34172	1043	14859	45645	11473

Table 11: Energy use for space heating and heating of ventilation air of the case study NZEH model with and without single-core ERV in Kuujjuaq.

Months	With single-core ERV unit				Without ERV unit		
	Space heating (kWh)	Heating of ventilation air (kWh)	Total heating energy use (kWh)	Defrost hours	Heating of ventilation air (kWh)	Total heating energy use (kWh)	Energy savings (kWh)
Sep.	1514	213	1727	0	702	2217	489
Oct.	2196	296	2492	0	1006	3203	710
Nov.	2741	336	3078	64	1292	4034	955
Dec.	3736	401	4138	141	1804	5541	1403
Jan.	3948	422	4371	145	1890	5838	1467
Feb.	3523	375	3899	139	1710	5233	1334
Mar.	3778	399	4178	149	1813	5592	1414
Apr.	2794	333	3128	60	1321	4116	987
May.	2171	287	2458	0	985	3156	698
June	168	20	188	0	71	239	51
Total	26574	3087	29661	702	12599	39173	9512

Table 12: Energy use for space heating and heating of ventilation air of the case study NZEH model with and without single-core ERV in Resolute.

Months	With the single-core ERV unit				Without ERV unit		
	Space heating (kWh)	Ventilation heating (kWh)	Total heating (kWh)	Defrost hours	Ventilation heating (kWh)	Total heating (kWh)	Energy saving (kWh)
Jan.	4863	482	5345	204.98	2325	7188	1842
Feb.	4391	441	4832	188.55	2106	6498	1665
Mar.	4920	495	5416	212.09	2395	7316	1900
Apr.	4151	423	4575	178.93	2011	6163	1588
May.	3045	371	3416	87.22	1452	4498	1081
June.	2186	338	2525	0.55	995	3182	656
July.	1852	273	2126	0	813	2666	540
Aug.	1994	309	2304	0	882	2876	572
Sep.	2406	375	2782	9.45	1259	3665	883
Oct.	3358	372	3731	121.58	1618	4976	1245
Nov.	4203	425	4629	174.83	1998	6202	1573
Dec.	4787	484	5272	208.16	2303	7090	1818
Total	42163	5012	47176	1379	20163	62326	15150

Table 13 presents a summary of annual heating energy use and defrost hours for all four locations, with and without single-core ERV unit. The use of single-core ERV unit contributes to the reduction of annual heating energy use of the NZEH house, from 25.2% in Inuvik to 23% in

Montreal. The reduction of annual energy use for heating the ventilation air, due to the use of ERV unit, is about 77% in Inuvik to 73% in Montreal.

However, the drawback of using single-core ERV unit is the reduction of outdoor airflow rate during the defrost by recirculation of exhaust air during 1043 hours in Inuvik, 701 hours in Kuujjuaq, and 1379 hours in Resolute, compared with 223 hours in Montreal. Normally, the reduction of ventilation air has an impact on indoor air quality.

Table 13: Comparison of annual heating energy use and defrost hours under three arctic climates (Inuvik, Kuujjuaq, and Resolute) compared with the cold climate of Montreal, in the case of NZEH model.

Location	With single-core ERV unit				Without ERV unit	
	Space heating (kWh)	Heating of ventilation air (kWh)	Total heating energy use (kWh)	Defrost hours	Heating of ventilation air (kWh)	Total heating energy use (kWh)
Inuvik	30710	3389	34099	1043	14863	45573
Kuujjuaq	26574	3087	29661	703	12599	39173
Resolute	42163	4794	46957	1379	20163	62326
Montreal	15566	1938	17504	223	7172	22738

With the decrease of the threshold temperature for the defrost, the airflow rate of the supply air will increase while the energy use for ventilation air increases as well. Since there is no impact on the thermal performance of the ERV unit [21] in case of the outdoor air temperature higher than -20 °C, -20 °C threshold temperature for defrost are selected to compare with the -10 °C threshold temperature (manufacturing set-up). **Tables 14 - 17** presents defrost hours and the comparison of energy use with -10 °C and -20 °C threshold temperature for defrost in the single-core ERV unit at four locations.

Table 14: Annual energy use and defrost hours of single-core ERV in the NZEH model in Montreal, comparison of the case of -10°C and -20°C threshold temperature for defrost of single-core ERV unit.

Months	-10 °C threshold temperature			-20 °C threshold temperature				
	Defrost hours	Ventilation heating (kWh)	Total heating (kWh)	Defrost hours	Ventilation heating (kWh)	Total heating (kWh)	Energy saving (kwh)	Defrost hours reduction
Oct.	0	237	970	0	237	970	0	0
Nov.	0	444	2321	0	447	2324	-3	0
Dec.	50	559	3564	0	637	3642	-78	50
Jan.	78	573	3817	19	672	3916	-99	59
Feb.	70	503	3349	11.3	601	3447	-98	59
Mar.	23	527	2891	0	562	2926	-35	23
Apr.	0	362	1679	0	362	1679	0	0
Sum.	223	3201	18595	30.3	3518	18912	-313	193

The defrost hours of the single-core unit with -10 °C threshold temperature for defrost is counted to be 223 hours per year, where 89 % of the defrost operation is in the cold winter months (e.g. Dec, Jan and Feb), while the defrost hours of -20 °C threshold temperature is counted to be 30 hours yearly, 100% of which are from the cold winter months. In addition, compared with -20 °C threshold temperature, the defrost operation of -10 °C threshold temperature saves 9 % (313 kWh) of ventilation heating and 1.6 % of total heating, whereas increase 6.5 times (193 hours) of defrost hours. Although increased fan power of defrost operation (0.076kw at 0 °C and 0.079kw at -25 °C) compared with normal operation (0.036kw) results in additional 6.3 kwh (4 % of fans energy use) energy use yearly, the application of -10 °C threshold temperature can still save 306 kWh energy yearly.

Table 15: Annual energy use and defrost hours of single-core ERV in the NZEH model in Inuvik, comparison of the case of -10°C and -20°C threshold temperature for defrost of single-core ERV unit.

Months	-10 °C threshold temperature			-20 °C threshold temperature				
	Defrost hours	Energy use for heating the outdoor air (kWh)	Total heating (kWh)	Defrost hours	Energy use for heating the outdoor air (kWh)	Total heating (kWh)	Energy saving (kWh)	Defrost hours reduction
Sep.	0	233	1865	0	233	1865	0	0
Oct.	57	354	3216	19	383	3245	-28	38
Nov.	162	392	4124	97	447	4179	-54	65
Dec.	191	449	4751	157	475	4777	-25	33
Jan.	191	458	4975	188	461	4979	-3	3
Feb.	169	414	4434	137	443	4463	-28	31
Mar.	175	429	4579	128	470	4620	-41	47
Apr.	93	350	3583	48	385	3619	-35	44
May.	1	283	2452	0	283	2453	-1	1
June	0	21	196	0	21	196	0	0
Sum.	1043	3389	34099	777	3608	34318	218	265

The defrost hours of -10 °C of the single-core unit with -10 °C threshold temperature for defrost is counted to be 1043 hours per year, where 94.35 % of the defrost operation is in the cold winter months (e.g. Nov, Dec, Jan, Feb and March and April), while the defrost hours of -20 °C threshold temperature is counted to be 777.22 hours yearly, 97.53% of which are from the cold winter months. In addition, compared with -20 °C threshold temperature, the defrost operation of -10 °C threshold temperature saves 6 % (218 kWh) of ventilation heating and 0.6 % of total heating, whereas increases by 34.1% (265.36 hours) of defrost hours. Although increased fan power of defrost operation (0.076kw at 0 °C and 0.079kw at -25 °C) versus normal operation (0.036kw) results in additional 9.04 kwh (3.2 % of fans energy use) energy use yearly, the application of -10 °C threshold temperature can still save 209 kWh energy yearly.

Table 16: Annual energy use and defrost hours of single-core ERV in the NZEH model in Kuujuaq, comparison of the case of -10°C and -20°C threshold temperature for defrost of single-core ERV unit.

Months	-10 °C threshold temperature			-20 °C threshold temperature			Energy saving (kwh)	Defrost hours reduction
	Defrost hours	Ventilation heating (kWh)	Total heating (kWh)	Defrost hours	Ventilation heating (kWh)	Total heating (kWh)		
Sep.	0	213	1727	0	213	1727	0	0
Oct.	0	296	2492	0	296	2493	0	0
Nov.	64	336	3078	6	376	3118	-40	58
Dec.	141	401	4138	88	443	4180	-41	53
Jan.	145	422	4371	126	438	4387	-15	19
Feb.	139	375	3899	98	409	3932	-33	41
Mar.	149	399	4178	88	447	4226	-48	60
Apr.	60	333	3128	13	373	3167	-39	47
May.	0	287	2458	0	287	2458	0	0
June.	0	20	188	0	20	188	0	0
Sum.	702	3087	29661	421	3307	29881	220	281

The defrost hours of -10 °C of the single-core unit with -10 °C threshold temperature for defrost is counted to be 702 hours per year, where 100 % of the defrost operation is in the cold winter months (e.g. Nov, Dec, Jan, Feb and March and April), while the defrost hours of -20 °C threshold temperature is counted to be 421 hours yearly, 100% of which are from the cold winter months. In addition, compared with -20 °C threshold temperature, the defrost operation of -10 °C threshold temperature saves 7 % (220 kWh) of ventilation heating and 0.7 % of total heating, whereas increases by 67 % (281 hours) of defrost hours. Although increased fan power of defrost operation (0.076kw at 0 °C and 0.079kw at -25 °C) versus normal operation (0.036kw) results in additional 9.7 kWh (4 % of fans energy use) energy use yearly, the application of -10 °C threshold temperature can still save 271 kWh energy yearly.

Table 17: Annual energy use and defrost hours of single-core ERV in the NZEH model in Resolute, comparison of the case of -10°C and -20°C threshold temperature for defrost of single-core ERV unit.

Months	-10 °C threshold temperature			-20 °C threshold temperature			Energy saving (kWh)	Defrost hours reduction
	Defrost hours	Ventilation heating (kWh)	Total heating (kWh)	Defrost hours	Ventilation heating (kWh)	Total heating (kWh)		
Jan.	204	482	5345	196	491	5354	-8	8
Feb.	188	441	4832	180	448	4840	-7	8
Mar.	212	495	5416	197	509	5429	-13	14
Apr.	178	423	4575	143	455	4607	-32	35
May.	87	371	3416	0	428	3474	-57	86
June	0	338	2525	0	339	2525	0	0
July	0	273	2126	0	273	2126	0	0
Aug.	0	309	2304	0	309	2304	0	0
Sep.	9	375	2782	0	381	2788	-6	9
Oct.	121	372	3731	32	437	3796	-65	89
Nov.	174	425	4629	145	453	4656	-27	28
Dec.	208	484	5272	208	484	5272	0	0
Sum.	1379	5012	47176	1112	5012	47176	217	281

The defrost hours of -10 °C of the single-core unit with -10 °C threshold temperature for defrost is counted to be 1379 hours per year, where 93 % of the defrost operation is in the cold winter months (e.g. Oct, Nov, Dec, Jan, Feb, March and April), while the defrost hours of -20 °C threshold temperature is counted to be 777.22 hours yearly, 100% of which are from the cold winter months. In addition, compared with -20 °C threshold temperature, the defrost operation of -10 °C threshold temperature saves 4 % (217 kWh) of ventilation heating and 0.6 % of total heating, whereas increase by 25% (281 hours) of defrost hours. Although increased fan power of defrost operation (0.076kw at 0 °C and 0.079kw at -25 °C) versus normal operation (0.036kw) results in additional 9.8 kwh (3 % of fans energy use) energy use yearly, the application of -10 °C threshold temperature can still save 209.41 kWh energy yearly.

Overall, -10 °C threshold temperature will decrease ventilation energy with the disadvantages of less fresh air supply due to the increased defrost hours compared with -20 °C threshold temperature in all three arctic locations and Montreal. To analyze the feasibility of -10 °C

threshold temperature versus -20 °C threshold temperature, the monthly energy saving rate

(Equation 18) is presented in Figure 27.

$$\text{Energy increase rate} = \frac{\text{energy increase}}{\text{operation hours increase}} \quad (18)$$

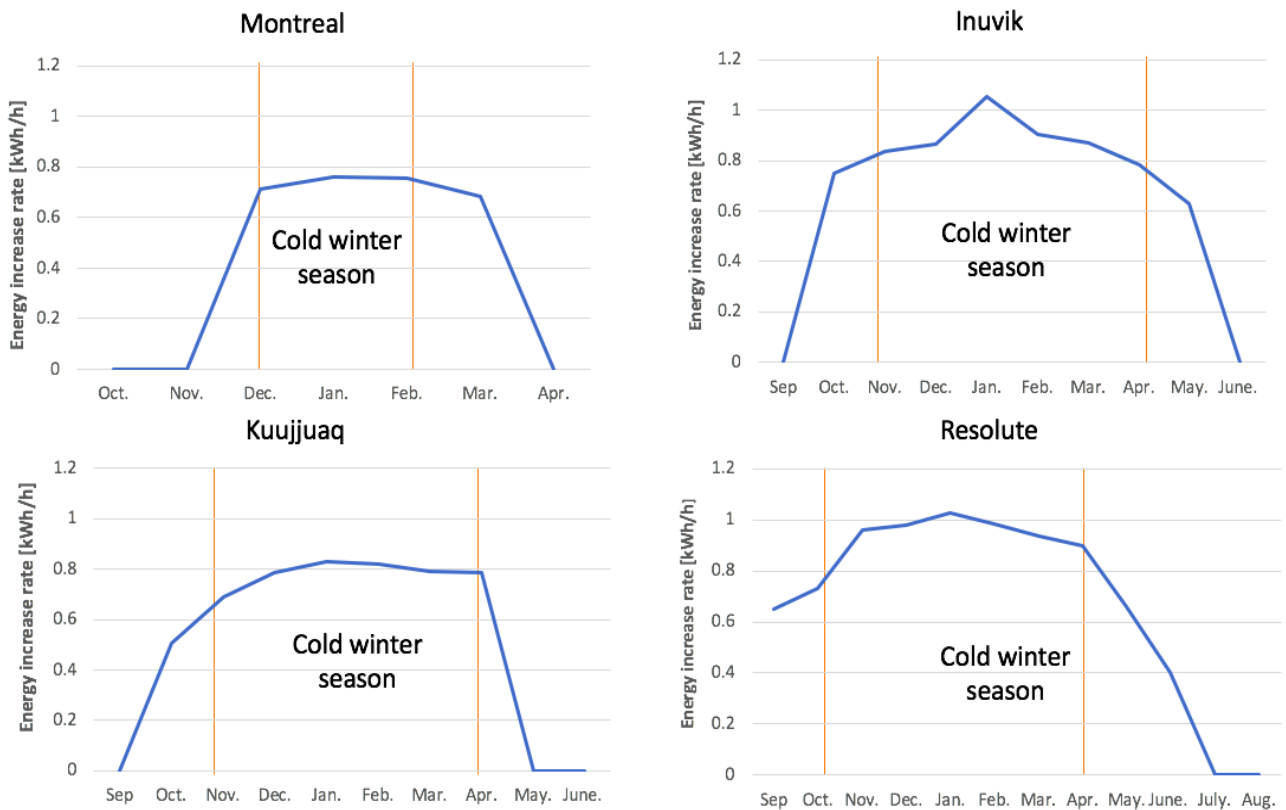


Figure 27: The monthly energy savings rate in three arctic locations (Inuvik, Kuujuaq and Resolute) and Montreal for the heating months.

It can be observed (Figure 27) that they all see higher energy increase rate in four locations in the cold winter months, meaning the colder the climate the higher energy cost to achieve the same number of hours reduction for defrost. Therefore, -10 °C threshold temperature for the defrost is recommended to implement during the cold winter months both in the northern cities (Inuvik, Kuujuaq and Resolute) and Montreal.

Preheating the outdoor air is another defrost strategy for the single-core ERV in arctic climates [31, 32]. The cold outdoor air is heated up to -10°C before entering the single-core ERV unit. Then, the ventilation air is heated from T_2 (supply air temperature leaving the ERV unit) up to T_5 that enters the house, as controlled by the heating coil (HC) that is installed after the ERV unit. The new preheating model (**Equation 19**), which is added in an equation box in TRNSYS program, estimates the energy use of heating the outdoor air from T_1 to T_5 :

$$Q_{preheating} = \int_0^t \frac{ach}{3600} \cdot V_{house} \cdot \rho_{air} \cdot C_p \cdot [(-10 - T_1) + (T_5 - T_2)] \cdot \Delta t \quad (19)$$

There is an uninterrupted operation of the single-core ERV as the cold outdoor air is preheated by the coil (PH), and hence a continuous supply of required outdoor airflow rate. However, the preheating defrost increases the annual energy use for heating the outdoor air by 230% in Inuvik, 200% in Kuujjuaq, 220% in Resolute, 156% in Montreal, compared with the recirculation defrost (**Table 18**). On the other hand, the implementation of dual-core reduces the annual energy use for heating the outdoor air (**Table 18**) by 63% (17% of decrease versus total heating energy use) in Inuvik, 62% (16%) in Kuujjuaq, 63% (17%) in Resolute, 61% (15%) in Montreal, compared with the pre-heating, which also can provide the continuous supply of outdoor air.

Table 18. Annual energy use for heating the outdoor air of NZEH. Comparison of single-core ERV with recirculation defrost, single-core ERV with preheating defrost, and dual-core ERV with recirculation defrost.

Location	Recirculation Heating of ventilation air (kWh)	Preheating Heating of ventilation air (kWh)	Dual-core Heating of ventilation air (kWh)	Recirculation v.s. Preheating Increase of energy for heating the outdoor air (%)	Preheating v.s. Dual-core Decrease of energy use for heating the outdoor air (%)	Dual-core Decrease of energy use for heating the outdoor air versus total heating energy use (space heating and heating the outdoor air) (%)
Inuvik	3389	11326	4173	230	63	17
Kuuujuaq	3087	9248	3507	200	62	16
Resolute	4794	15378	5748	220	63	17
Montreal	1938	4969	1935	156	61	15

Due to the moisture exchange inside the single-core ERV unit, and moisture transfer during the recirculation defrost, the indoor humidity ratio increases at all four locations, when compared with the case without ERV (**Figure 28**). For instance, the average indoor humidity ratio in January in Inuvik increases from 1.7 g/kg (without ERV unit) to 4.9 g/kg (with ERV unit).

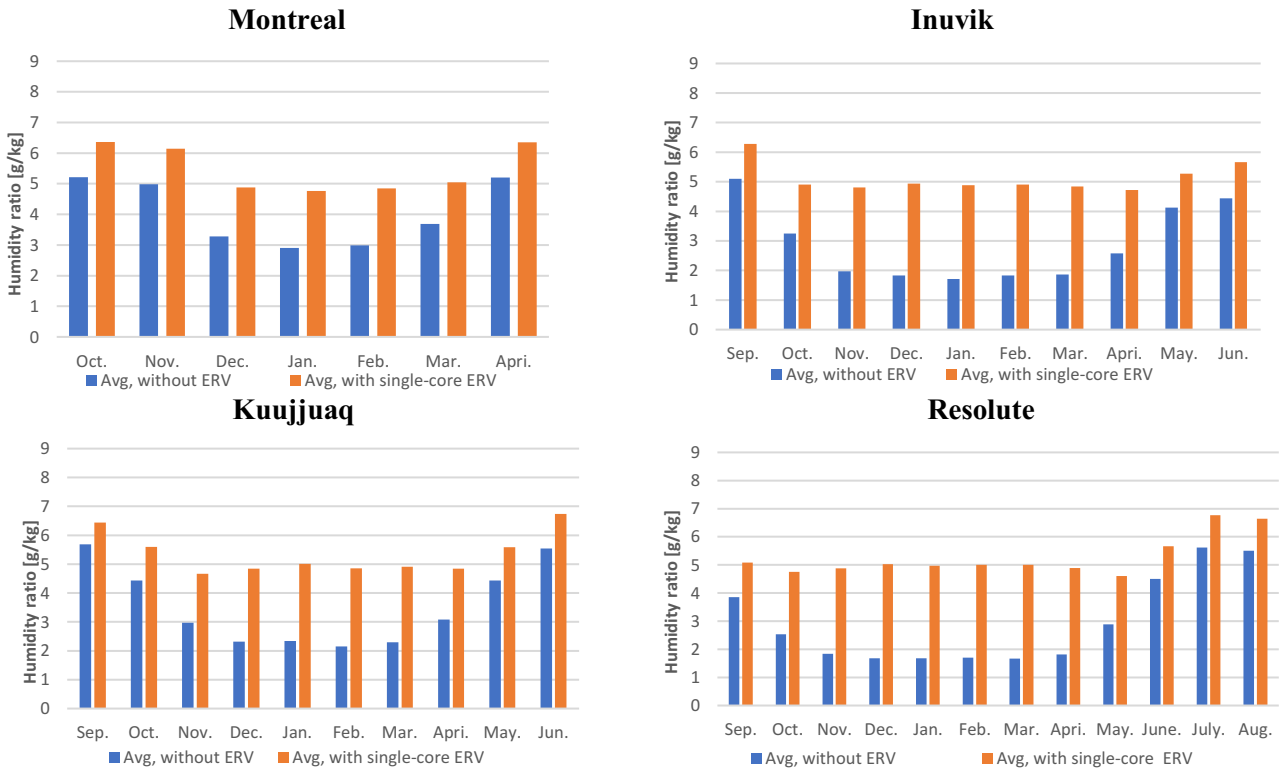


Figure 28: Indoor humidity ratio with and without single-core ERV unit during the heating season.

4.3. Impact of different operation schedules of the single-core ERV with the NZEH model

As discussed in Section 4, With longer normal operation time of the ERV unit at low outdoor air temperature T_1 , more ice is accumulated, and the supply air temperature T_2 is lower. On the other hand, longer normal operation time reduces the defrost frequency and the risk of reduced outdoor supply airflow rate. The impact of the longer normal operation time, i.e., 30, 40, and 50 minutes, then the manufacturer’s set schedule (**Table 19**) is presented in this section.

When the duration of normal operation is increased, the heating energy use for ventilation air increases compared with the manufacture’s set schedules (**Table 4**), while the percentage of defrosting hours out of total operation hours decreases, at four selected locations (Inuvik, Kuujuaq and Resolute, and Montreal) (**Table 19**).

Table 19: Increase of annual energy use for heating ventilation air and decrease of percentage of defrost hours of the NZEH model with the increase of normal operation time.

Normal operation time [min]	Energy use for heating the outdoor air [kWh]				decrease of percentage of defrost hours (%)			
	Inuvik	Kuujuuaq	Resolute	Montreal	Inuvik	Kuujuuaq	Resolute	Montreal
30	88	86	167	15	15.5 %	10.5 %	20.4 %	3.4 %
40	147	120	456	19	12.6 %	8.2 %	17.3 %	2.4 %
50	428	343	1241	31	12 %	8 %	11.3 %	2.5 %

Table 20: The fan energy use of the single-core ERV in the NZEH model with the increase of normal operation time.

Duration of normal operation [min]	Fan energy use (kWh)			
	Inuvik	Kuujuuaq	Resolute	Montreal
25 (factory set schedule)	455	262.83	371.35	295
30	453	263.35	363.03	295
40	416	257.32	359.51	294
50	439	256.63	359.51	292

There is no significant impact of changing the operation schedules in Montreal: increase of heating energy use for outdoor air by 31 kWh at 50 minutes normal operation and 2.5% of defrost hours, and decrease by 3 kWh of fan energy use (**Table 20**). However, the impact is greater at the three arctic locations. The ventilation energy use increases by 428.16 kWh at Inuvik, and 1241 kWh at Resolute; while there is a slight decrease of 16 kWh of fan energy use at Inuvik, 6 kWh at Kuujuaq, and 12 kWh at Resolute. One can conclude, based on these results, that the manufacturer's set schedules of normal operation duration should be used in the three arctic locations, when the single-core ERV unit is used for NZEH model.

4.4. Dual-core ERV with the NZEH model

When the dual-core ERV unit is used, the required outdoor air ventilation rate is supplied continuously, and it can keep the indoor air quality at desired level. However, this comes at the cost

of increasing the energy use for ventilation. At the three northern locations, the heating energy use for ventilation air and fans increases by 15% at Kuujuaq and 22.7 % at Inuvik (**Table 21**). There is no impact in the case of NZEH in Montreal.

Table 21: Annual energy use for heating the outdoor air and fans: comparison between the single-core ERV and dual-core ERV, in the case of NZEH model.

Location	Single-core		Dual-core		Increase of total energy use for fans and heating of ventilation air (%) (dual-core v.s. single-core)
	Heating of ventilation air (kWh)	Fans energy use (kWh)	Heating of ventilation air (kWh)	Fans energy use (kWh)	
Inuvik	3390	277.15	4173	318.84	22.7
Kuujuaq	3087	262.83	3507	348.18	15
Resolute	4795	371.35	5748	502.87	20.1
Montreal	1938	223.35	1935	235.33	0.4

The use of dual-core and single-core ERV units significantly increases the indoor humidity ratio of the case study NZEH model at four locations, compared to the case without ERV unit (**Figure 29**). The highest increase of indoor humidity ratio is obtained in January in Resolute, from 1.8 g/kg to 4.3 g/kg. There is a slight difference between the indoor humidity ratio due to the dual-core ERV unit versus single-core unit.

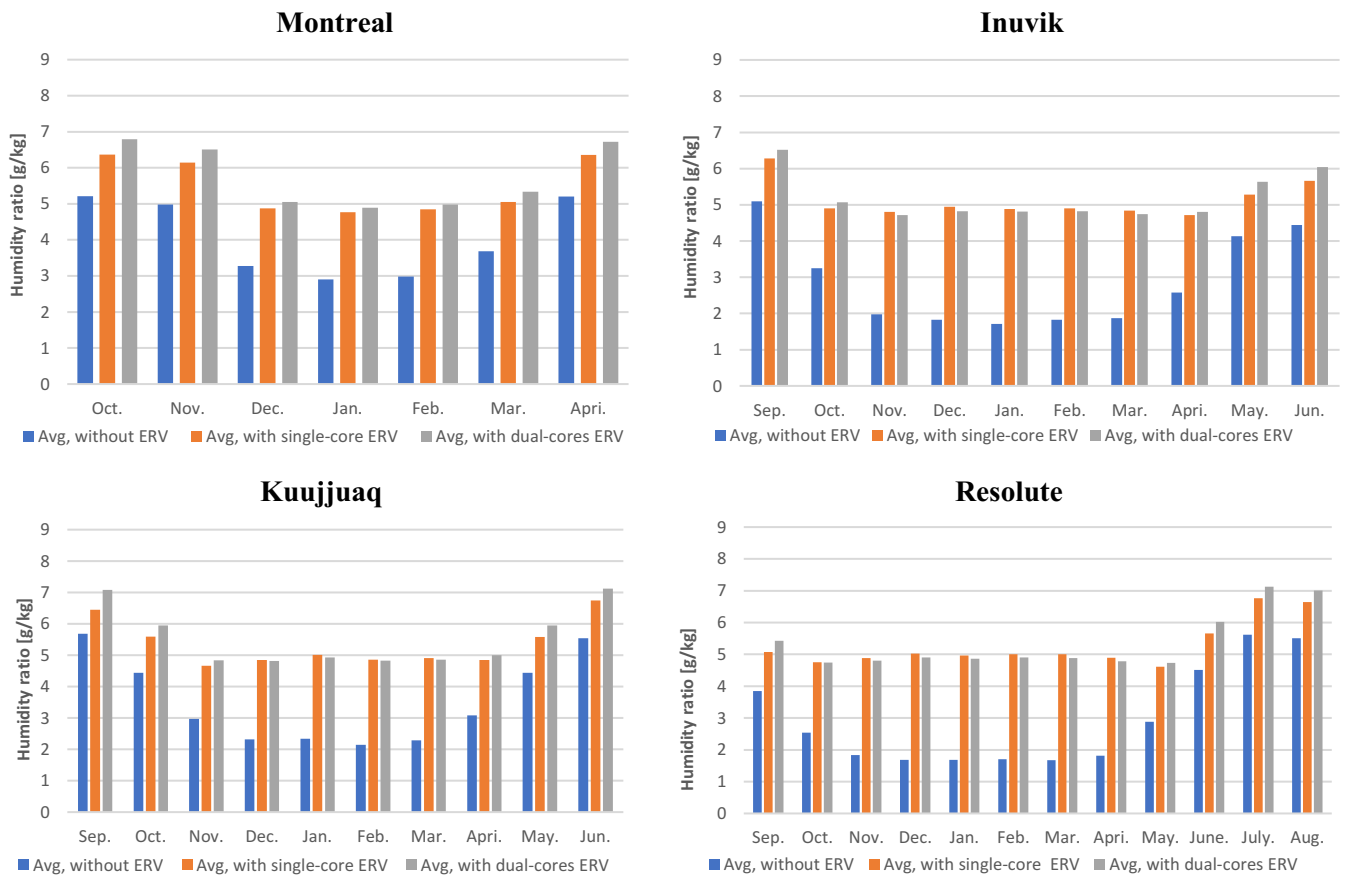


Figure 29: Monthly average indoor humidity ratio: comparison of cases without ERV, single-core ERV and dual-cores ERV units for NZEH model.

4.5. Single-core versus dual-core ERV with northern CNH and NSH Models.

This section presents the results from the simulation of dual-core and single-core ERV units, when installed in the ventilation systems of CNH and NSH, at the same four locations.

Since CNH and NSH models have the same ventilation rate and house volume, the predicted annual energy use for heating the ventilation air and fans are identical. The increase in energy use for heating the outdoor air and fans is between 2.2% to 21.5% when the dual-core ERV units are used instead of the single-core ERV unit (**Table 22**). The increase of annual energy use of heating the outdoor air and fans are different between the NZEH model and CNH and NSH models due to the different house volume that they have. Compared with the pre-heating, dual-core leads to a significant reduction in energy use for heating the outdoor air (**Table 23**) for CNH and NSH

models, which is about 56-62% for all four locations. The energy use for heating outdoor air, for instance in Inuvik, accounts for 27% and 32% of the total heating energy use (space heating plus heating for ventilation air) in CNH and NSH, respectively, when pre-heating is used, while this portion becomes 12% and 15% when dual-core ERV is used.

Table 22: Annual energy use for heating the outdoor air: comparison between single-core and dual-core ERV units used in CNH and NSH models.

Locations	Single-core			Dual-core		Increase of total energy use for heating of ventilation air and fans (%) (dual-core v.s. single-core)
	Defrost hours (%)	Heating of ventilation air (kWh)	Fans energy use (kWh)	Heating of ventilation air (kWh)	Fans energy use (kWh)	
Inuvik	16.11	5298	455	6370	593	21
Kuujuuaq	10.85	4928	434	5433	560	11.8
Resolute	15.74	7296	610	8798	808	21.5
Montreal	4.74	3201	295	3198	375	2.2

Table 23: Annual space heating energy use and energy use of heating the outdoor air: comparison between dual-core and pre-heating ERV used with CNH and NSH models.

Locations	Space heating (kWh)		Heating of ventilation air (kWh)			Decrease in total heating energy use (space+ventilation) (dual-core v.s. pre-heating) (%)	
	CNH	NSH	Pre-heating	Dual-core	Energy saving (dual-core v.s. pre-heating) (%)	CNH	NSH
Inuvik	45192	35934	16768	6370	62	17	20
Kuujuuaq	37492	28894	13653	5433	60	16	19
Resolute	63532	48373	22779	8798	61	16	20
Montreal	20551	15394	7303	3198	56	15	18

Figure 26 presents the monthly average indoor humidity ratio of both CNH and NSH models incorporating either single-core or dual-core. CNH and NSH have the same house humidity ratio, due to the same infiltration rate, occupancy humidity, ventilation rate. Compared with the case without ERV, there is a considerable increase in the humidity ratio in both CNH and NSH

models when using the single-core and dual-core ERV units (**Figure 30**). The highest increase occurs in January in Resolute, from 2.1 g/kg to 6 g/kg.

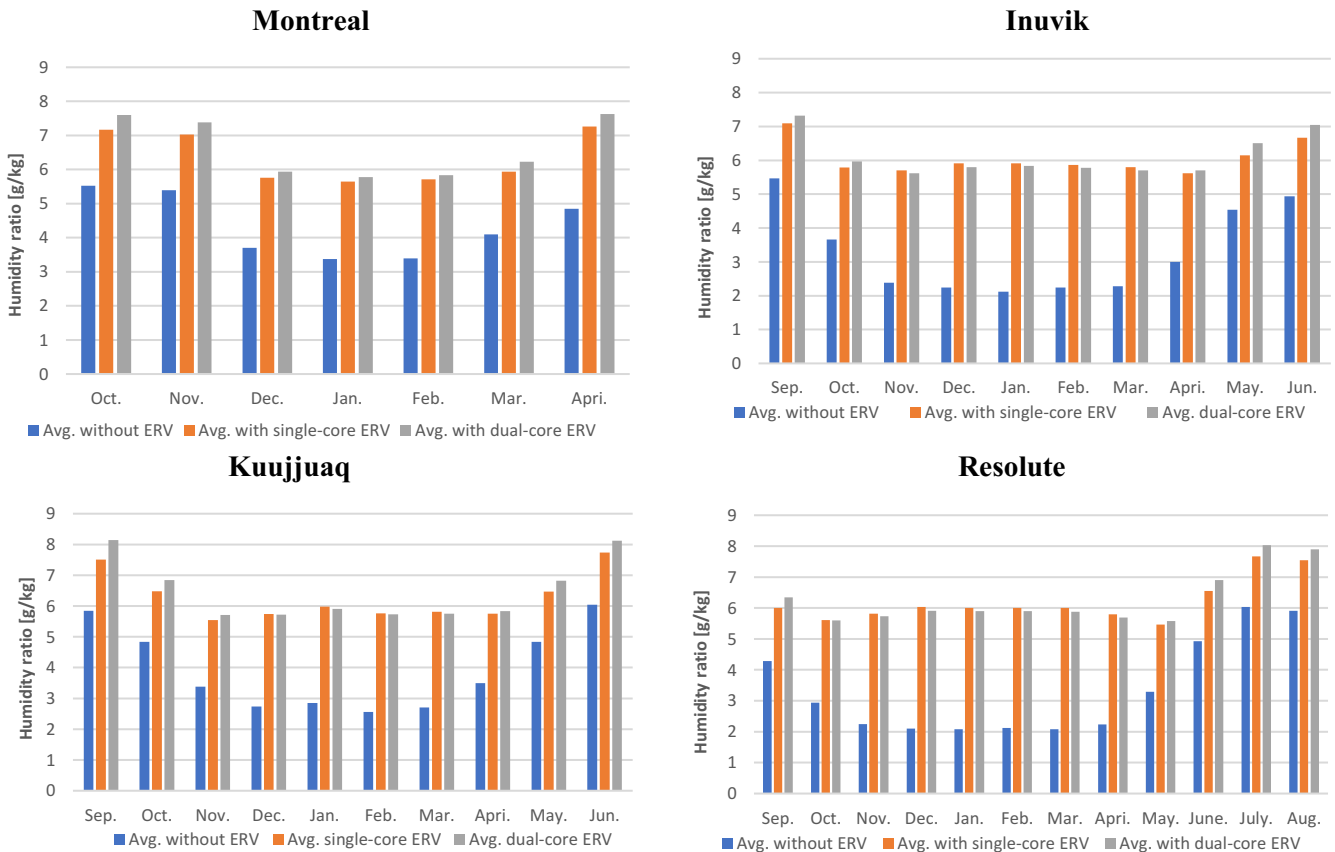


Figure 30: Monthly average indoor humidity ratio: comparison of cases without ERV, single-core ERV and dual-cores ERV units for CNH and NSH models.

4.6. Summary

The ERV ais studied in NZEH model in the three arctic cities (Inuvik, Kuujuaq and Resolute) in terms of three case studies as follow: i) with and without single-core ERV, ii) different threshold temperature for the defrost of single-core ERV, iii) different operation time and iv) preheating and recirculating defrost. Compared with the built-in ERV unit (667 b) in TRNSYS, the correlation-based models of ERV unit, adopted under frosting condition, can provide more accurate results on the energy use of heating the ventilation air and supply air temperature and relative humidity with

16 % of accuracy increase. Compared without the single-core ERV unit, the single-core ERV unit with the recirculating defrost see the significant energy savings of heating the ventilation air, for instance, in Inuvik with the largest decrease of 26 % among three arctic cities, while reduces 13% of airflow rate. The indoor humidity was also increased significantly due to the increased humidity ratio of supply air of the unit. Moreover, the single-core ERV unit with -10 °C of threshold temperature for defrost can significantly reduce energy use of heating the ventilation air but the airflow rate decrease considerably, compared with the case with -20 °C of threshold temperature. Lastly, the increase of the normal operation time leads to a significant increase of the energy use of heating the ventilation air (e.g. 428. 16 kWh in Inuvik). The preheating defrost, commonly used in the arctic but not optimal due to its significant energy use, is tested to compare with the recirculating defrost which shows the significant energy increase (e.g. 230% in Inuvik) by using the recirculating defrost.

The case studies regarding the preheating defrost and dual-core operation are carried out in section 4. The use of dual-core provides the continuous supply of outdoor air while increases the total energy use for heating outdoor air and fans, by 22.7 % in Inuvik in NZEH, 21% in CNH and NSH, compared with the single-core ERV with recirculation defrost. In the meanwhile, compared with pre-heating defrost, dual-core ERV significantly reduces the annual energy use for heating the outdoor air. for instance, by 63% in Inuvik in NZEH. This energy savings represents 17% of heating energy use in NZEH, 17% in CNH and 20% in NSH, respectively.

5. CONCLUSIONS

The thesis presented the development of new correlation-based models to be used for the simulation of thermal performance during the normal versus defrost by recirculation of single-core and dual-core ERV units, based on previous laboratory-controlled measurements. The model was validated by measurements in [34]. Comparison between TRANSYS model and the correlation-based model including frost/defrost is made, and showed that the correlation-based model provides more accurate calculation in energy use by ERV and indoor humidity with 16 % of accuracy increase. Therefore, the new correlation-based models of ERV unit are recommended whenever the frosting of the unit is observed. In addition, the models were linked with the TRNSYS model of a case study NZEH to study the impact at three arctic locations in comparison with the cold climate of Montreal. The developed models in equation box and built-in ERV models (Type 667b) in TRNSYS are combined to simulate the thermal performance of ERV unit in NZEH model. Developed models are used when the frost is observed, otherwise only built-in ERV (Type 667b) is deployed.

Main conclusions are:

1. The main contribution of this thesis is the development of correlation-based ERV models. This model can be used in the energy models to simulate the energy impact of ERV unit under the cold (arctic) climate.
2. Compared with the case without ERV, the single-core ERV with the recirculation simulated in NZEH model reduces the energy use for heating the outdoor air, at the cost of reduced air ventilation rate in three arctic cities (Inuvik, Kuujuaq and Resolute) and Montreal. For instance, the heating energy use in Inuvik is reduced by 26 % while the airflow rate is reduced by 13% (701 defrost hours), which is the highest among the three arctic locations.
3. Single-core with the recirculation defrost, simulated in NZEH, CNH and NSH models, can increase indoor relative humidity given the higher air humidity of the supply air of the ERV unit during the defrost. For instance, the average indoor humidity ratio in January in Inuvik

increased from 1.7g/kg (without ERV unit) to 4.9 g/kg (with ERV unit), which is the increase of indoor relative humidity from 10.9 % to 31.9 % with the largest increase among the three arctic cities.

4. Different proposed operation schedules (30, 40 and 50 minutes of normal operation) are also tested in the single-core ERV in NZEH model. The increase of normal operation time results in a significant increase of ventilation energy use in all three arctic cities (e. g., Inuvik with 428.16 kWh of increase of heating energy use for outdoor air in 50 minutes operation). Therefore, the factory set operation schedules should be used in the arctic climates.
5. The single-core ERV with -10 °C and -20 °C of threshold temperature for the recirculating defrost are assessed in the NZEH model. The single-core ERV with -10 °C compared with -20 °C of threshold temperature significantly reduce the energy use of heating the outdoor air (e.g. 7% in Kuujjuaq) at the cost of the considerable decrease of airflow rate (e.g. 67% in Kuujjuaq)
6. The preheating defrost, commonly used in the arctic but not optimal due to its significant energy use, is tested to compare with the recirculating defrost, which shows the significant energy increase (e.g. 230% in Inuvik in NZEH) by using the preheating defrost.
7. Dual-core ERV unit, simulated in NZEH, CNH and NSH models, has the advantage of continuously supplying outdoor air at the cost of increasing the total energy use for heating outdoor air and fans, by 22.7 % in Inuvik in NZEH, 21% in CNH and NSH, respectively, compared with the single-core ERV with recirculation defrost.
8. Compared with pre-heating defrost, dual-core ERV, simulated in NZEH, CNH and NSH, significantly reduces the annual energy use for heating the outdoor air. for instance, by 63% in Inuvik in NZEH. This energy savings represents 17% of heating energy use in NZEH, 17% in CNH and 20% in NSH, respectively.
9. Dual-core ERV unit, simulated in NZEH, CNH and NSH models, increases the indoor air humidity during the heating season. For instance, the average indoor humidity ratio in

January in Inuvik increased from 1.7g/kg (without ERV unit) to 4.7 g/kg (dual-core ERV unit), which is the increase of indoor relative humidity from 10.9 % to 30.9 % with the largest increase among the three arctic cities.

Future work should include the development of correlation-based models for the other types of ERV, from different manufacturers, and using different strategies for controlling the defrost operation, for example, MERV 1 with recirculation or preheating defrost in NZEH and two northern houses (MNECH house and NSH house, respectively, in an arctic climate).

REFERENCES

- [1] “Northern Canada,” Wikipedia. Jul. 13, 2021. Accessed: Jul. 14, 2021. [Online Available]: https://en.wikipedia.org/w/index.php?title=Northern_Canada&oldid=1033451059
- [2] N. E. Board, “Energy Facts - Energy Use in Canada’s North,” 2011. <https://www.cer-rec.gc.ca/en/data-analysis/energy-markets/archive/energy-use-canada-north-facts-2011/energy-use-in-canadas-north-overview-yukon-northwest-territories-nunavut-energy-facts.html>
- [3] J. Kruse, B. Poppel, L. Abryutina, G. Duhaime, S. Martin, M. Poppel, M. Kruse, E. Ward, P. Cochran, and V. Hanna, “Survey of Living Conditions in the Arctic (SLiCa),” in *Barometers of Quality of Life Around the Globe*, pp. 107–134, 2008.
- [4] N.H. Corporation, “The GN Long-Term Comprehensive Housing and Homeless Strategy Tamapta,” accessed: May 09 2021 <http://blueprintforaction.ca/docs/other/nhc-homelessness-en.pdf>
- [5] S. Canada, “Focus on Geography Series, 2011 Census - Census subdivision of Iqaluit,” no. 98-310-XWE2011004, 2012. <https://www12.statcan.gc.ca/census-recensement/2011/as-sa/fogs-spg/Facts-csd-eng.cfm?Lang=eng&GK=CSD&GC=6204003>.
- [6] Statistics Canada, “Focus on Geography Series, 2011 Census - Census subdivision of Iqaluit,” no. 98-310-XWE2011004, 2012. [Online]. <https://www12.statcan.gc.ca/census-recensement/2011/as-sa/fogs-spg/Facts-csd-eng.cfm?Lang=eng&GK=CSD&GC=6204003>.
- [7] Housing in Inuit Nunangat.” Accessed: May 05, 2021. [Online]. <https://www.nunivaat.org/doc/document/2019-12-19-02.pdf>.
- [8] M. Rousseau, M. Manning, M. N. Said, S. M. Cornick, and M. C. Swinton, “Characterization of Indoor Hygrothermal Conditions in Houses in Different Northern Climates,” in *Thermal Performance of Exterior Envelopes of Whole Buildings X*, 2007.
- [9] P. at: J. 27 2019-08:47 / U. at: J. 27 2019-08:47 F. G. Sharp, “Tackling the Housing Crisis in Northern Canada.” Accessed: May 06, 2021. <https://www.highnorthnews.com/en/tackling-housing-crisis-northern-canada>
- [10] N. H. Corporation, “Nunavut Housing Needs Survey Backgrounder Nunavut Housing Needs Survey Backgrounder,” 2010. <http://www.stats.gov.nu.ca/en/Housing.aspx>
- [11] N. News, “Overcrowded housing crippling the North’s future: report,” *Nunatsiaq News*, Dec. 16, 2011. https://nunatsiaq.com/stories/article/65674overcrowded_housing_crippling_the_norths_future_report/
- [12] S. G. Donaldson, J. Van Oostdam, C. Tikhonov, M. Feeley, B. Armstrong, P. Ayotte, O. Boucher, W. Bowers, L. Chan, F. Dallaire, R. Dallaire, E. Dewailly, J. Edwards, G. M. Egeland, J. Fontaine, C. Furgal, T. Leech, E. Loring, G. Muckle, T. Nancarrow, D. Pereg, P.

- Plusquellec, M. Potyrala, O. Receveur, and R. G. Shearer, “Environmental contaminants and human health in the Canadian Arctic,” *Sci. Total Environ.*, vol. 408, no. 22, pp. 5165–234, Oct. 2010.
- [13] J. Kruse, B. Poppel, L. Abryutina, G. Duhaime, S. Martin, M. Poppel, M. Kruse, E. Ward, P. Cochran, and V. Hanna, “Survey of Living Conditions in the Arctic (SLiCa),” in *Barometers of Quality of Life Around the Globe*, pp. 107–134. 2008
- [14] D. R. International, Ltd., and under contract to P. N. N. Laboratory, “2011 Buildings Energy Data Book (U.S. Department of Energy) - Institute for Energy and Environmental Research,” accessed Jan. 20, 2021.
<https://ieer.org/resource/energy-issues/2011-buildings-energy-data-book/>.
- [15] N. R. Canada, “R-2000: environmentally friendly homes,” accessed Feb. 02, 2018.
<https://www.nrcan.gc.ca/homes/buying-energy-efficient-new-home/r-2000-environmentally-friendly-homes/20575>.
- [16] ASHRAE. 1997. ASHRAE handbook: Fundamentals, American Society of Heating, Refrigerating and Air-Conditioning Engineers, Atlanta, GA.
- [17] F Steimle, J Roben, “Ventilation requirements in modern buildings”, In: *Proceedings of the 13th AIVC conference Nice. France*, p. 414e22, 1992.
- [18] M. Justo Alonso, P. Liu, H. M. Mathisen, G. Ge, and C. Simonson, “Review of heat/energy recovery exchangers for use in ZEBs in cold climate countries,” *Build. Environ.*, vol. 84, pp. 228–237, Jan. 2015.
- [19] J. Zhang and A. S. Fung, “Experimental and numerical investigation of the thermal impact of defrost cycle of residential heat and energy recovery ventilators,” *Energy Build.*, vol. 97, pp. 129–136, Jun. 2015.
- [20] P. Liu *et al.*, “A theoretical model to predict frosting limits in cross-flow air-to-air flat plate heat/energy exchangers,” *Energy Build.*, vol. 110, pp. 404–414, Jan. 2016.
- [21] C. Beattie, P. Fazio, R. Zmeureanu, and J. Rao, “Experimental study of air-to-air heat exchangers for use in arctic housing,” *Appl. Therm. Eng.*, vol. 129, pp. 1281–1291, Jan. 2018.
- [22] R. Östin, “A study of heat exchange under frosting conditions,” *Heat Recovery Syst. CHP*, vol. 12, no. 2, pp. 89–103, Mar. 1992.
- [23] D. W. Schulte and R. H. Howell, “The Effects of Air Turbulence on the rate of Frost Growth on a Horizontal Plate,” *ASHRAE Trans.*, vol. 88, no. pt. 2, pp. 201–217, 1982.
- [24] M. R. Nasr, M. Fauchoux, R. W. Besant, and C. J. Simonson, “A review of frosting in air-to-air energy exchangers,” *Renew. Sustain. Energy Rev.*, vol. 30, pp. 538–554, Feb. 2014.
- [25] WJ Fisk, RE Chant, KM Archer, D Hekmat, FJ Offermann, BS Pedersen, “Performance of residential air-to-air heat exchangers during operation with freezing and periodic defrosts,” *ASHRAE Trans*, vol. 91, pt.1, pp. 159-172, 1985.

- [26] EG Phillips, RE Chant, BC Bradley, DR Fisher. “A model to compare freezing control strategies for residential air-to-air heat recovery ventilators,” *ASHRAE Trans*, vol. 95, pt. 2, pp. 454-483, 1989.
- [27] E. G. Phillips, D. R. Fisher, R. E. Chant, and B. C. Bradley, “Freeze-control strategy and air-to-air energy recovery performance,” *ASHRAE J*, vol. 34, no. 12, pp. 44–49, Dec. 1992.
- [28] “Frost-Control-Strategies-for-Airxchange-Wheels.pdf,” *Airxchange Inc*, Accessed: Jan. 16, 2021.
<https://www.airxchange.com/wp-content/uploads/2019/10/Frost-Control-Strategies-for-Airxchange-Wheels.pdf>.
- [29] J. Y. Jang, H. H. Bae, S. J. Lee, and M. Y. Ha, “Continuous heating of an air-source heat pump during defrosting and improvement of energy efficiency,” *Appl. Energy*, vol. 110, pp. 9–16, Oct. 2013.
- [30] S. Gendebien, A. Parthoens, and V. Lemort, “Investigation of a single room ventilation heat recovery exchanger under frosting conditions: Modeling, experimental validation and operating strategies evaluation,” *Energy Build.*, vol. 186, pp. 1–16, 2019.
- [31] M. Kassai, “A developed method for energy saving prediction of heat-and energy recovery units,” *Energy Procedia*, vol. 85, no. November 2015, pp. 311–319, 2016.
- [32] J. Berquist, C. Banister, and D. Krysz, “Performance of an advanced heat recovery ventilation system in the Canadian Arctic,” *Int. J. Vent*, pp. 1–10, 2020.
- [33] J. Rose, T. R. Nielsen, J. Kragh, and S. Svendsen, “Quasi-steady-state model of a counterflow air-to-air heat-exchanger with phase change,” *Appl. Energy*, vol. 85, no. 5, pp. 312-325, May 2008.
- [34] J. Zhang and A. S. Fung, “Experimental study and analysis of an energy recovery ventilator and the impacts of defrost cycle,” *Energy Build.*, vol. 87, pp. 265–271, Jan. 2015.
- [35] M. Leckner, R. Zmeureanu, “Life Cycle Cost and Energy Analysis of a Net Zero Energy House with Solar Combisystem,” *Applied Energy*, Vol. 88, pp. 232-241, 2011.
- [36] C. M. H. Corporation. (2014), “Northern Housing Project Profile: The Inuvik Northern Sustainable House”, *Canada Mortgage and Housing Corporation*, 2014.
- [37] C. M. H. Corporation. (2014), “Northern Housing Project Profile: The Arviat Northern Sustainable House,” *Canada Mortgage and Housing Corporation*, 2014.
- [38] C. M. H. Corporation. (2014), “Northern Housing Project Profile: The Dawson E/2 Northern Sustainable House,” *Canada Mortgage and Housing Corporation*, 2014.
- [39] C. M. H. Corporation. (2014), “Northern Housing Project Profile: The Dawson E/9 Northern Sustainable House,” *Canada Mortgage and Housing Corporation*, 2014.
- [40] C. Zeng, S. Liu, and A. Shukla, “A review on the air-to-air heat and mass exchanger technologies for building applications,” *Renew. Sustain. Energy Rev.*, vol. 75, pp. 753–774, Aug. 2017, doi: 10.1016/j.rser.2016.11.052.

- [41] D. O'Connor, J. K. S. Calautit, and B. R. Hughes, "A review of heat recovery technology for passive ventilation applications," *Renew. Sustain. Energy Rev.*, vol. 54, pp. 1481–1493, Feb. 2016, doi: 10.1016/j.rser.2015.10.039.
- [42] E. Zender-Świercz, "A Review of Heat Recovery in Ventilation," *Energies*, vol. 14, no. 6, Art. no. 6, Jan. 2021, doi: 10.3390/en14061759.
- [43] L. Z. Zhang and J. L. Niu, "Energy requirements for conditioning fresh air and the long-term savings with a membrane-based energy recovery ventilator in Hong Kong," *Energy*, vol. 26, pp. 119–135, 2001.
- [44] M. Nasif, R. AL-Waked, G. Morrison, and M. Behnia, "Membrane heat exchanger in HVAC energy recovery systems, systems energy analysis," *Energy Build.*, vol. 42, pp. 1833–1840, Oct. 2010.
- [45] B. K. Ouazia, M. Julien, M. C. Swinton, and M. Manning, "Assessment of the Enthalpy Performance of Houses Using Energy Recovery Technology," *ASHRAE Trans.*, vol. 112, no. 1, pp. 26–34, 2006.
- [46] C. G. Barringer and C. A. McGugan, "Effects of Residential air-to-air Heat and Moisture Exchangers on indoor humidity.pdf," *ASHRAE Trans.*, vol. 95, no. Part 2, pp. 461–474, 1989.
- [47] R. N. Huizing, "Coated Membranes for Enthalpy Exchange and Other Applications," US 2012/0061045 A1, 2012.
- [48] J. L. Niu and L. Z. Zhang, "Membrane-based Enthalpy Exchanger: material considerations and clarification of moisture resistance," *J. Memb. Sci.*, vol. 189, pp. 179–191, 2001.
- [49] Y. Zhang, Y. Jiang, L. Z. Zhang, Y. Deng, and Z. Jin, "Analysis of thermal performance and energy savings of membrane-based heat recovery ventilator," *Energy*, vol. 25, no. 6, pp. 515–527, Jun. 2000.
- [50] P. Taylor, J. Nie, J. Yang, L. Fang, and X. Kong, "Experimental evaluation of enthalpy efficiency and gas-phase contaminant transfer in an enthalpy recovery unit with polymer membrane foils Experimental evaluation of enthalpy efficiency and gas-phase contaminant transfer in an enthalpy recovery unit with," *Sci. Technol. Built Environ.*, vol. 21, pp. 150–159, 2015.
- [51] L.-Z. Zhang, "Progress on heat and moisture recovery with membranes: From fundamentals to engineering applications," *Energy Convers. Manag.*, vol. 63, pp. 173–195, Nov. 2012.
- [52] E. G. Phillips, L. C. Bradley, R. E. Chant, and D. R. Fisher, "Comparison of freezing control strategies for residential air-to-air heat recovery ventilators," *ASHRAE Trans*, vol. 95, pt 2, pp. 25-28, Jan. 1989,
- [53] P.T. Ninomura, R. Bhargava, "Heat recovery ventilators in multifamily residences in the arctic," *ASHRAE Trans*, vol. 101, pt. 2, pp. 14-97, 1995.
- [54] G. B. Davis, "Energy recovery ventilator: means for defrosting heat exchanger medium and damper motor actuation means," *US. Patent 5497823A*, vol 5, pp. 497-823, 1996.

- [55] J. Berquist, C. Banister, and M. Pellissier, “Comparison of Heat Recovery Ventilator Frost Control Techniques in the Canadian Arctic: Preheat and Recirculation,” in *Cold Climate HVAC & Energy*, vol. 246, pp. 11010, 2021.
- [56] M. Rafati Nasr, M. Kassai, G. Ge, and C. J. Simonson, “Evaluation of defrosting methods for air-to-air heat/energy exchangers on energy consumption of ventilation,” *Appl. Energy*, vol. 151, pp. 32–40, Aug. 2015.
- [57] J. Liu, W. Li, J. Liu, and B. Wang, “Efficiency of energy recovery ventilator with various weathers and its energy saving performance in a residential apartment,” *Energy Build.*, vol. 42, no. 1, pp. 43–49, Jan. 2010.
- [58] Y. P. Zhou, J. Y. Wu, and R. Z. Wang, “Performance of energy recovery ventilator with various weathers and temperature set-points,” *Energy Build.*, vol. 39, no. 12, pp. 1202–1210, Dec. 2007.
- [59] M. Rasouli, C. J. Simonson, and R. W. Besant, “Applicability and optimum control strategy of energy recovery ventilators in different climatic conditions,” *Energy Build.*, vol. 42, no. 9, pp. 1376–1385, Sep. 2010.
- [60] J. Jokisalo, J. Kurnitski, M. Vuolle, and A. Torkki, “Performance of Balanced Ventilation with Heat Recovery in Residential Buildings in a Cold Climate,” *Int. J. Vent.*, vol. 2, no. 3, pp. 223–236, Dec. 2003.
- [61] S. Anisimov, A. Jedlikowski, and D. Pandelidis, “Frost formation in the cross-flow plate heat exchanger for energy recovery,” *Int. J. Heat Mass Transf.*, vol. 90, pp. 201–217, Nov. 2015.
- [62] T. R. Nielsen, J. Rose, and J. Kragh, “Dynamic model of counter flow air to air heat exchanger for comfort ventilation with condensation and frost formation,” *Appl. Therm. Eng.*, vol. 29, no. 2–3, pp. 462–468, Feb. 2009.
- [63] J. Kragh, J. Rose, T. R. Nielsen, and S. Svendsen, “New counter flow heat exchanger designed for ventilation systems in cold climates,” *Energy Build.*, vol. 39, no. 11, pp. 1151–1158, Nov. 2007.
- [64] B. Ouazia, C. Arsenault, Y. Li, M. Brown, and C. Chisholm, “Long-term performance and resiliency testing of a dual core energy recovery ventilation system for the Arctic,” *National Research Council of Canada*, 2019.
- [65] J. Kragh, J. Rose, and S. Svendsen, “Mechanical ventilation with heat recovery in cold climates,” *Proc. Seventh Nord. Symp. Build. Phys. Nord. Ctries.*, Jan. 2005.
- [66] P. Vladykova, C. Rode, J. Kragh, M. Kotol, “Low-energy house in arctic climate : five years of experience,” *J. Cold Reg. Eng.* Vol. 26, pp. 79–100, 2012.
- [67] B. Ouazia, G. Gnanamurugan, C. Arsenault, and Y. Li, “Performance of a dual core energy recovery ventilation system for use in Arctic housing,” *National Research Council of Canada*, 2018
https://www.aivc.org/sites/default/files/D1_S4B-02.pdf

- [68] S. E. Laboratory at U. of Wisconsin-Madison. USA, "Type 667b: Air-to-air heat exchanger," *TRNSYS 17 TESS Libraries*. Vol. 6, 2017.
<https://sel.me.wisc.edu/trnsys/>
- [69] F. Breque, M. Nemer, "Frosting modeling on a cold flat plate: Comparison of the different assumptions and impacts on frost growth predictions," *Int. J. Refrig*, Vol. 69, pp. 340-360, 2016"
- [70] Venmar AVS, "Product Sheet: Venmar AVS ERV EKO 1.5," no. 120309. 2012.
<https://www.venmar.ca/111-air-exchangers-eko-1-5-erv.html>
- [71] N. R. C of Canada, "Model national energy code of Canada for houses 1997," *Ottawa: Institute for Research in Construction, National Research Council of Canada*, 1997.
- [72] Klein, SA, Beckman, WA, Mitchell, JW, Duffie, JA, Duffie, NA, Freeman, TL, Mitchell, JC, Braun, JE, Evans, BL, Kummer, JP, Urban, RE, Fiksel, A, Thornton, JW, Blair, NJ, Williams, PM, Bradley, DE, McDowell, TP, Kummert, M & Arias, D 2006, *TRNSYS16 - A TRaNsient System Simulation program*. *The University of Wisconsin Madison, WI*
<http://sel.me.wisc.edu/trnsys/>
- [73] Solar Energy Industries Association 2006, *Photovoltaic*. Retrieved January 23, 2006, www.seia.org/solartypes.php#
- [74] *EnergyPlus Weather Data*, accessed Nov. 21, 2020
<https://energyplus.net/weather>
- [75] L. Xing, "Estimations of undisturbed ground temperatures using numerical and analytical modeling," no. 406. 2008.
- [76] American Society of Heating, Refrigerating and Air-Conditioning Engineers (ASHRAE), "2017 ASHRAE handbook: Fundamentals," *Atlanta, GA: ASHRAE*, 2017.
- [77] T.Kasuda, PR , Archenbach, 'Earth Temperature and Thermal Diffusivity at Selected Stations in the United States', *ASHRAE Transactions*, Vol. 71, Part 1, 1965.

APPENDIX A. THE DEVELOPMENTS OF CORRELATION-BASED MODELS.

A.1. Supply air temperature T_2 / humidity w_2 during the defrost.

Table A.1: Supply air temperature T_2 at the beginning and end of defrost operation [21].

T_1 [°C]	T_3 [°C]	T_2 at the beginning of defrost operation [°C]	T_2 at the end of defrost operation [°C]
-10	21.7	14.1	18
-15	21.7	13.8	18
-20	21.7	12	18
-25	21.7	10.45	18
-35	21.7	8	18

Table A.2: Supply air humidity w_2 at the beginning and end of the defrost operation [21]

T_1 [°C]	[g/kg]	at the beginning of defrost operation [g/kg]	at the end of defrost operation [g/kg]
-10	5.44	3.74	6.1
-15	5.44	3.63	6.1
-20	5.44	3.46	6.1
-25	5.44	3.20	6.1
-35	5.44	2.75	6.1

A.2. Different proposed operation schedules.

For the 30 minutes normal operation, The coefficients (**Equation 1**) at -10°C, -15°C, -20°C and -25°C are A=0.006126236, B=0.328184136, C=0.097176434 and D=1.102336623, and the coefficients (**Equation 1**) at -35 are A=0.00409994, B=0.55968648, C=0.18028934 and D=1.12599307.

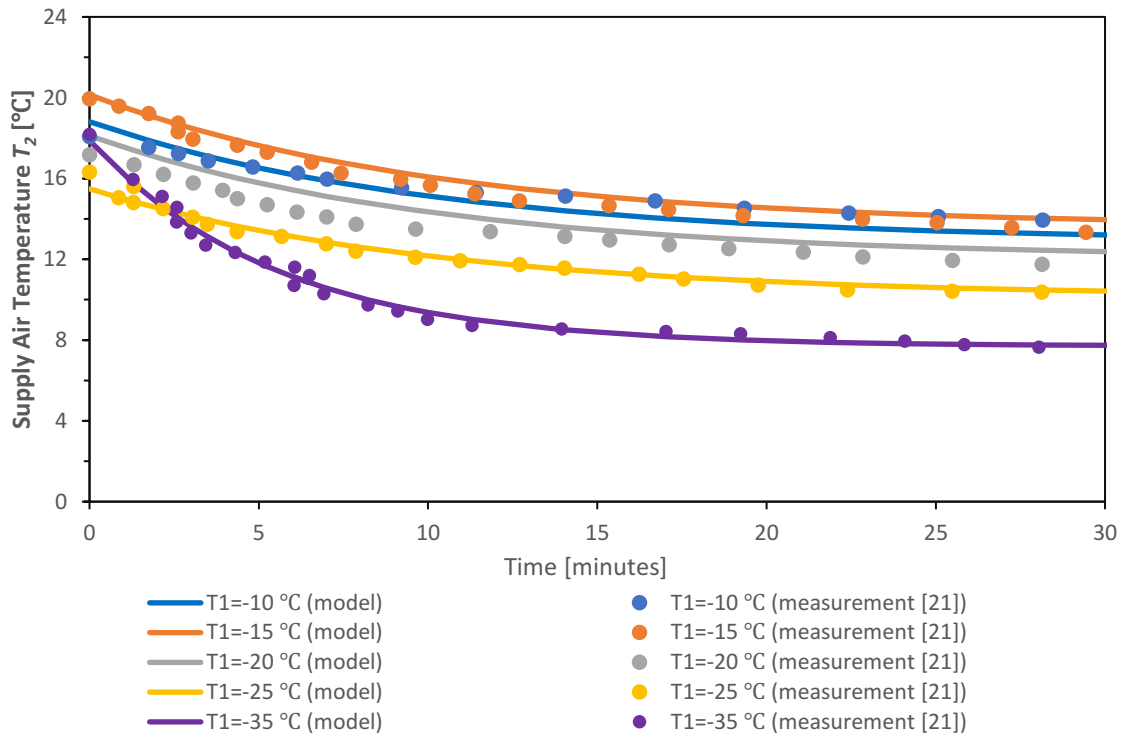


Figure A.1: Predicted versus measured [21] supply air temperature at different outdoor air temperature T_1 during 30 minutes normal operation

Table A.3: Supply air temperature T_2 at the beginning and end of the defrost operation.

T_1 [°C]	T_3 [°C]	T_2 at the beginning of defrost operation [°C]	T_2 at the end of defrost operation [°C]
-10	21.7	13.69	18
-15	21.7	13.026	18
-20	21.7	11.517	18
-25	21.7	10.188	18
-35	21.7	7.6	18

The coefficients at -10°C, -15°C and -20°C and -25°C (**Equation 3**) are determined as follow:

$A = -0.007$ and $B = 0.51$, $C = 0.2517$ and $D = 16.489$, and the coefficients (**Equation 3**) at -35°C are

$A = -0.002$ and $B = 0.47$.

For the 40 minutes normal operation, the predicted supply air temperature T_2 (**Figure A.2**) agrees well with the measured supply air temperature T_2 (**Figure A. 2**) as the coefficient of determination R^2 has values from 0.97 to 0.99. The coefficients at -10°C, -15°C, -20°C and -25°C

are $A=0.00625835$, $B=0.30775931$, $C=0.08453033$ and $D=1.07038996$, and the coefficients at -35°C is $A=0.00625835$, $B=0.55943099$, $C=0.20376209$ and $D=0.97782175$.

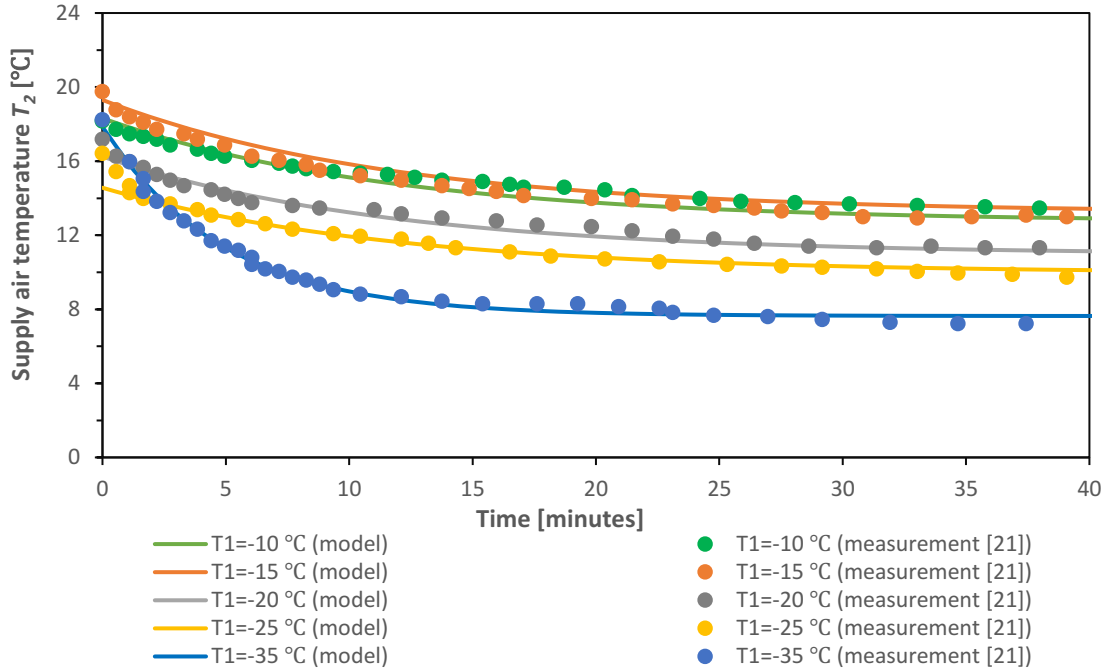


Figure A.2: Predicted versus measured [21] supply air temperature at different outdoor air temperature T_1 during 40 minutes normal operation

Table A.4: Supply air temperature T_2 at the beginning and end of the defrost operation corresponding to 40 minutes normal operation.

T_1 [°C]	T_3 [°C]	T_2 at the beginning of defrost operation [°C]	T_2 at the end of defrost operation [°C]
-10	21.7	13.39	18
-15	21.7	12.86	18
-20	21.7	11.26	18
-25	21.7	9.74	18
-35	21.7	7.23	18

The coefficients at -10°C , -15°C and -20°C (**Equation 3**) are determined as follow: $A=0.007$ and $B=0.51$, $C=0.2582$ and $D=16.318$, and the coefficients at -25°C and -35°C are $A=-0.006$ and $B=0.51$ and $A=-0.0005$ and $B=0.48$, respectively.

For the 50 minutes normal operation, The coefficients (**Equation 3**) at -10°C , -15°C , -20°C and -25°C are $A=0.00706$, $B=0.307315604$, $C=0.083378394$ and $D=1.079394069$, and the coefficients (**Equation 3**) at -35 is $A=0.00706001$, $B=0.56440413$, $C=0.18874996$ and $D=0.96889102$.

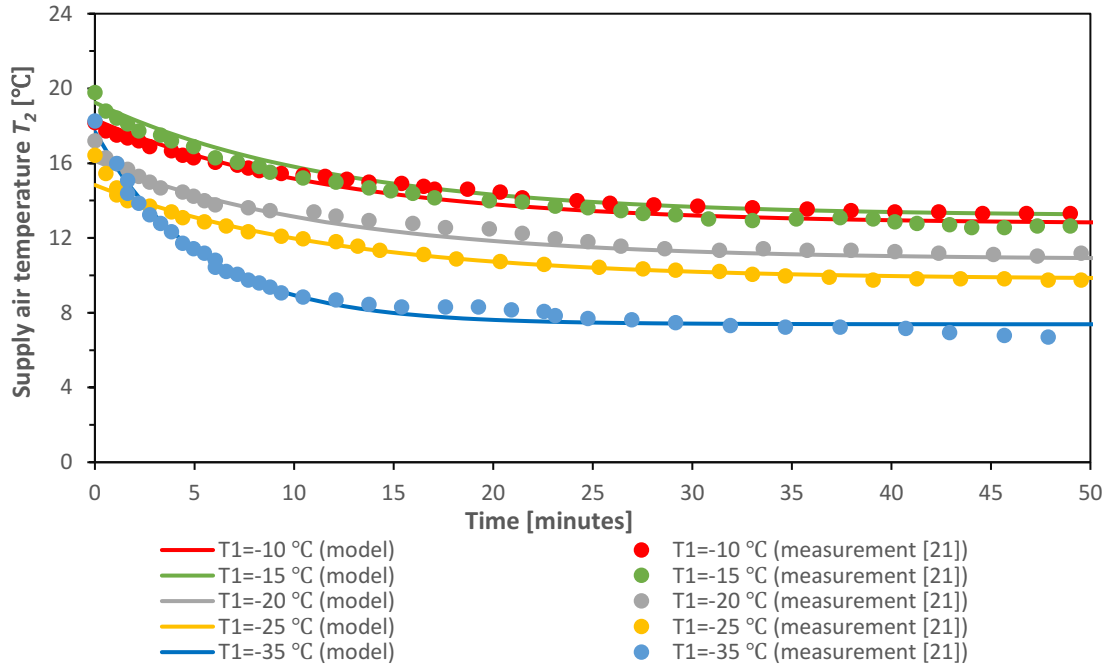


Figure A.3: Predicted versus measured [21] supply air temperature at different outdoor air temperature T_1 during 50 minutes normal operation

Table A.5: Supply air temperature T_2 at the beginning and end of the defrost operation for the 50 minutes normal operation.

Outdoor air temperature, T_1 [$^{\circ}\text{C}$]	Inlet exhaust air temperature, T_3 [$^{\circ}\text{C}$]	Supply air temperature, T_2 at the beginning of defrost operation [$^{\circ}\text{C}$]	Supply air temperature T_2 at the end of defrost operation [$^{\circ}\text{C}$]
-10	21.7	13.39	18
-15	21.7	12.63	18
-20	21.7	11.19	18
-25	21.7	9.74	18
-35	21.7	6.79	18

The coefficients at at -10°C, -15°C and -20°C (**Equation 3**) are determined as follow: A= -0.004 and B=0.51,C=0.2685 and D=16.371, and the coefficients at -25 °C and -35°C (**Equation 3**) are A= -0.002 and B= 0.51 and A= -0.0006 and B= 0.49, respectively.

APPENDIX B. PARAMETERS AND INPUTS FROM TRNSYS TYPE

B.1. Ground coupling – TYPE 1244.

Parameter 1, Amplitude of Surface Temperature [75]: 12.8°C in Inuvik; 12.7°C in Montreal; 9.1°C in Kuujjuaq; 14.5°C in Resolute.

Parameter 2, Deep earth temperature [75]: -4.2°C in Inuvik; 6.9°C in Montreal; -0.2°C in Kuujjuaq; -12.2°C in Resolute

Parameter 3, Day of min surface temp: Day 44 in Inuvik; Day 34 in Montreal; Day 30 in Resolute; Day 35 in Kuujjuaq. This value is obtained in TRNSYS by determining the minimum outdoor air temperature of the year from the weather file (Type 55).

The prominent soil in Inuvik is a brown gravel with sand, silt or Clay. The clay and sand are selected as the soil type around the Inuvik home. Similarly, the soil type in this model is defined as clay or sandy in Montreal and Kuujjuaq. The soil type in Resolute is determined as the sand by referencing with Iqaluit, Nunavut being closed to Resolute and built beyond the very sandy soil.

Parameter 4, Soil thermal conductivity: 1.8 W/mK in Montreal, Inuvik and Kuujjuaq; This value comes from [76], p. 26.21. It is based on the high conductivity values for clay and sand, but closer to the clay value since the soil is more clay. The high conductivity value was used to calculate the maximum heat loss through soil in winter. 2.25 W/mK in Resolute; Value taken from the sand [76], p. 26.2.

Parameter 5, Soil Density: 1260 Kg/m³ in Montreal, Inuvik and Kuujjuaq; This is an average between clay and sand from [12], p. 33.3. 1520 Kg/m³ in Resolute; This value is taken from the

sand [76], p. 33.3.

Parameter 6, Soil Specific Heat: 860 J/KgK in Montreal, Inuvik and Kuujuaq; Value taken between clay (920 J/KgK) and sand (800 J/KgK) [12], p. 33.3. 800 J/KgK in Resolute; Value taken from the sand [76], p. 33.3.

Input 1, Air temperature: Connected with the weather component (Type 15) (°C)

Input 2, Soil to Ambient Convection Coefficient: 104.400011 (W/m² ·K)

Input 3, Sky Temperature: Connected with the weather component (Type 15) (°C)

Input 4, Incident Solar Radiation: Connected with the weather component (Type 15)
(KJ/hr.m²)

Input 5, Zone Temperature-1: The air temperature of basement (heated zone A1); Connected with *TAIR_ZONE_A1* of the building component (Type 56)

Input 6-11, Boundary Heat Transfer Rate from the six sides of basement in heated zone A1:
The rate at which energy is transferred out of the interior surface to the ground. This input is connected to the *Qcomo* output from Type 56 (KJ/hr)

Input 12, Zone Temperature-1 : The air temperature of basement (heated zone A1); Connected with *TAIR_GARAGE* of the building component (Type 56)

Input 13-18, Boundary Heat Transfer Rate from the six sides of basement in unheated garage: The rate at which energy is transferred out of the interior surface to the ground. This input is connected to the *Qcomo* output from Type 56 (KJ/hr)

In this model, the basement walls and floors in all directions (N, E, S, W) will affect the earth in a range of 4 m around the house. The initial soil surface temperatures are calculated by using the long-term average (Kusuda correlation [76]) based on the time of year.

B.2. Energy recovery component – Type 667b.

Parameter 1, Humidity mode: 1 (Fraction); the humidity ratio is used as the input.

Input 1, Exhaust air temperature: 22 (°C)

Input 2, Humidity ratio: connected with the output of Type 694 (Fraction)

Input 3, Exhaust air flow rate: 213 in the NZEH model; 321 in the CNH and NSH models (kg/hr)

Input 4, Exhaust air pressure: 0.0229 (atm)

Input 5, Exhaust air drop: 0 (atm) as the default in TRNSYS

Input 6, Fresh air temperature: Connected with the weather component (Type 15) (°C)

Input 7, Humidity ratio [21]: Connected with the weather component (Type 15) (Fraction)

Input 8, Fresh air flowrate [35]: 213 in the NZEH model; 321 in the CNH and NSH models (kg/hr)

Input 9, Fresh air pressure [21]: 0.0000987 (atm)

Input 10, Fresh air drop: 0 (atm) as the default in TRNSYS

Input 11, Sensible effectiveness [21]: 0.7/ 0.73 at single-core/dual-core in the NZEH model; 0.67/0.72 at single-core/dual-core in the CNH and NSH models (Fraction)

Input 12, Latent effectiveness [21]: 0.5/0.59 at single-core/dual-core in the NZEH model; 0.46/0.55 at single-core/dual-core in the CNH and NSH models (Fraction)

APPENDIX. C. SIMULATION RESULTS

C.1. Single-core ERV in compliance with the different proposed normal/defrost operation schedules in the NZEH house model.

Table C.1: Annual energy use for the space heating and heating the outdoor air and defrost hours in the NZEH house in Montreal with the increase of normal operation time, comparison of the case with the single-core ERV unit and without ERV unit

Normal operation minutes	Defrost hours	Space heating (kWh)	With single-core ERV unit		Without ERV unit		
			Energy use for heating the outdoor ait (kWh)	Total heating (kWh)	Energy use for heating the outdoor ait (kWh)	Total heating (kWh)	Energy saving (kWh)
25	223.35	15394	3201	18595	10923	26317	7722
30	219.2	15394	3224	18618	10923	26317	7699
40	153.43	15394	3220	18614	10923	26317	7703
50	160.4	15394	3232	18626	10923	26317	7691

It can be seen (**Table C.1**) that the use of the single ERV unit can all reduce the energy consumption (around 73% ventilation heating savings or 23% total heating savings during the heating months yearly) in the NZEH house regardless of the normal/defrosting schedules involved. The energy us of ventilation heating will slightly increase by 18kw at maximum at 50 min normal operation (0.9% of the ventilation heating or 0.1% of the total heating compared with the manufactured operation schedules) as the normal operation period lasts longer from 25 min to 60 min while the defrost hours will decrease, with 60 min seeing the highest decrease by 38% compared with the manufactured operation schedules. **Table C.2** presents the fan energy use at the different normal/defrost operation schedules.

Table C.2: Annual energy use for the space heating and heating the outdoor air and defrost hours in the NZEH house in Inuvik with the increase of normal operation time, comparison of the case with the single-core ERV unit and without ERV unit

Normal operation minutes	Defrost hours	Space heating (kWh)	With single-core ERV unit		Without ERV unit		
			Energy use for heating the outdoor air (kWh)	Total heating (kWh)	Energy use for heating the outdoor air (kWh)	Total heating (kWh)	Energy saving (kWh)
25	1043	35934	5298	41232	25923	61857	20625
30	1012	35934	5410	41344	25923	61857	20513
40	823.16	35934	5445	41379	25923	61857	20478
50	782.07	35934	5930	41864	25923	61857	19993

It can be observed (**Table C.2**) that the use of single-core ERV unit can all lead to lower energy use (from 74 % to 77% of ventilation heating reduction or around 25 % total energy heating reduction) for all proposed normal/defrost operation schedules. In addition, the longer period of the normal operation leads to the reduction of the defrost hours up to 28% at maximum of the defrost hours reduction at 60 min normal operation. In the meanwhile, the ventilation heating for the proposed different operation schedules sees a significant increase by, at maximum, 11% of the ventilation heating or 1% of the total heating versus the manufactured operation schedules. The total heating demand with the fan powers is presented in **Table C.3**.

Table C.3: Annual energy use for the space heating and heating the outdoor air and defrost hours in the NZEH house in Kuujjuaq with the increase of normal operation time, comparison of the case with the single-core ERV unit and without ERV unit

		With single-core ERV unit			Without ERV unit		
Normal operation minutes	Defrost hours	Space heating (kWh)	Energy use for heating the outdoor ait (kWh)	Total heating (kWh)	Energy use for heating the outdoor ait (kWh)	Total heating (kWh)	Energy saving (kWh)
25	702.5	26574	3087	29661	12599	39173	9512
30	687.17	26574	3144	29718	12599	39173	9454
40	537.26	26574	3207	29781	12599	39173	9392
50	523.45	26574	3313	29887	12599	39173	9286

It can be seen (**Table C.3**) that the application of the single-core ERV unit plays a key role in reducing the energy USE (around 74 ventilation heating reduction or 24 total heating reduction) in the NZEH house regardless of the normal operation period of the single-core ERV unit.

Compared with the manufactured defrost schedules, the single-core ERV unit experiences 2, 23, 25.4 and 30.6 defrost hours drop when the normal operation periods are 30min, 40min, 50 min and 60 min, respectively. Conversely, 1.85, 2.8%, 7.3% and 6% ventilation increases are witnessed.

Table C.4: Annual energy use for the space heating and heating the outdoor air and defrost hours in the NZEH house in Resolute with the increase of normal operation time, comparison of the case with the single-core ERV unit and without ERV unit

		With single-core ERV unit			Without ERV unit		
Normal operation minutes	Defrost hours	Space heating (kWh)	Energy use for heating the outdoor ait (kWh)	Total heating (kWh)	Energy use for heating the outdoor ait (kWh)	Total heating (kWh)	Energy saving (kWh)
25	1379.08	42163.66	4650	46814	20163	62326.79	15512
30	1333.33	42163.66	4782	46946	20163	62326.79	15380
40	1130.17	42163.66	5115	47056	20163	62326.79	15048
50	734.47	42163.66	5376	47540	20163	62326.79	14786

It can be noticed (**Table C.4**) that the introduction of the single-core ERV unit made a significant contribution (from 73% to 76 ventilation heating reduction or 24.5 total heating reduction) to the energy savings in the NZEH house. The extension on the normal operation period (25min, 30 min, 40 min, 50 min and 60 min, respectively) result in significant defrost hours reduction as follow: 3.3% at 30 min normal operation, 18% at 40 min normal operation, 47% at 50 min normal operation and 45% at 60 min normal operation. However, the longer period of the normal operation of the single-core ERV unit also leads to the increased ventilation heating energy use, where 15.6% ventilation heating increase, as the highest for all, is seen at 60 min normal operation.